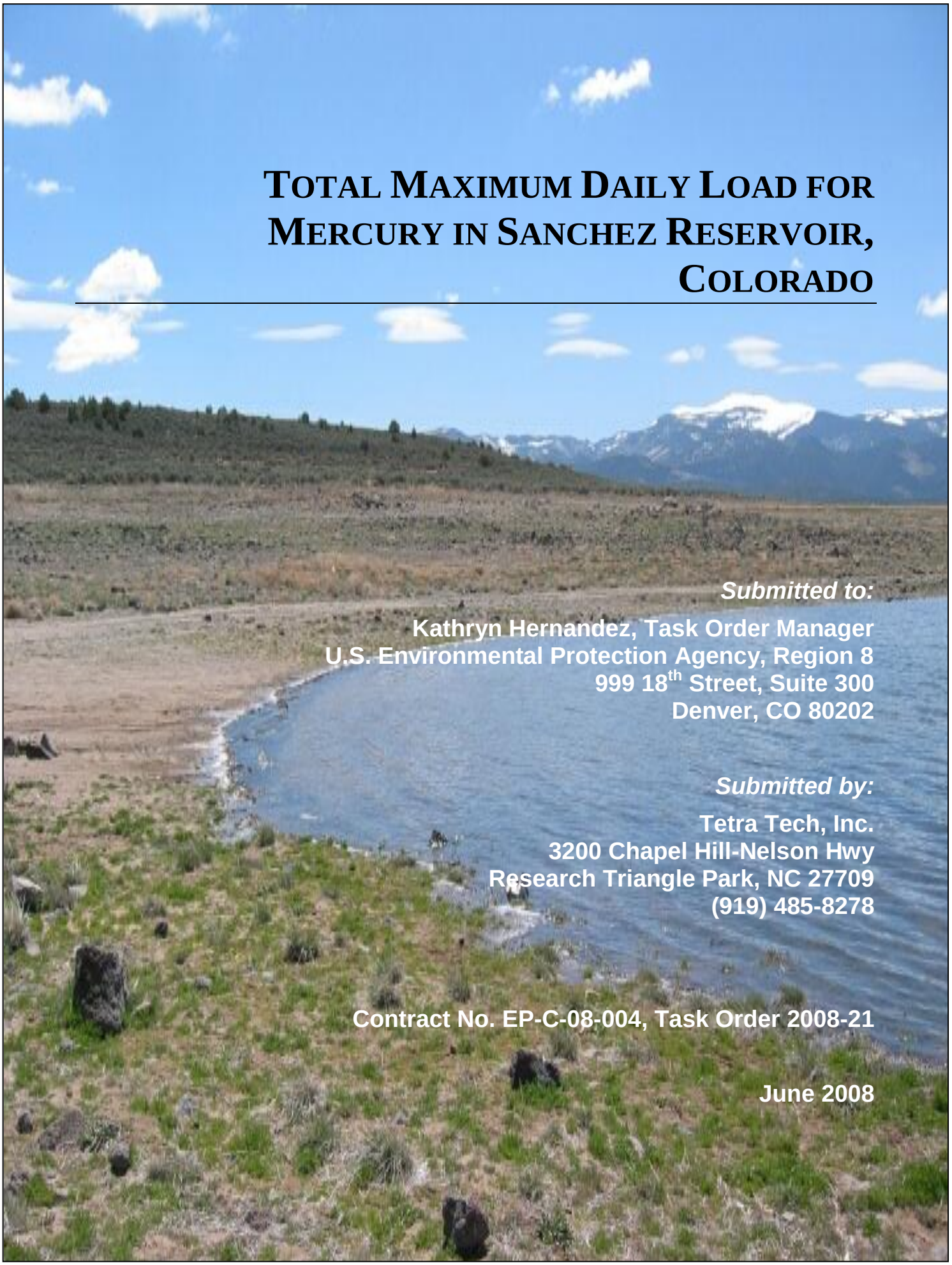

TOTAL MAXIMUM DAILY LOAD FOR MERCURY IN SANCHEZ RESERVOIR, COLORADO

Submitted to:

Kathryn Hernandez, Task Order Manager
U.S. Environmental Protection Agency, Region 8
999 18th Street, Suite 300
Denver, CO 80202

Submitted by:

Tetra Tech, Inc.
3200 Chapel Hill-Nelson Hwy
Research Triangle Park, NC 27709
(919) 485-8278

Contract No. EP-C-08-004, Task Order 2008-21

June 2008

Acknowledgments

This document was developed for the Colorado Department of Public Health and the Environment (CDPHE) and the U.S. Environmental Protection Agency (EPA), Region 8, under the direction of Kathryn Hernandez, EPA Task Order Manager, based on studies prepared by Tetra Tech, Inc. Support for additional sediment sampling was provided by CDPHE.

TOTAL MAXIMUM DAILY LOAD FOR MERCURY IN SANCHEZ RESERVOIR

Table of Contents

List of Tables

List of Figures

(This page left intentionally blank.)

Executive Summary

The Colorado Department of Public Health and the Environment (CDPHE) has identified Sanchez Reservoir in Costilla County as not supporting its designated uses due to the presence of elevated fish tissue concentrations of mercury that have resulted in Fish Consumption Advisories. Mercury concentrations at the levels observed present a significant health risk to persons who consume listed fish from the reservoir. Ambient water quality criteria for concentrations of mercury in water have not been exceeded; however, the physical and chemical characteristics of the lake leads to a situation in which mercury builds up in fish tissue to levels that present a risk to human health. Small amounts of mercury enter invertebrates and small fish at the bottom of the food chain; these amounts are further concentrated in predatory fish, such as walleye, that consume smaller fish. Because Sanchez Reservoir does not support its designated uses, a Total Maximum Daily Load (TMDL) is required for mercury loading to the lake. The TMDL is a mechanism established in the Clean Water Act for situations in which water quality impairment has not been mitigated by imposition of the minimum required levels of technology-based effluent limits on permitted point sources. The TMDL process requires that the acceptable level of loading that is consistent with supporting uses (the loading capacity) be established. The U.S. Environmental Protection Agency (EPA), Region 8, is supporting CDPHE in the development of this TMDL. Support provided by Region 8 has included a technical assessment of mercury loads and potential allocations and determination of the appropriate TMDL target.

The target for the TMDL is established in terms of mercury concentrations in fillets of walleye of 20 inches or greater length. The walleye is a top predator in the system and thus at high risk for bioaccumulation of mercury. It is also frequently sought by sport fishermen on the reservoir. The target set by CDPHE and Region 8 is an average of 0.3 mg/kg methylmercury in fish tissue. The average is based on composite samples of not more than 10 fish per size and species class.

The TMDL, according to federal regulations, consists of an allocation of the amount of pollutant loading that is consistent with attaining designated uses (the loading capacity) to permitted point sources, nonpoint sources, and a margin of safety. As described in this document, the loading capacity of Sanchez Reservoir associated with attaining the target fish tissue concentration of 0.3 mg/kg is approximately 154 grams of mercury per year. The existing load is estimated as 495 g/yr, of which 389 g/yr (78 percent) derives from the watershed. Thus, significant reductions in loads will likely be needed to achieve target concentrations in fish tissue.

All of the loading capacity is allocated to nonpoint sources (atmospheric load and watershed background load which itself appears to be derived primarily from atmospheric deposition) and a Margin of Safety. An explicit Margin of Safety is applied by determining a 95-percent upper confidence limit on the relationship between fish tissue concentrations and mercury concentrations in the reservoir. The difference between the loading capacity determined using the best estimate of needed load reductions and that determined using the upper confidence limit constitutes the Margin of Safety – which amounts to approximately 14 percent of the annual average mercury load to Sanchez Reservoir.

Sanchez Reservoir has no permitted point sources of mercury loading. In addition, the geology of the watershed is not indicative of elevated mercury loading potential, and human activities (such as improper waste disposal) appear to contribute only a small portion of the mercury problem. Instead, the major source of mercury input to Sanchez Reservoir appears to be atmospheric deposition – both direct to the lake and to the watershed. Observed data and atmospheric modeling suggest that atmospheric deposition adds up to 21 grams of mercury per square kilometer per year to the Sanchez watershed – or about 12 kilograms per year over the entire watershed. Only a small portion of this atmospheric load would account for the observed watershed mercury loads to the reservoir. Some of this mercury load derives from coal-fired power plants and other point source emissions in Colorado, New Mexico, and Arizona. However, a large portion of the load appears to derive from the global atmospheric cycling of mercury,

much of it derived from foreign sources that do not have the emission controls required in the United States.

While atmospheric deposition appears to be the major ultimate source of mercury loading to Sanchez Reservoir, the watershed load reflects the net impact of decades of atmospheric deposition, whereas the direct input to the reservoir surface is driven by current deposition rates. Significant time may be required to reduce watershed loading of mercury to the lake even if atmospheric sources are reduced.

TMDL allocations to achieve water quality standards include reductions in both direct atmospheric deposition to the lake and mercury loading from the watershed. Because much of the watershed mercury load tends to travel with sediment, efforts that reduce sediment loading to Sanchez Reservoir by controlling soil erosion will also reduce mercury loading. Efforts to reduce local inputs of mercury to the watershed (for example, contaminated dredge spoil from the Sanchez Canal, illegal trash dumps, and uncontrolled automobile graveyards) will also have a beneficial effect, but appear unlikely to yield a significant reduction in the total mercury load. In addition, Sanchez Reservoir appears to be at high risk for mercury bioaccumulation in fish in part because a relatively large fraction of the mercury that is carried into the reservoir is methylmercury – the form that accumulates in fish. Methylmercury is created by biological activity under low oxygen conditions, particularly in wetlands. However, there may be possibilities for reducing the rate of mercury methylation in the watershed and thus improving fish tissue concentrations. The limited data available from the watershed are not, however, sufficient to evaluate the potential benefits of such interventions at this time.

The conclusion that the loading of mercury to Sanchez Reservoir is driven by regional and local atmospheric mercury transport means that it will be difficult to reduce mercury to acceptable levels based solely on local efforts within the watershed. Even if it is possible to reduce the rates of mercury delivery and/or mercury methylation in the watershed, it appears likely that reduction in the atmospheric mercury loads will ultimately be needed to meet water quality standards in the reservoir. Atmospheric deposition of mercury in remote areas of Colorado like Costilla County is, at least in part, a global issue. Fully achieving safe fish tissue concentrations of mercury in Sanchez Reservoir may require global action to reduce mercury emissions worldwide.

The analysis presented in this report is based on a limited number of sampling events for mercury in water, sediment, and biota. While a watershed loading model has been constructed, there are not sufficient data available to develop a detailed understanding of mercury cycling within Sanchez Reservoir at this time. Because there is considerable uncertainty in the estimation of the appropriate mercury loading limits for the reservoir, continued monitoring to assess the status of fish tissue concentrations in the reservoir is strongly recommended.

Glossary and Acronyms

7Q10. Seven-day, consecutive low flow with a 10-year return frequency.

Acute toxicity. A stimulus severe enough to rapidly induce a toxic effect. In aquatic toxicity tests, an effect observed within 96 hours or less is considered acute.

Aerobic. Environmental condition characterized by the presence of dissolved oxygen. Used to describe chemical or biological processes that occur in the presence of oxygen.

Algae. Any organisms of a group of chiefly aquatic microscopic nonvascular plants. Most algae have chlorophyll as the primary pigment for carbon fixation.

Anaerobic. Environmental condition characterized by the absence of dissolved oxygen. Used to describe chemical or biological processes that occur in the absence of oxygen.

Anoxic. Aquatic environmental conditions containing zero or minimal dissolved oxygen.

ASCE. American Society of Civil Engineers.

AV SWAT. ArcView Soil and Water Assessment Tool.

Benthic. Refers to material, especially sediment, at the bottom of an aquatic ecosystem.

Benthic organisms. Organisms living in or on bottom substrates in an aquatic ecosystem.

Bioaccumulation. The process by which a contaminant accumulates in the tissues of an organism.

BMP. Best Management Practice.

CAA. Colorado Acequia Association.

CAMR. Clean Air Mercury Rule.

CDPHE. Colorado Department of Public Health and Environment.

CDOW. Colorado Division of Wildlife.

CFR. Code of Federal Regulations.

Chronic toxicity. Toxic impacts that occur over relatively long periods of time, often one-tenth of the life span or more. Chronic effects may include mortality, reduced growth, or reduced reproduction.

Cinnabar. A compound of sulfide and mercury (HgS), also known as red mercuric sulfide, that is the primary naturally occurring ore of mercury.

CMAQ. Community Multiscale Air Quality.

CSFS. Colorado State Forest Service.

CWA. Clean Water Act.

DEM. Digital Elevation Model.

Designated uses. Those beneficial uses of a waterbody identified in state water quality standards that must be achieved and maintained as required under the Clean Water Act.

DR. Delivery ratio.

EMNRD. New Mexico Energy, Minerals, and Natural Resources Department.

Epilimnion. The surface water layer overlying the thermocline of a lake. This water layer is in direct contact with the atmosphere.

Evapotranspiration. Water loss from the land surface by the combined effects of direct evaporation and transpiration by plants.

FDA. U.S. Food and Drug Administration.

FRV. Final Residue Value.

GIRAS. Geographic Information Retrieval and Analysis System.

GIS. Geographic Information System.

GWLF. Generalized Watershed Loading Functions Model.

Hg. Chemical symbol for mercury.

Hg(0). Elemental mercury.

Hg(I). Monovalent ionic mercury.

Hg(II). Divalent ionic mercury.

Hg-P. Particle-associated mercury.

HgS. See cinnabar.

Hydrophobic. A compound that lacks affinity for water and thus tends to have low solubility in water.

Hypolimnion. The bottom water layer underlying the thermocline of a lake. This layer is isolated from direct contact with the atmosphere.

ICR. U.S. EPA Information Collection Request.

IEM. Indirect Exposure Methodology Model.

Lipophilic. A compound that has a high affinity for lipids (fats and oils) and is thus prone to be stored in body tissues.

Load Allocation. The portion of a receiving water's loading capacity that is attributed either to one of its existing or future nonpoint sources of pollution or to natural background.

Loading capacity. The amount of contaminant load (expressed as mass per unit time) that can be loaded to a waterbody without exceeding water quality standards or criteria.

Macrophytes. Macroscopic, multicellular forms of aquatic vegetation, including macroalgae and aquatic vascular plants.

Margin of Safety. A required component of the TMDL that accounts for uncertainty in the relationship between the pollutant loads and the quality of the receiving waterbody.

MDN. Mercury Deposition Network. A monitoring network for wet deposition of mercury operated in association with NADP.

MeHg. See Methylmercury.

Metalimnion. The water stratum between the epilimnion and hypolimnion that contains the thermocline.

Methylation. The process of adding a methyl group (CH_3) to a compound, often occurring as a result of bacterial activity under anaerobic conditions.

Methylmercury (MeHg). A compound formed from a mercury ion and a methyl molecule, CH_3Hg, usually by bacterial activity. Methylmercury exhibits the chemical behavior of an organic compound and is the form of mercury most likely to be taken up and retained by organisms.

mg. Milligram (10^{-3} grams).

Morphometry. The shape, size, area, and volumetric characteristics of a waterbody.

MOS. Margin of Safety.

MT. Metric ton (10^6 grams).

MUID. Mapping Unit Identifier.

MW. Megawatt (10^6 watts).

NADP. National Atmospheric Deposition Program. A monitoring network maintained by USEPA to monitor wet deposition of NOx and sulfate.

NASA. National Aeronautics and Space Administration.

ng. Nanogram (10^{-9} grams).

NHAP. National High Altitude Photography.

NOAA. National Oceanic and Atmospheric Administration.

Nonpoint source pollution. Pollution that is not released through pipes but rather originates from multiple sources over a relatively large area.

NOx. Nitrate plus nitrite nitrogen.

NPDES. National Pollutant Discharge Elimination System.

NRCS. Natural Resources Conservation Service of the U.S. Department of Agriculture.

Oligotrophic. Waterbodies characterized by low rates of internal production, usually due to the presence of low levels of nutrients to support algal growth.

PCS. U.S. EPA Permit Compliance System.

pg. Picogram (10^{-12} grams).

pH. A measure of acidity and alkalinity of a solution that is a number on a scale on which the value of 7 represents neutrality and lower numbers indicate increasing acidity. pH is equivalent to the negative logarithm of hydrogen ion activity.

Photodegradation/photolysis. Degradation of compounds by light energy.

Piscivorous. Fish-eating.

Potential evapotranspiration (PET). An estimate of the evapotranspiration that would occur in response to available solar energy if water supply was not limiting.

RADM. Regional Atmospheric Deposition Model.

Redox potential. A measure of the energy available for oxidation and reduction reactions, represented as the negative logarithm of electron activity in a solution.

RELMAP. Regional Lagrangian Model of Air Pollution.

REMSAD. Regional Modeling System for Aerosols and Deposition.

RfD. Reference dose.

RGM. Reactive gaseous mercury.

SO_4. Sulfate.

SOD. Summary of the day weather station.

STATSGO. State Soil Geographic Database (U.S. Department of Agriculture).

Stratification (of waterbody). Formation of water layers with distinct physical and chemical properties that inhibit vertical mixing. Most commonly, thermal stratification occurs when warmer surface water overlies colder bottom water.

Tailings. Residue of raw material or waste separated out during the processing of mineral ores.

TEAM. Trace Element Atmospheric Model.

Total Maximum Daily Load (TMDL). The sum of the individual wasteload allocations for point sources, load allocations for nonpoint sources and natural background, and a margin of safety as specified in the Clean Water Act. The TMDL must be less than or equal to the loading capacity and can be expressed in terms of mass per time, toxicity, or other appropriate measures that relate to a state's water quality standards.

TRI. U.S. EPA Toxics Release Inventory.

Trophic level. One of the hierarchical strata of a food web characterized by organisms that are the same number of steps removed from the primary producers (such as photosynthetic algae). Animals that consume other animals are at higher trophic levels. Certain pollutants such as methylmercury tend to accumulate at higher concentrations in animals at higher trophic levels.

UCL. Upper Confidence Limit.

µg. Microgram (10^{-6} grams).

UPI. Upper Prediction Interval.

USEPA. U.S. Environmental Protection Agency.

USFWS. U.S. Fish and Wildlife Service.

USGS. U.S. Geological Survey.

USLE. Universal Soil Loss Equation.

Wasteload Allocation. The portion of a receiving water's loading capacity that is allocated to one of its existing or future permitted point sources of pollution.

Watershed. The entire upstream land area that drains to a given waterbody.

WEPP. Water Erosion Prediction Project.

1 Introduction and Problem Statement

1.1 DESCRIPTION OF TMDL PROCESS

High-quality water is an extremely valuable commodity in Colorado. Water quality standards are established to protect the designated uses of Colorado's waters. When states and local communities identify problems in meeting water quality standards, a Total Maximum Daily Load (TMDL) can be part of a plan to fix the water quality problems. The purpose of this TMDL is to provide an estimate of pollutant loading reductions needed to restore the beneficial uses of Sanchez Reservoir.

Section 303(d) of the Clean Water Act (CWA) requires states to identify the waters that are water quality impaired. A water quality impaired segment does not meet the standards for its assigned use classification. The states must also rank these impaired waterbodies by priority, taking into account the severity of the pollution and the uses to be made of the waters. Lists of prioritized impaired waterbodies are known as the "303(d) lists" and must be submitted to EPA every two years.

A TMDL represents the total load of a pollutant that can be discharged to a waterbody and still meet the applicable water quality standards. The TMDL can be expressed as the total mass or quantity of a pollutant that can enter the waterbody within a unit of time. In most cases, the TMDL determines the allowable load for a constituent and divides it among the various contributors in the watershed as wasteload (i.e., point source discharge) and load (i.e., nonpoint source) allocations. The TMDL also accounts for natural background sources and provides a margin of safety. For some nonpoint sources it might not be feasible or useful to derive an allocation in mass per time units. In such cases, a percent reduction in pollutant discharge may be proposed.

TMDLs must include specific information to be approved by USEPA, Region 8. This information can be summarized in the following seven elements:

1) **Plan to meet state water quality standards:** The TMDL includes a study and a plan for the specific water and pollutants that must be addressed to ensure that applicable water quality standards are attained.

2) **Describe quantified water quality goals, targets, or endpoints:** The TMDL must establish numeric endpoints for the water quality standards, including beneficial uses to be protected, as a result of implementing the TMDL. This often requires an interpretation that clearly describes the linkage(s) between factors impacting water quality standards.

3) **Analyze/account for all sources of pollutants:** All significant pollutant sources are described, including the magnitude and location of sources.

4) **Identify pollution reduction goals:** The TMDL plan includes pollutant reduction targets for all point and nonpoint sources of pollution.

5) **Describe the linkage between water quality endpoints and pollutants of concern:** The TMDL must explain the relationship between the numeric targets and the pollutants of concern. That is, do the recommended pollutant load allocations exceed the loading capacity of the receiving water?

6) **Develop Margin of Safety that considers uncertainties, seasonal variations, and critical conditions:** The TMDL must describe how any uncertainties regarding the ability of the plan to meet water quality standards have been addressed. The plan must consider these issues in its recommended pollution reduction targets.

7) **Include an appropriate level of public involvement in the TMDL process:** This is usually achieved by publishing public notice of the TMDL, circulating the TMDL for public comment, and

holding public meetings in local communities. Public involvement must be documented in the state's TMDL submittal.

1.2 WATERBODY NAME AND LOCATION

This document sets forth the technical basis for a mercury TMDL for Sanchez Reservoir (List ID: CORGRG30) in Costilla County, southcentral Colorado. General characteristics of the reservoir and its watershed are described in Tetra Tech (2000) and are summarized only briefly here.

A private irrigation company, Costilla Estates Development Company, constructed Sanchez Reservoir approximately 6 miles south of San Luis in 1912 in order to supply irrigation water. In 1956, ownership of the reservoir was transferred to the Sanchez Ditch and Reservoir Company. The Colorado Division of Wildlife (CDOW) began fishery management in 1978, although fish stocking records exist from 1952.

With a drainage area of 226.6 square miles (588 km^2), the reservoir receives flow from Culebra Creek, Vallejos Creek, and San Francisco Creek via the Sanchez canal as well as directly from five intermittent streams. The majority of the watershed is contained within Costilla County, CO, with a small portion in Taos County, NM. The reservoir has a surface area of 3,145 acres and a storage capacity of 103,000 acre-feet at 8,300 ft. MSL. The reservoir rarely approaches full storage however, and typically contains about 40,000 acre-feet with an area of about 1,600 ac.

The location of the Sanchez Reservoir watershed is shown in Figure 1-1 and a detailed view of the watershed is provided in Figure 1-2. All land within the watershed is held by private ownership. Land uses in the watershed are discussed in Section 4.3.4.

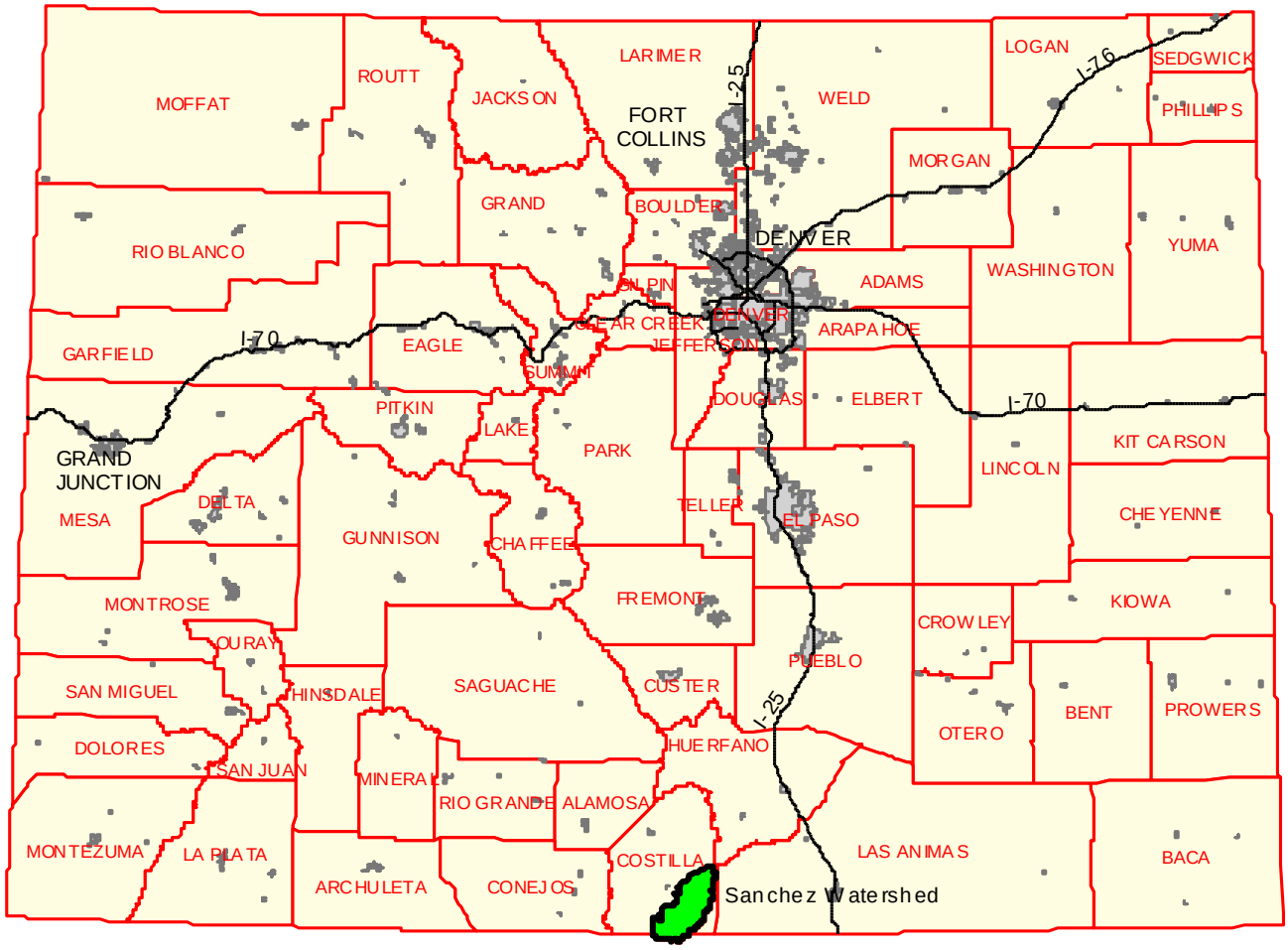

Figure 1-1. Location of Sanchez Watershed

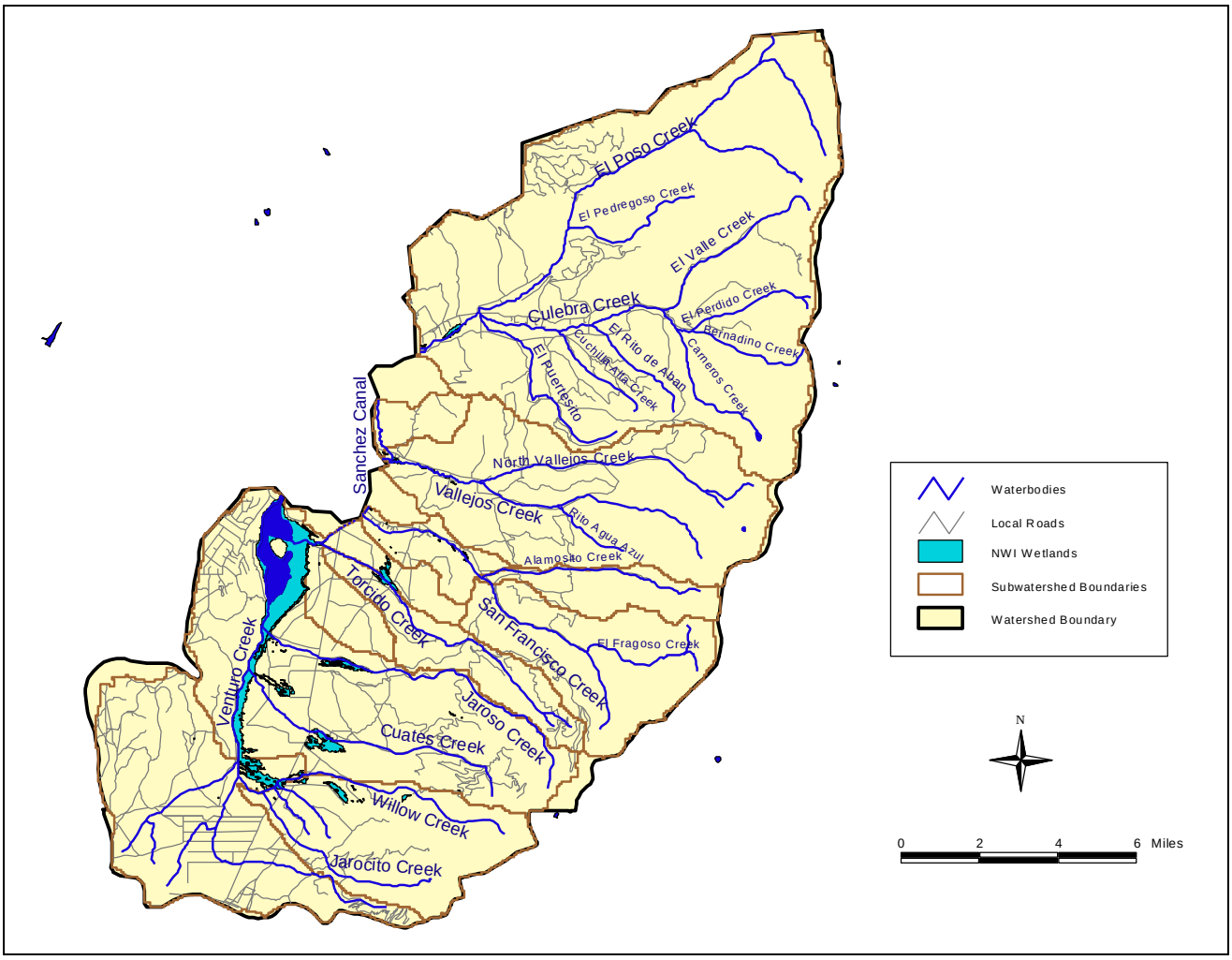

Figure 1-2. Detail of Sanchez Reservoir Watershed

1.3 GEOGRAPHIC COVERAGE OF TMDL

Water quality and beneficial uses are documented as impaired only within the reservoir itself. As evidenced by the observed mercury concentrations in the tributaries, mercury loads arise within the entire upstream watershed area, including sources from soil background and atmospheric deposition. Therefore, the geographic coverage of the TMDL is the entire upstream drainage of the reservoir. In addition, consideration is given to atmospheric transport of mercury from outside the watershed.

1.4 TMDL PRIORITY AND TARGETING

Sanchez Reservoir is listed on the Colorado 2008 303(d) list as high priority for development of a mercury TMDL (List ID: CORGRG30).

1.5 WATER QUALITY SUMMARY

1.5.1 Mercury in Water and Sediment

Historical sampling of Sanchez Reservoir and its watershed is summarized in Tetra Tech (2000). Data on mercury prior to 1999 are limited in number, did not use ultra-clean sampling and analysis, and are generally characterized by high detection limits that are not sufficient to resolve concentrations that lead to bioaccumulation in fish. They are therefore of limited use in developing the TMDL.

Ultra-clean sampling methods are important because mercury is highly mobile in gaseous form and can readily contaminate samples that are not handled properly. Additional intensive sampling of the reservoir was conducted in June and August of 1999 using ultra-clean methods, as described in Tetra Tech (2000). Tetra Tech collected supplementary sediment samples from the Sanchez Canal in November 2005 (Tetra Tech, 2006). These results are summarized briefly here. Sampling locations within the watershed are shown in Figure 1-3 and Table 1-1.

The Sanchez Reservoir water quality was alkaline with low dissolved solids concentrations in both June (110 to 120 mg/L) and August (84 to 100 mg/L) of 1999. The major ions were calcium (22 to 23 mg/L in June and 21 to 23 mg/L in August) and bicarbonate. Sulfate concentrations were low, <10 mg/L in June and 5.3 to 5.7 mg/L in August. Chloride concentrations were also low, 1 to 2 mg/L in June and about 1 mg/L in August. Nitrate was below detection in all the samples for both the June and August events. Ammonia was detected in only one sample at SAN-B at a depth of 8.5 ft, located in the shallow eastern part of the reservoir, at 0.2 mg/L. Phosphorus was <0.1 to 0.05 mg/L in June and 0.07 to 0.1 mg/L in August. Dissolved organic carbon was 3 to 4 mg/L in June and 4 to 6 mg/L in August. Suspended solids were low for both sampling dates, less than 2 mg/L. The Secchi depths ranged from 6.5 to 12.5 ft, and represented 38 to 65 percent of the total water depth.

In June, dissolved oxygen was above 6 mg/L at all the profile locations. The Sanchez Reservoir profiles in June showed a temperature difference of about 2 ˚C at SAN-C, and about a 4 ˚C difference at the deepest location at about 65 ft (Tetra Tech, 2000). In August, the reservoir at SAN-A was fully mixed to a depth of 22 ft with dissolved oxygen of 5 mg/L at a temperature of 18.8 ˚C. SAN-B was weakly stratified with respect to temperature, but dissolved oxygen was high, over 8 mg/L throughout the water column. The deeper location, SAN-C, was more strongly stratified, with a small temperature difference of 2 ˚C, but a large decrease in dissolved oxygen from 7 mg/L at the surface to less than 1 mg/L at a depth of 32 ft.

Mercury sampling results for the water column of Sanchez Reservoir are summarized in Table 1-2. In June, samples from the upper reaches of streams had higher total mercury concentrations than the samples from the lower reaches of the streams or the reservoir. The highest total mercury concentrations were in Alamosito Creek (SAN-7A) and two beaver ponds on Jaroso Creek (SAN-5) and San Francisco Creek (SAN-7B). The highest total methylmercury concentration was measured in an unnamed tributary to Ventero Creek in the southern part of the watershed (SAN-2). In August, the highest mercury concentrations were in wetlands in the southern part of the watershed (SAN-3 and SAN-14).

The Sanchez Reservoir water column samples in June had total mercury ranging from 6.7E-04 to 1.26E-03 µg/L and dissolved mercury from 5.2E-04 to 9.4E-04 µg/L. In August, total mercury ranged from 4.6E-04 to 8.4E-03 µg/L and dissolved mercury from 2.6E-04 to 7.7E-04 µg/L. Total methylmercury ranged from 4.7E-05 to 1.06E-04 µg/L and was higher in August than in July.

Mercury sampling results for the sediment in the Sanchez Reservoir watershed are summarized in Table 1-3 and Table 1-5. The June 1999 sediment samples had high total mercury in the southern part of the watershed. Methylmercury was measured in only one sample (SAN-11). In August 1999, the highest

sediment mercury was also in the southern part of the watershed with the highest concentration at SAN-11 (0.035 mg/kg).

The 2005 sediment samples ranged from 7.3E-04 to 0.025 mg/kg, with the highest concentrations at the head of the canal, just below the Culebra Creek diversion.

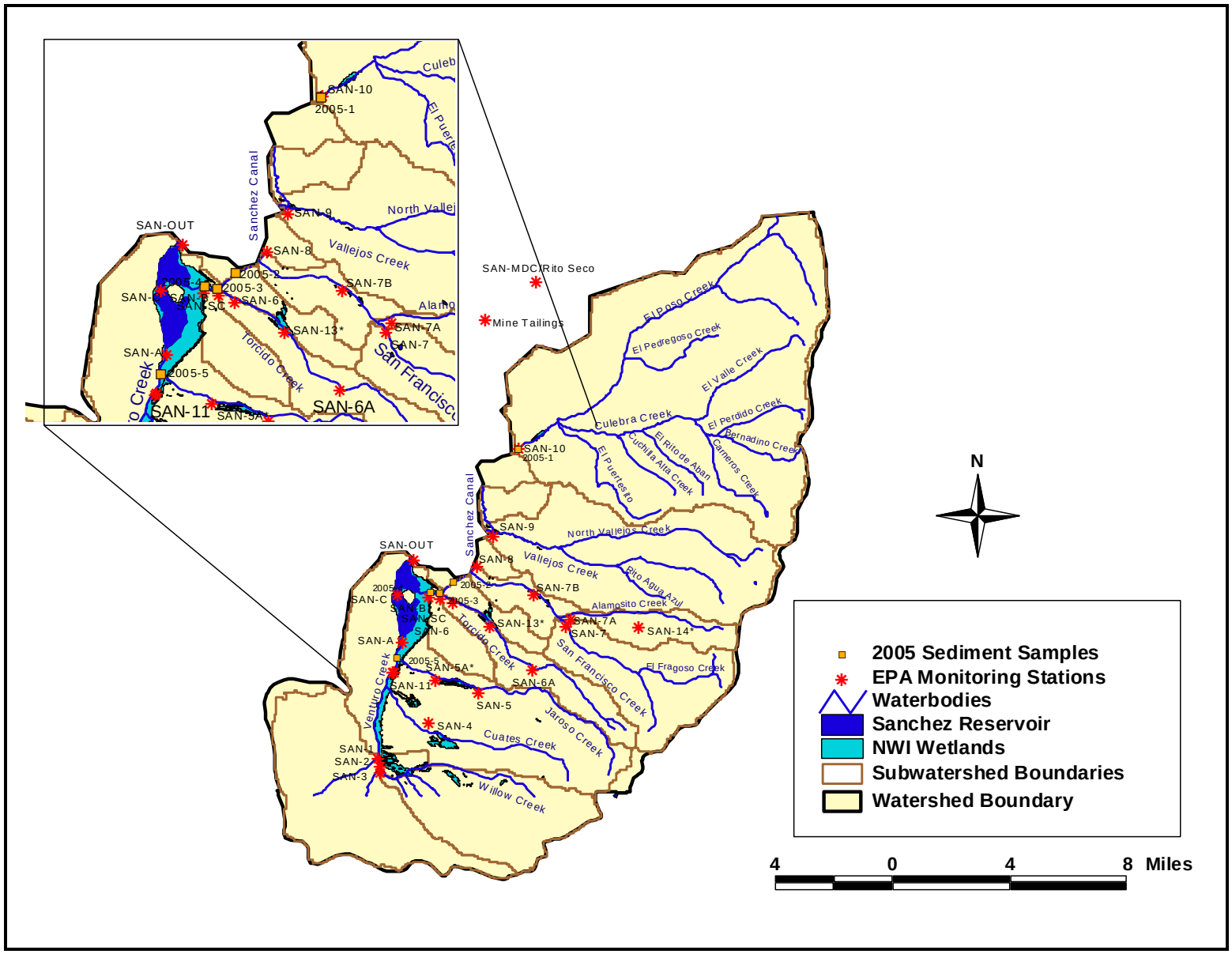

Figure 1-3. Sanchez Reservoir Sampling Stations, 1999

Table 1-1. Sanchez Sampling Locations, 1999 Water and Sediment Sampling

Table 1-1, Part A

Site Name	Site Location	Latitude	Longitude
SAN-1	Ventero Creek - Pond	37.016529	105.430412
SAN-2	Unnamed Tributary to Ventero Creek	37.012397	105.429553
SAN-3	Willow Creek	37.009298	105.429124
SAN-4	Cuates Creek	37.034364	105.399485
SAN-5	Jaroso Creek - Upper Beaver Pond	37.049242	105.368986
SAN-5A*	Jaroso Creek - Lower	37.055441	105.395189
SAN-6	Torcido Creek - Lower	37.093320	105.384880
SAN-6A	Torcido Creek - Upper	37.060778	105.335911
SAN-7	San Francisco Creek - Seep	37.082300	105.315077
SAN-7A	Alamosito Creek	37.085744	105.312285
SAN-7B	San Francisco Creek at Beaver Pond	37.097452	105.335481
SAN-8	Sanchez Canal – Middle (above San Francisco Creek)	37.111915	105.369845
SAN-9	Vallejos Creek	37.126377	105.360395
SAN-10	Culebra Creek	37.168044	105.344072
SAN-11	Ventero Creek near Inlet to Reservoir	37.059229	105.420962
SAN-13*	Torcido Creek - Middle	37.081956	105.362113
SAN-14*	Unnamed Tributary to Alamosito Creek	37.081612	105.270618
SAN-A	Sanchez Reservoir off Inlet from Ventero Creek	37.073864	105.416237
SAN-B	Sanchez Reservoir off Inlet from Sanchez Canal	37.096419	105.399485
SAN-C	Sanchez Reservoir between Island and West Side	37.097451	105.419243
SAN-OUT	Outlet from Sanchez Reservoir - Ventero Creek	37.114325	105.408935
SAN-SC	Sanchez Canal near Inlet to Reservoir	37.095730	105.392612

* New sample location added for August 1999 sampling.

Table 1-1, Part B. Sanchez Sampling Locations, 2005 Sediment Sampling

2005-1	Head of Sanchez Canal	37.16809	105.34440
2005-2	Sanchez Canal, ½ mi. below San Francisco Creek	37.10212	105.38460
2005-3	Sanchez Canal below Torcido Creek	37.09599	105.39324
2005-4	Canal at Alluvial Deposition	37.09691	105.39928
2005-5	Wetlands area, southeast of reservoir	37.06432	105.41932

Table 1-2. Mercury in Water Column Samples, Sanchez Reservoir, 1999

Sample ID	Date	Unfiltered Total Mercury (µg/L)	Dissolved Total Mercury (µg/L)	Unfiltered Methylmercury (µg/L)	Dissolved Methylmercury (µg/L)
Sanchez Streams					
SAN-1	6/5/1999	2.35E-03	1.65E-03	1.85E-04	1.12E-04
SAN-2	6/5/1999	2.82E-03	2.33E-03	3.01E-04	2.06E-04
SAN-3	6/5/1999	4.35E-03	3.23E-03	2.06E-04	1.58E-04
SAN-4	6/4/1999	3.41E-03	3.37E-03	1.09E-04	8.90E-05
SAN-5	6/4/1999	7.60E-03	2.43E-03	1.74E-04	3.20E-05
SAN-6	6/5/1999	3.48E-03	2.72E-03	2.32E-04	2.21E-04
SAN-6A	6/4/1999	6.24E-03	3.98E-03	6.80E-05	4.10E-05
SAN-7	6/4/1999	7.40E-04	4.90E-04	3.40E-05	1.10E-05
SAN-7A	6/4/1999	1.07E-02	3.88E-03	2.08E-04	3.30E-05
SAN-7B	6/4/1999	7.03E-03	2.73E-03	1.61E-04	1.00E-05
SAN-8	6/3/1999	2.43E-03	1.43E-03	5.20E-05	1.30E-05
SAN-9	6/4/1999	3.24E-03	2.08E-03	7.50E-05	3.00E-05
SAN-10	6/3/1999	1.80E-03	1.27E-03	1.40E-05	3.00E-06
SAN-11	6/6/1999	1.08E-03	1.04E-03	1.40E-04	1.48E-04
SAN-SC	6/3/1999	3.29E-03	1.75E-03	1.08E-04	1.00E-06
SAN-OUT	6/3/1999	1.03E-03	6.50E-04	9.30E-05	2.40E-05
SAN-1	8/4/1999	2.76E-03	2.12E-03	1.73E-04	NA
SAN-2	8/4/1999	1.18E-03	1.05E-03	1.86E-04	NA
SAN-3	8/4/1999	6.65E-03	2.92E-03	3.34E-04	NA
SAN-4	8/4/1999	1.32E-03	1.09E-03	2.25E-04	NA
SAN-5	8/4/1999	3.04E-03	1.52E-03	1.69E-04	NA
SAN-5A	8/4/1999	3.51E-03	1.35E-03	1.38E-04	NA
SAN-6A	8/3/1999	2.48E-03	1.26E-03	8.50E-05	NA
SAN-7	8/2/1999	4.00E-04	5.40E-04	8.60E-05	NA
SAN-7A	8/2/1999	1.48E-03	1.04E-03	8.40E-05	NA
SAN-7B	8/2/1999	1.61E-03	8.20E-04	1.05E-04	NA
SAN-8	8/2/1999	1.12E-03	6.40E-04	7.20E-05	NA
SAN-9	8/2/1999	8.60E-04	6.20E-04	6.60E-05	NA
SAN-10	8/2/1999	1.57E-03	8.00E-04	4.80E-05	NA

Sample ID	Date	Unfiltered Total Mercury (µg/L)	Dissolved Total Mercury (µg/L)	Unfiltered Methylmercury (µg/L)	Dissolved Methylmercury (µg/L)
SAN-11	8/6/1999	1.58E-03	1.31E-03	1.07E-04	NA
SAN-13	8/3/1999	6.20E-04	5.80E-04	5.20E-05	NA
SAN-14	8/2/1999	4.58E-03	1.32E-03	6.50E-05	NA
SAN-SC	8/2/1999	1.41E-03	7.40E-04	8.40E-05	NA
SAN-OUT	8/3/1999	1.00E-03	8.00E-04	4.39E-04	NA
Sanchez Reservoir					
SAN-A (1')	6/6/1999	7.00E-04	7.50E-04	1.00E-06	8.00E-06
SAN-A (1') rep.	6/6/1999	7.60E-04	6.80E-04	9.00E-06	6.00E-06
SAN-A (9')	6/6/1999	6.70E-04	6.80E-04	1.01E-04	1.70E-05
SAN-B (1.5')	6/17/1999	7.40E-04	6.90E-04	4.20E-05	1.60E-05
SAN-B (8.5')	6/17/1999	1.26E-03	9.40E-04	9.50E-05	6.20E-05
SAN-C (1.5')	6/17/1999	8.30E-04	7.60E-04	2.60E-05	3.80E-05
SAN-C (33')	6/17/1999	7.80E-04	5.20E-04	4.00E-05	1.30E-05
SAN-E (1')	6/17/1999	7.10E-04	6.80E-04	3.70E-05	1.40E-05
SAN-A (3')	8/6/1999	6.20E-04	5.90E-04	8.70E-05	<3.60E-5
SAN-A (18')	8/6/1999	7.50E-04	5.10E-04	5.90E-05	<3.60E-5
SAN-B (3')	8/6/1999	9.10E-04	7.70E-04	9.60E-05	<3.60E-5
SAN-B (8')	8/6/1999	8.39E-03	5.40E-04	1.06E-04	4.00E-05
SAN-C (20')	8/5/1999	1.56E-03	5.00E-04	9.20E-05	2.90E-05
SAN-C (30')	8/5/1999	6.40E-04	2.60E-04	6.20E-05	2.90E-05
SAN-E (3')	8/5/1999	4.60E-04	3.50E-04	4.70E-05	3.50E-05

Note: Depth of reservoir samples given in parentheses.

Table 1-3. Mercury in Sediment Samples, Sanchez Reservoir, 1999

Sample ID	Date	% Moisture	Sediment pH (S.U.)	Total Hg (mg/kg) dry wt.	Methyl Hg (mg/kg) dry wt.	Carbonate Carbon (%)	TOC (%)	Sulfide-S (mg/kg - dry)
Sanchez Streams								
SAN-1	6/5/1999	49.8	-	1.22E-02	-	0.01	2.31	20
SAN-2	6/5/1999	50.3	-	1.71E-02	-	0.01	3.25	<1
SAN-4	6/4/1999	35.9	-	9.38E-03	-	ND	2.31	<1
SAN-5	6/4/1999	29.5	-	6.82E-03	-	ND	1.35	<1

Sample ID	Date	% Moisture	Sediment pH (S.U.)	Total Hg (mg/kg) dry wt.	Methyl Hg (mg/kg) dry wt.	Carbonate Carbon (%)	TOC (%)	Sulfide-S (mg/kg - dry)
SAN-6	6/5/1999	29.9	-	6.87E-03	-	ND	1.35	<1
SAN-6A	6/4/1999	27.1	-	3.17E-03	-	ND	0.68	<1
SAN-7	6/4/1999	41.4	-	5.91E-03	-	0.11(0.09)	5.79	22
SAN-7A	6/4/1999	24.8	-	2.01E-03	-	0.01	1.12	4
SAN-7B	6/4/1999	47.1	-	1.54E-02	-	ND	3.88	9
SAN-8	6/3/1999	36.9	-	8.96E-03	-	0.03	1.09	1
SAN-9	6/4/1999	27.1	-	8.50E-04	-	ND	0.14	2
SAN-10	6/17/1999	38.2	-	4.54E-03	-	0.01	0.33	<1
SAN-11	6/6/1999	53.6	-	2.72E-02	9.30E-05	ND	3.85	8
SAN-SC	6/3/1999	34.6	-	1.13E-03	-	ND	0.23	<1
SAN-DAM (soil)	6/17/1999	11.9	-	2.58E-03	-	-	-	-
SAN-1	8/4/1999	61.2	-	1.28E-02	1.41E-04	0.86	-	31
SAN-2	8/4/1999	45.3	-	3.12E-02	1.57E-04 (1.91E-04)	2.25	-	<7.5
SAN-3	8/4/1999	61.6	-	1.70E-02	2.47E-04	2.32	-	9.1
SAN-4	8/4/1999	58.4	-	2.13E-02	6.42E-04	1.23	-	<6.9
SAN-5	8/4/1999	49.7	-	3.15E-02	2.69E-03 (3.12E-03)	1.17	-	10
SAN-5A	8/4/1999	77.5	-	<2.00E-03	2.03E-04	0.67	-	<6.8
SAN-6	8/3/1999	84.4	7.2	4.56E-03	2.70E-05	0.36	-	<4.9
SAN-6A	8/3/1999	78.5	7.6	<2.00E-03	6.00E-06	0.28	-	<4.9
SAN-7	8/2/1999	16.7	6.7	<4.70E-02	6.11E-04	1.2	-	3.1
SAN-7A	8/2/1999	77.1	6.8	<2.00E-03	1.88E-04	0.84	-	<5.7
SAN-7B	8/2/1999	73.6	7.5	5.26E-03	3.22E-04	0.42	-	<5.8
SAN-8	8/2/1999	67.4	7.3	1.33E-02 (1.19E-02)	8.44E-04	0.59	-	5
SAN-9	8/2/1999	85.0	7.2	<2.00E-03	1.42E-04	0.43	-	<6
SAN-10	8/2/1999	73.0	7.2	<3.00E-03	4.14E-04	0.72	-	<6.2
SAN-11	8/6/1999	71.3	7.2	3.53E-02	4.70E-05	0.9	-	<4.4
SAN-13	8/3/1999	75.8	-	7.00E-03	5.50E-05	0.63	-	<10
SAN-14	8/2/1999	77.1	-	1.41E-02	1.04E-04	0.89	-	<5.7
SAN-SC	8/2/1999	68.8	7.4	<3.00E-03	1.04E-03	0.16	-	3.1

Sample ID	Date	% Moisture	Sediment pH (S.U.)	Total Hg (mg/kg) dry wt.	Methyl Hg (mg/kg) dry wt.	Carbonate Carbon (%)	TOC (%)	Sulfide-S (mg/kg - dry)
SAN-OUT	8/3/1999	64.0	-	<3.00E-03	2.88E-04	1.5	-	<6.6
Sanchez Reservoir								
SAN-B-B	6/17/1999	38.3	-	6.95E-03	3.05E-04	0.04(0.05)	0.93	54
SAN-C-B	6/17/1999	69.6	-	1.97E-02	2.07E-04	ND	1.63	108(117)
SAN-A-B	8/6/1999	66.0	6.8	4.05E-02	1.90E-05	0.68	2.7	11
SAN-B-B	8/6/1999	70.9	6.6	2.18E-02	7.90E-05	0.49	1.9	<7.3
SAN-C-B	8/5/1999	43.5	6.9	1.57E-02	4.23E-04	0.68	7.8	21
SAN-E-S	8/5/1999	53.4	6.5	2.17E-02	2.68E-04	0.64	<1.8	11
Sanchez Wetlands								
SANW	8/6/1999	45.2	6.8	1.43E-02	6.90E-05	1.94	<2	<7.9

Notes: Replicates listed in parentheses.

Carbonate carbon and TOC determined on <2 mm fraction of sediment from June samples. Grain size distribution is shown in separate table.

Table 1-4. Mercury in Sediment Samples, Sanchez Reservoir, 2005

Sample ID	Date	% Moisture	Sediment pH (S.U.)	Total Hg (mg/kg) dry wt.	Methyl Hg (mg/kg) dry wt.	Carbonate Carbon (%)	TOC (%)	Sulfide-S (mg/kg - dry)
2005-1 (instream)	11/21/2005	-	-	2.54E-02	1.98E-03	-	6.80	< 3.5
2005-1 (berm)	11/21/2005	-	-	9.30E-03	1.13E-03	-	1.93	< 1.1
2005-2 (instream)	11/21/2005	-	-	4.02E-03	1.31E-04	-	0.879	< 1.3
2005-2 (berm)	11/21/2005	-	-	1.41E-02	5.55E-04	-	3.88	< 1.5
2005-3 (instream)	11/21/2005	-	-	7.30E-04	2.40E-05	-	1.31	< 0.96
2005-4 (instream)	11/21/2005	-	-	3.24E-03	7.60E-05	-	0.238	< 0.90
2005-5 (berm)	11/21/2005	-	-	1.14E-02	3.89E-04	-	2.26	< 1.5
2005-5 (berm)	11/21/2005	-	-	1.57E-02	3.32E-04	-	3.98	< 1.6

1.5.2 Mercury in Biota

Fish tissue sampling was also conducted during 1999 by Colorado Division of Wildlife (CDOW). Samples were collected in October, two months after the second water column sampling round. Results are summarized in Table 1-5. The fish species analyzed in Sanchez Reservoir included northern pike,

walleye, and yellow perch. The highest mercury concentration in 1999 (1.6 mg/kg) was in a 20-inch walleye. Out of 22 fish sampled, there were 7 fish with mercury above 1 mg/kg and 11 fish above 0.5 mg/kg. All the fish above 0.5 mg/kg were either walleye or northern pike, both piscivorous fish that can grow quite large. A small yellow perch had the lowest mercury concentration.

A variety of benthic invertebrates were also sampled in the reservoir in 1999 as discussed in Tetra Tech (2000). Three samples from Sanchez Reservoir ranged from 3.29E-03 to 0.0124 mg/kg total mercury. The results for sampling throughout the Sanchez Reservoir watershed are summarized in Table 1-6.

Table 1-5. Fish Tissue Samples from Sanchez Reservoir, 1999

Species	Sample No.	Length (in.)	Weight (g)	Total Mercury (mg/kg-wet wt.)	Tissue Wt. (g)	Percent Moisture	Date
Northern pike (female)	SAN01	45.67	8,900	1.25	1000	76	10/5/1999
Northern pike (female)	SAN02	44.09	7,600	1.03	950	77	10/5/1999
Northern pike	SAN03	38.19	5,100	1.15	550	79	10/5/1999
Northern pike	SAN04	15.35	330	0.128	46	80.2	10/5/1999
Northern pike	SAN05	14.96	272	0.098	38	82.2	10/5/1999
Walleye	SAN06	18.90	1,000	0.0993	160	77.6	10/5/1999
Walleye	SAN07	18.90	1,025	0.899	175	75.7	10/5/1999
Walleye	SAN08	15.16	610	0.289	135	73.6	10/5/1999
Walleye	SAN09	22.44	1,850	0.835	300	78.7	10/5/1999
Walleye	SAN10	18.31	1,100	0.292	209	79.4	10/5/1999
Walleye	SAN11	19.69	1,250	1.58	200	76	10/5/1999
Walleye	SAN12	18.11	950	0.598	158	79	10/5/1999
Walleye	SAN13	18.50	1,150	1.3 (1.35)	205	76.5	10/5/1999
Walleye	SAN14	18.90	1,150	0.441	218	74.9	10/5/1999
Walleye	SAN15	15.75	650	0.429	116	78.4	10/5/1999
Northern pike	SAN16	20.47	800	0.382	171	80	10/5/1999
Northern pike	SAN17	23.43	1,070	0.328	203	79.2	10/5/1999
Yellow perch	SAN18	6.89	84	0.051	18	81.1	10/5/1999
Walleye	SAN19	17.32	850	0.933	159	77.7	10/5/1999
Walleye	SAN20	17.13	925	0.491	162	72.1	10/5/1999
Walleye	SAN21	18.50	1,020	1.14	175	77	10/5/1999

Note: All samples were left fillet from one fish; parentheses indicate replicate analyses.

Table 1-6. Benthic Macroinvertebrate Samples from Sanchez Reservoir, 1999

Sample ID	Date	Species Collected	Total Hg (mg/kg ww)	Methyl Hg (mg/kg ww)
Sanchez Streams				
SAN-1	6/5/1999	Mayfly, Damselfly, and Dragonfly Larvae	3.96E-03	NA
SAN-2	6/5/1999	Water Beetles	2.89E-02	NA
SAN-3	6/5/1999	Water Beetles	4.85E-02	NA
SAN-5	6/4/1999	Composite Benthic Invertebrates	4.06E-02	NA
SAN-6	6/5/1999	Midge Larvae	<2.1E-04	NA
SAN-6A	6/4/1999	Composite Benthic Invertebrates	1.23E-02	NA
SAN-7A (a)	6/4/1999	Composite Benthic Invertebrates	4.49E-03	NA
SAN-7A (b)	6/5/1999	Composite Benthic Invertebrates	1.66E-03	NA
SAN-7B	6/4/1999	Composite Benthic Invertebrates	1.58E-02	NA
SAN-9 (a)	6/4/1999	Mayfly and Caddisfly Larvae	1.33E-02	NA
SAN-9 (b)	6/4/1999	Stonefly Larvae	8.30E-03	NA
SAN-10	6/17/1999	Mayfly and Dragonfly Larvae	4.20E-03	NA
SAN-11	6/6/1999	Amphipods, Flatworms, and Oligochaetes	1.43E-03	NA
SAN-1	8/4/1999	Dragonfly Larvae and Water Beetles	2.83E-02	1.99E-02
SAN-2	8/4/1999	Leeches, Mayfly, and Fly Larvae	2.56E-02	1.18E-02
SAN-3	8/4/1999	Water Beetles	1.11E-01	3.74E-02
SAN-4	8/4/1999	Mayfly Larvae and Water Beetles	9.90E-02	6.23E-02
SAN-5	8/4/1999	Mayfly and Fly Larvae	NA	1.86E-02
SAN-5A	8/4/1999	Mayfly, Caddisfly and Fly Larvae	NA	1.21E-02
SAN-6A	8/3/1999	Stonefly, Mayfly and Water Beetle Larvae	4.60E-02	4.15E-02
SAN-7A	8/2/1999	Stonefly, Mayfly and Water Beetle Larvae	5.84E-02	3.41E-02
SAN-7B	8/2/1999	Stonefly, Mayfly, Fly, and Water Beetle Larvae	2.17E-02	1.68E-02
SAN-8	8/2/1999	Mayfly and Water Beetle Larvae	2.49E-02	1.79E-02
SAN-9	8/2/1999	Stonefly, Mayfly, Fly, and Water Beetle Larvae	2.06E-02	1.83E-02
SAN-10	8/2/1999	Stonefly, Mayfly, Caddisfly, and Water Beetle Larvae	1.69E-02	1.20E-02
SAN-11	8/6/1999	Mayfly Larvae and Mysid Shrimp	1.20E-02	6.18E-03
SAN-13	8/3/1999	Water Beetles and Mayfly Larvae	1.18E-01	2.92E-02
SAN-14	8/2/1999	Stonefly and Mayfly Larvae	NA	1.01E-02
SAN-SC	8/2/1999	Stonefly Larvae, Mayfly Larvae	1.25E-02	8.30E-03

Sample ID	Date	Species Collected	Total Hg (mg/kg ww)	Methyl Hg (mg/kg ww)
Sanchez Reservoir				
SAN-B-B	6/17/1999	Oligochaetes (red worms) and Midge Larvae	3.29E-03	NA
SAN-A-B	8/6/1999	Oligochaetes (red worms)	1.24E-02	4.64E-03
SAN-B-B	8/6/1999	Oligochaetes (red worms) and Mysid Shrimp	NA	5.47E-03
SAN-C-B	8/5/1999	Oligochaetes (red worms)	8.20E-03	<1.00E-03

Note: Mercury concentrations are on a wet weight basis. Parenthetical designations in the Sample ID (e.g., "(a)") refer to co-located samples.

Other fish tissue data from Sanchez Reservoir were collected in 1991 by CDOW, 2004 by CDPHE and in 1990 and 1991 by US Fish and Wildlife Service (USFWS). These results are summarized in Table 1-7, along with a limited number of samples from tributaries collected by USFWS. The highest concentration on record is 2.17 mg/kg, in a 17-in walleye analyzed by USFWS in 1992. In 2004, the highest concentration (1.45 mg/kg) was found in a relatively small (22-in) northern pike, while concentrations in walleye ranged up to 1.44 mg/kg. Of the 48 samples collected, 19 exceeded 0.5 mg/kg.

Though additional fish mercury concentration sampling has not been conducted in Sanchez since June 2004, CDPHE collected additional species type, length, and weight data in October 2005. During this event, 63 walleye were caught ranging in length from 14 to 21 inches.

Table 1-7. Additional Fish Tissue Samples from Sanchez Reservoir and Watershed

Species	Length (in)	Weight (g)	Total Mercury (mg/kg-wet weight)	Number in Sample	Sample Type	Date	Agency
Samples from Sanchez Reservoir							
Brown Trout	18 – 24	-	0.84	1	Fillet	6/91	CDOW
Brown Trout	6 – 12	-	0.05	1	Fillet	6/91	CDOW
Carp	24 – 30	-	0.42	3	Fillet	6/91	CDOW
Northern Pike	12 – 18	-	0.38	1	Fillet	6/91	CDOW
Northern Pike	22		1.45	1	Fillet	6/8/04	CDPHE
Northern Pike	24 – 30	-	1.24	1	Fillet	6/91	CDOW
Northern Pike	25	-	0.98	1	Fillet	3/91	USFWS
Northern Pike	30 – 35	-	0.99	1	Fillet	6/91	CDOW
Northern Pike	40	7,100	1.10	1	Fillet	5/92	USFWS
Northern Pike	40		0.4	1	Fillet	6/8/04	CDPHE
Walleye	-	-	0.183	3	Whole Body	5/92	USFWS

Species	Length (in)	Weight (g)	Total Mercury (mg/kg-wet weight)	Number in Sample	Sample Type	Date	Agency
Walleye	15	-	0.45	1	Fillet	6/91	CDOW
Walleye	15 – 17	412 – 708	1.20	5	Fillet	5/92	USFWS
Walleye	16		<0.3	1	Fillet	6/8/04	CDPHE
Walleye	16		0.33	1	Fillet	6/8/04	CDPHE
Walleye	16		<0.3	1	Fillet	6/8/04	CDPHE
Walleye	17	731	2.17	1	Fillet	5/92	USFWS
Walleye	17	750	1.76	1	Fillet	5/92	USFWS
Walleye	17		0.51	1	Fillet	6/8/04	CDPHE
Walleye	17		0.67	1	Fillet	6/8/04	CDPHE
Walleye	17		0.39	1	Fillet	6/8/04	CDPHE
Walleye	20	-	1.60	1	Fillet	3/91	USFWS
Walleye	20		1.02	1	Fillet	6/8/04	CDPHE
Walleye	20		1.44	1	Fillet	6/8/04	CDPHE
Walleye	21		1.11	1	Fillet	6/8/04	CDPHE
Walleye	22		1.27	1	Fillet	6/8/04	CDPHE
Walleye	22		1.42	1	Fillet	6/8/04	CDPHE
Walleye	24		1.33	1	Fillet	6/8/04	CDPHE
White Sucker	-	-	0.166	3	Whole Body	5/92	USFWS
White Sucker	17 – 20	-	0.32	9	Fillet	5/91	CDOW
Yellow Perch	-	-	0.058	3	Whole Body	5/92	USFWS
Yellow Perch	11	523	0.44	1	Fillet	5/92	USFWS
Yellow Perch	11		<0.3	3	Fillet	6/8/04	CDPHE
Yellow Perch	11		<0.3	3	Fillet	6/8/04	CDPHE
Yellow Perch	11		<0.3	3	Fillet	6/8/04	CDPHE
Yellow Perch	12		0.37	3	Fillet	6/8/04	CDPHE
Yellow Perch	12		<0.3	3	Fillet	6/8/04	CDPHE
Yellow Perch	12 – 18	-	0.75	4	Fillet	6/91	CDOW
Yellow Perch	12 – 18	-	0.48	1	Fillet	6/91	CDOW

Species	Length (in)	Weight (g)	Total Mercury (mg/kg-wet weight)	Number in Sample	Sample Type	Date	Agency
Yellow Perch	6 – 12	-	0.45	7	Fillet	5/91	CDOW
Yellow Perch	6 – 12	-	0.45	7	Fillet	5/91	CDOW
Yellow Perch	9 – 11	227 – 274	0.40	5	Fillet	5/92	USFWS
Samples from Sanchez Reservoir Tributaries – San Francisco Creek on Taylor Ranch							
Brown Trout	-	-	0.068	10	Whole Body (less head and gills)	5/92	USFWS
Brown Trout	-	-	0.106	5	Whole Body	5/92	USFWS
Samples from Sanchez Reservoir Tributaries – Ventero Creek							
Brown Trout	-	-	0.036	1	Fillet	5/92	USFWS
Brown Trout	-	-	< 0.029	10	Whole Body (less head and gills)	5/92	USFWS
Brown Trout	-	-	< 0.032	5	Whole Body	5/92	USFWS
Rio Grande Sucker	-	-	0.044	5	Whole Body	5/92	USFWS

Fish in Sanchez tributaries do not exceed the fish tissue guidelines. This is expected because the fish in the tributaries are very small and are not larger predators that concentrate mercury by consumption of other fish. Trout, which consume many terrestrial insects, typically show low mercury body burdens. The low concentrations in tributary fish do *not* indicate that tributaries are free of mercury load.

Tetra Tech combined the available fish data for Sanchez and plotted tissue concentration versus length for different species (Figure 1-4 through Figure 1-6). Concentrations are high in many cases, but the size of fish (particularly walleye) was also quite large. Length is an approximate surrogate for age, and fish, particularly piscivorous fish, tend to have increased tissue concentrations with increased age.

Fish tissue mercury concentrations in Sanchez are high relative to most other Colorado lakes. To investigate this issue qualitatively, Sanchez Reservoir results are compared to 1999 samples from Narraguinnep Reservoir, another Colorado reservoir impaired by elevated fish tissue concentrations, on a concentration versus length basis (Figure 1-7 through Figure 1-9). The comparison to Narraguinnep is appropriate because similar species are present.

For yellow perch and northern pike, the Narraguinnep samples appear to show the same concentration-length relationship as in Sanchez. For walleye, fish of a given length in Narraguinnep tended to have a somewhat higher mercury tissue concentration than those in Sanchez – possibly due to faster growth rates in Sanchez. Thus, the high concentrations of mercury in fish observed in Sanchez seem to be primarily a result of the larger size of the sport fish present in the reservoir. Size and age are typically strongly correlated, although no age information is available for Sanchez fish samples.

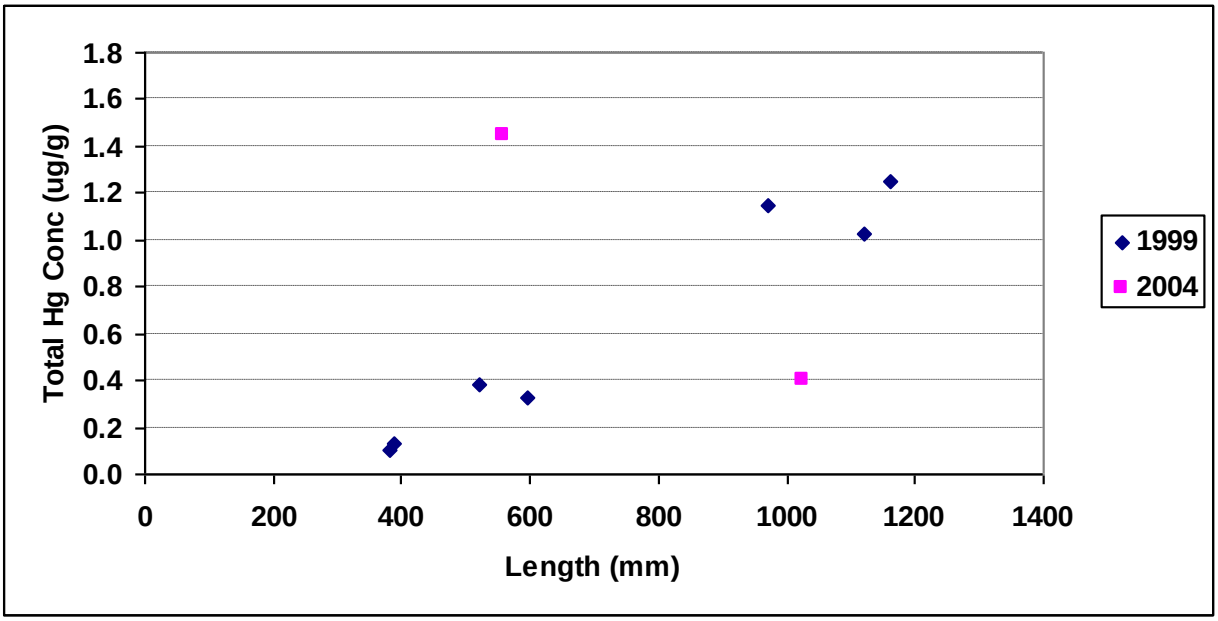

Figure 1-4. Tissue Concentrations of Total Mercury in Northern Pike by Sampling Year, Sanchez Reservoir

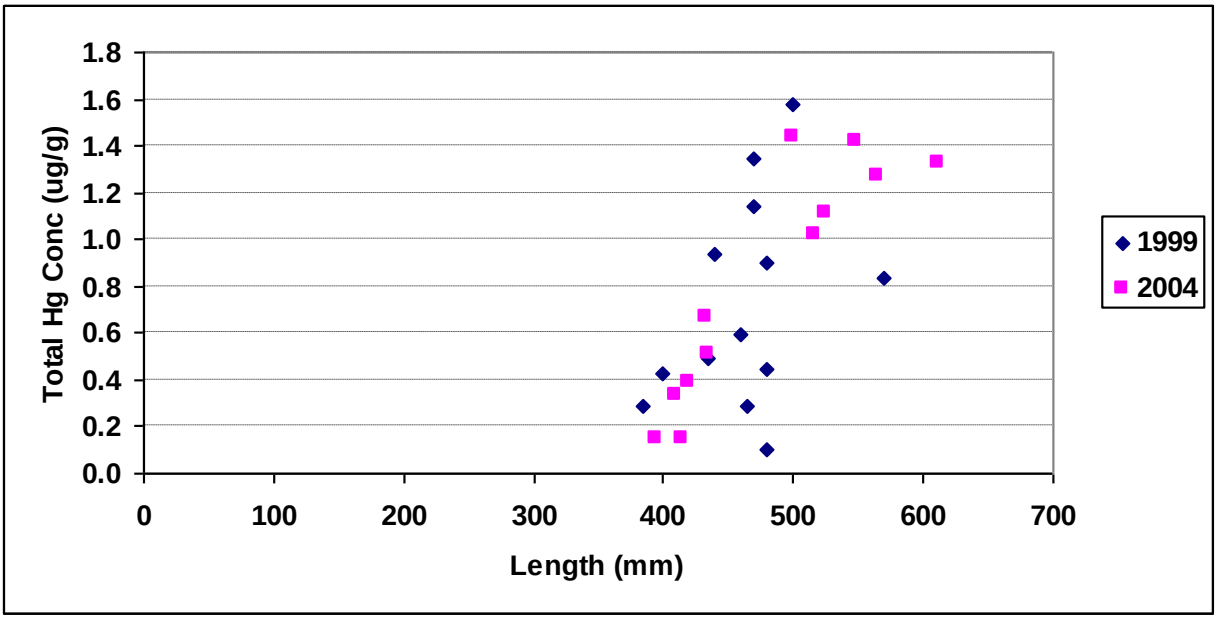

Figure 1-5. Tissue Concentrations of Total Mercury in Walleye by Sampling Year, Sanchez Reservoir

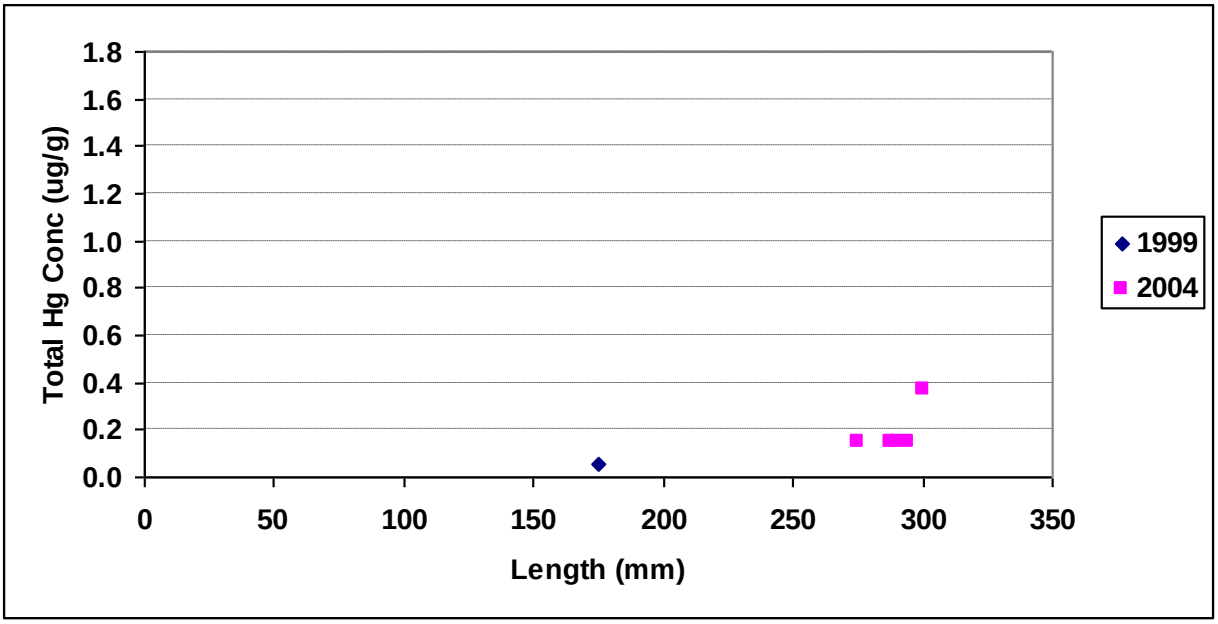

Figure 1-6. Tissue Concentrations of Total Mercury in Yellow Perch by Sampling Year, Sanchez Reservoir

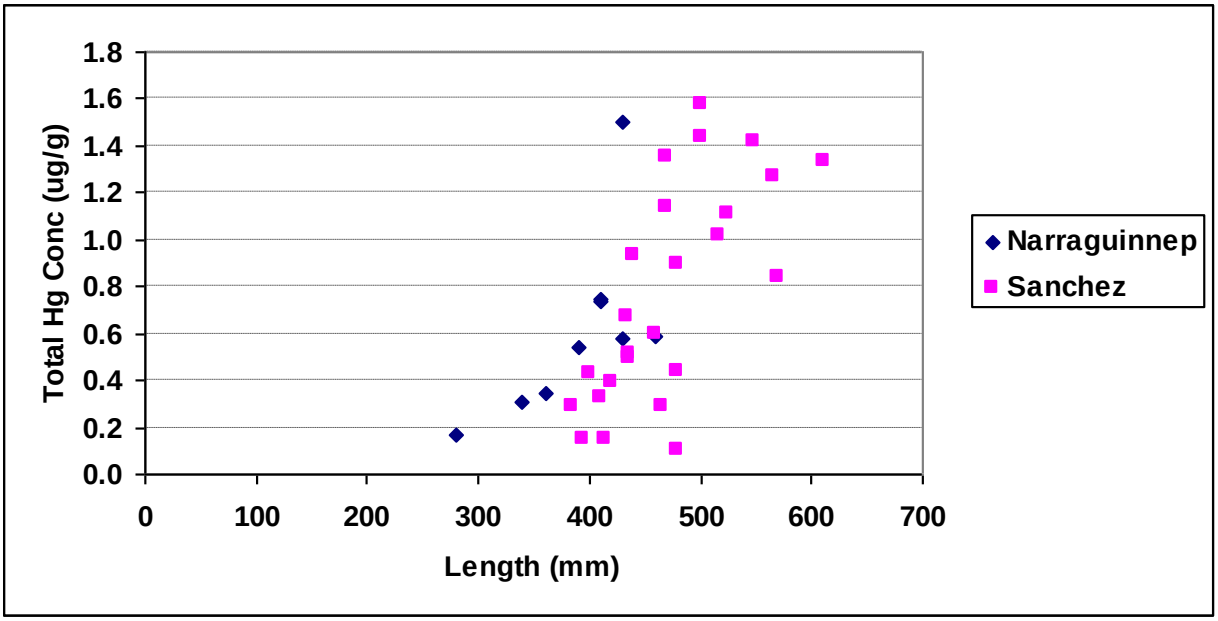

Figure 1-7. Comparison of Total Mercury Concentrations in Walleye from Sanchez and Narraguinnep Reservoirs

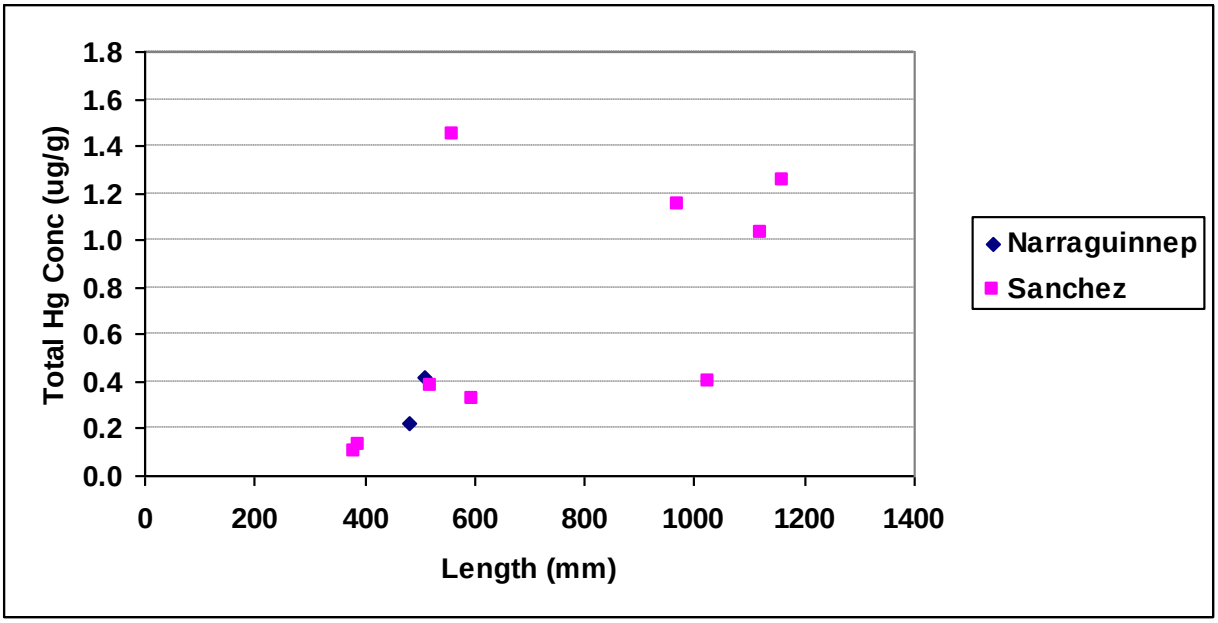

Figure 1-8. Comparison of Total Mercury Concentrations in Northern Pike from Sanchez and Narraguinnep Reservoirs

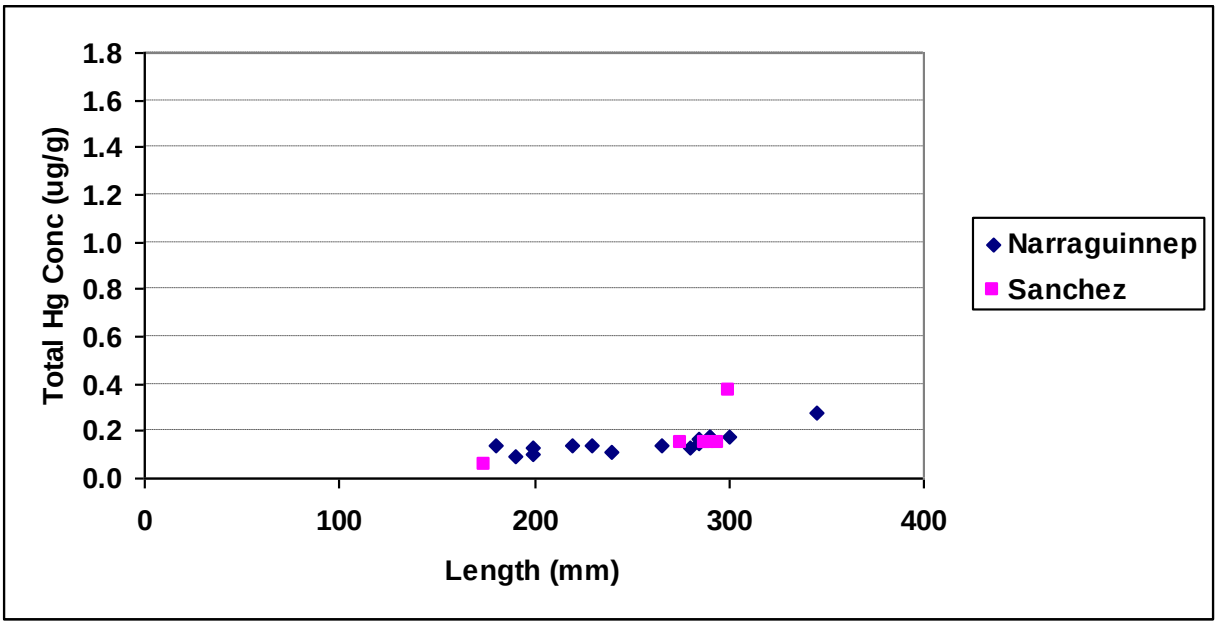

Figure 1-9. Comparison of Total Mercury Concentrations in Yellow Perch from Sanchez and Narraguinnep Reservoirs

(This page left intentionally blank.)

2 Applicable Water Quality Standards

TMDLs are developed to meet applicable water quality standards. These may include numeric water quality standards, narrative standards for the support of designated uses, and other associated indicators of support of beneficial uses. A numeric target identifies the specific goals or endpoints for the TMDL that equate to attainment of the water quality standard. The numeric target may be equivalent to a numeric water quality standard (where one exists), or it may represent a quantitative interpretation of a narrative standard. This section reviews the applicable water quality standards and identifies an appropriate numeric indicator and associated numeric target level for the calculation of the mercury TMDL for Sanchez Reservoir.

2.1 NUMERIC WATER QUALITY STANDARDS

The designated use classifications of Sanchez Reservoir are Aquatic Life Cold 1, Water Supply, Recreation 1E, and Agriculture. Colorado has adopted water quality standards for mercury that apply to these designated uses, specifying a Final Residue Value (FRV)-based criterion of 0.01 ug/L total mercury in water (Colorado DPHE Water Quality Control Commission, Regulation No. 31, effective July 1, 2007, Table III). The mercury criterion is not hardness-dependent. The applicable criterion is the most restrictive of values derived for the protection of aquatic life, fish tissue concentrations, and drinking water supplies, and is based on the maximum allowed concentration of total mercury in the water that will present "bioconcentration or bioaccumulation of methylmercury in edible fish tissue at the U.S. Food and Drug Administration's (FDA) action level of 1 ppm" (CDPHE Water Quality Control Commission, Regulation No. 31 effective July 1, 2007, Table III, Footnote 6).

To date, mercury concentrations in water in Sanchez Reservoir have not exceeded the applicable water quality standards, and the reservoir is listed as not supporting designated uses based on the presence of a Fish Consumption Advisory rather than excursions of ambient water quality standards for mercury.

2.2 NARRATIVE STANDARDS

The state's narrative language for toxics is expressed in part as follows (CDPHE Water Quality Control Commission, Regulation No. 31 [Effective July 1, 2007], Section 31.11(1)):

> Except where authorized...state surface waters shall be free from substances attributable to human-caused point source or nonpoint source discharges in amounts, concentrations, or combinations which:
>
> (a) for all surface waters except wetlands:
>
> (iv) are harmful to the beneficial uses or toxic to humans, animals, plants, or aquatic life...

This clause may be taken to generally prohibit loading of mercury to the lake in amounts that result in fish tissue contamination levels sufficient to impair recreational uses or present a risk to human health.

2.3 FISH CONSUMPTION GUIDELINES

Colorado's numeric criterion for mercury in water is intended to ensure protection of the general population from potential adverse health impacts from the ingestion of sport-caught or local fish. As noted above, the water quality criterion is based on a Final Residual Value in fish tissue at the FDA action

level of 1 ppm (1 ppm = 1 mg/kg). Footnote 6 to Table III in Regulation 31 provides the following discussion relative to this criterion (pp. 55–56):

> FRV means Final Residue Value and should be expressed as "Total" because many forms of mercury are readily converted to toxic forms under natural conditions. The FRV value of 0.01 µg/liter is the maximum allowed concentration of total mercury in the water that will present bioconcentration or bioaccumulation of methylmercury in edible fish tissue at the U.S. Food and Drug Administration's (FDA) action level of 1 ppm. The FDA action level is intended to protect the average consumer of commercial fish; it is not stratified for sensitive populations who may regularly eat fish.
>
> A 1990 health risk assessment conducted by the Colorado Department of Public Health and Environment indicates that when sensitive subpopulations are considered, methylmercury levels in sport-caught fish as much as one-fifth lower (0.2 ppm) than the FDA level may pose a health risk.

In 2006, CDPHE updated the health risk assessment, which will be used to revise the Basic Standards during the June 2010 Rulemaking. This assessment concludes that methylmercury levels of 0.093 ppm may cause toxicological effects in children and levels of 0.154 ppm should not be consumed by women of childbearing age.

Colorado does not have a formal regulation establishing a mercury guideline for the issuance of fish consumption advisories. However, the Colorado DPHE (CDPHE) has issued fish consumption advisories for waterbodies where concentrations of mercury in composite samples of not more than 10 fish fillets from a given species and size class are equal to or exceed the action level of 0.5 mg/kg (wet weight) total mercury (personal communication, Philip Hegeman, CDPHE to A. Matos, Tetra Tech, 4/23/2008). CDPHE listings are based on the risk analysis presented in the June 2006, Disease Control and Environmental Epidemiology Division *Methylmercury Fish Consumption Limit Guidelines: Toxicological Basis and Development*. This paper, which is based on a toxicity value RfD of 0.0001 mg/kg/day, establishes a fish tissue concentration of 0.17 mg/kg as the approximate center of the range at which the safe consumption level is four meals per month for nonpregnant adults. For women who are pregnant, nursing, or planning to become pregnant, the center concentration is 0.12 mg/kg, and for children 6 years of age or younger, the concentration is 0.07 mg/kg.

2.4 SELECTED NUMERIC TARGET FOR COMPLETING THE TMDL

In 2001, USEPA issued a methylmercury criterion of 0.3 mg/kg in fish tissue (USEPA, 2001). The applicable numeric targets for the Sanchez TMDLs are the Colorado ambient water quality criterion of 0.01 ug/L total mercury in the water column and the USEPA criterion of 0.3 mg/kg methylmercury concentration in fish tissue. Water column mercury concentrations have not been found in excess of the ambient water quality standard; however, tissue concentrations have exceeded the action level. Fish in Sanchez Reservoir accumulate unacceptable tissue concentrations of mercury even though the ambient water quality standard appears to be met. The most binding regulatory criterion is the fish tissue concentration criterion of 0.3 mg/kg methylmercury, which is selected as the primary numeric target for calculating this TMDL. Attaining this criterion will better protect human health while also resulting in removal of the fish consumption advisory.

Mercury bioaccumulates in the food chain with concentrations increasing in larger fish that consume smaller fish. Within a lake fish community, top predators usually have higher mercury concentrations than forage fish, and tissue concentrations generally increase with age class. Top predators (such as bass or walleye) are often target species for sport fishermen. Risks to human health from the consumption of mercury-contaminated fish are based on long-term, cumulative effects, rather than concentrations in individual fish. Therefore, the criterion should not be applied to the extreme case of the most-contaminated fish within a target species; instead, the criterion is most applicable to average concentrations in a top predator species of a size likely to be caught and consumed.

Within Sanchez Reservoir, the top predator sport fish, and also the fish with the highest reported tissue methylmercury body burden, is walleye. Walleye continue to bioaccumulate mercury with increasing size and age. There are no size limits on walleye catch in Sanchez at present (CDOW, 2008); however, angler activity is likely to be focused on larger fish, for which Sanchez is renowned. Many walleye in the available sampling are greater than 500 mm (about 20") in length, and the highest observed mercury tissue concentrations occur in this range (see Figure 1-5). Therefore, the selected target for the TMDL analysis in Sanchez Reservoir is an average tissue concentration in walleye greater than 20" length (508 mm) that meets the target level of 0.3 mg/kg or less.

(This page left intentionally blank.)

3 Pollutant Source Assessment

The number of identified sources of mercury loading to the Sanchez Reservoir is limited. The sources external to the reservoir can be separated into direct atmospheric deposition onto the water surface (both from near- and far-field sources) and transport into the reservoir from the watershed. The watershed loading of mercury occurs in both dissolved and sediment-sorbed forms. Potential sources of mercury in the watershed include: parent geologic formations, tailings and residue associated with mining techniques, point source discharges, and atmospheric deposition to the watershed, including deposition and storage in the snowpack. Monitoring of mercury in streams and stream sediments typically reflects the combined impact of these potential sources.

3.1 POINT SOURCES

Mercury can be found in the effluent from wastewater treatment plants and certain industrial processes. The EPA Permit Compliance System (PCS) does not identify any permitted dischargers to waters regulated under the NPDES system within the Sanchez Reservoir watershed. Three permitted dischargers are located in Costilla County and discharge to Culebra Creek; however, the effluent enters the creek downstream of the diversion structure at the head of the Sanchez Canal. Stormwater within this rural watershed is not subject to EPA Phase 2 Municipal Separate Storm Sewer System permitting requirements, and is thus treated as a nonpoint source. Therefore, permitted point source discharges are not expected to provide a source of mercury loading to Sanchez Reservoir.

3.2 ATMOSPHERIC DEPOSITION

Atmospheric deposition is an important source of inorganic mercury loading to surface waters. Much of this mercury is from a variety of anthropogenic sources. Atmospheric deposition can be divided into short-range or near-field deposition, which includes deposition from sources located near the watershed, and long-range or far-field deposition, which includes mercury deposition from regional and global sources. As described below in Section 3.2.5, near-field deposition appears to constitute, at most, a small fraction of the total atmospheric deposition of mercury to the Sanchez watershed.

3.2.1 Near-Field Atmospheric Mercury Sources

Significant atmospheric point sources of mercury can cause locally elevated areas of near-field atmospheric deposition downwind. Mercury emitted from man-made sources usually contains both gaseous elemental mercury (Hg(0)) and divalent mercury (Hg(II)). Hg(II) species, because of their solubility and their tendency to attach to particles, are redeposited relatively close to their source (probably within a few hundred miles), whereas Hg(0) remains in the atmosphere much longer, contributing to long-range transport.

The fact that there is low precipitation in southcentral Colorado means that less mercury is likely to be deposited near the source than in more humid regions; i.e., Hg(II) forms of mercury probably have time to migrate farther from their source before being scavenged by precipitation or dry depositing as particle-attached mercury.

Significant potential point sources of airborne mercury include coal-fired power plants, steel recycling facilities, waste incinerators, cement and lime kilns, smelters and gold mine roasters, pulp and paper mills, and chlor-alkali factories. There are two large coal-fired power plants in the Four Corners area at the intersection of Colorado, Utah, New Mexico, and Arizona: (1) Arizona Public Service – Four Corners Station, which has a 2,270 MW capacity and (2) the Public Service Company of New Mexico-San Juan

plant, which has a 1,779 MW capacity. Another large coal-fired power plant is located north of the watershed: Xcel Energy – Cherokee Station, which has a 717 MW capacity. Six other coal-fired power plants are located within a 200 mile radius of the center of Sanchez Reservoir. Together, these plants generated nearly 58,000,000 MWh of electricity during 1998 (Pechan, 2003).

Because mercury is a volatile element, much of the mercury present in coal used for power plants is discharged via the stack to the atmosphere, unless technology is implemented to limit emissions. The discharged mercury may be in elemental, oxidized (ionic), or particulate form, with the mix depending on temperature and mercury reaction conditions, including chlorine and sulfur content (EPRI, 2000). In general, the oxidized and particulate forms of mercury are amenable to removal by control technology, while the elemental forms are not.

A rough estimate of the emissions of mercury from coal-fired power plants without advanced emission controls is about 70 percent of the amount contained in the incoming coal (EPRI, 1999). Split sample analyses of mercury content of coal used for power production during the winter of 1999–2000 in the Four Corners area are reported by Ingersoll (2000). These range from about 0.04 mg/kg at Navajo to 0.09 mg/kg at Four Corners.

After July 1999, large power plants were required to estimate their mercury emissions and provide the data to the USEPA Toxics Release Inventory (TRI). Total releases for 2000 are summarized in Pechan (2003). Detailed mercury data for a large number of plants were collected during 1999 as part of EPA's Information Collection Rule. Detailed estimates of emissions for 1999 by plant and boiler are contained in the draft National Emissions Inventory (RTI, 2001). These estimates include influent and stack effluent mercury load after accounting for reduction expected for a given control technology. There is considerable uncertainty in the estimated rate of removal, as shown by the summaries in EPRI (2000). The control technologies (combination of boiler type, fuel, and sulfate, NO_x, and particulate matter controls) are identified by a group number or "bin." An accompanying table (http://www.epa.gov/ttn/atw/combust/utiltox/control2.zip, accessed 7/17/01) summarizes the average mercury speciation among particulate mercury, oxidized mercury, and elemental mercury as reported by control bin for the U.S. EPA Information Collection Request (ICR). These fractions can be applied to the total mercury emission estimates to obtain estimates of the reactive mercury (particulate plus oxidized mercury) generated by each source.

Mercury emissions for the 10 coal-fired power plants within 200 miles of Sanchez are presented in Part 1 of Table 3-1, based on 2006 TRI data (USEPA, 2008). These estimates differ somewhat from those presented in EPRI (2000) and RTI (2001), but are generally similar. Plant locations are shown in Figure 3-1. Total mercury emissions from the nine coal-fired plants amount to 754.4 kg-Hg/yr, of which more than 63 percent are associated with the San Juan and Four Corners generating plants. Reactive mercury emissions from the 10 plants totaled 234 kg in 2006. A distance limit of 200 miles was selected for this analysis because most near-field deposition of power plant emissions should occur within a range smaller than this distance.

Part 2 of Table 3-1 lists mercury air emissions from sources other than coal-fired power plants that emitted more than 5 kg/yr in 1999, 2003, or 2006. As of the 2006 TRI (USEPA, 2008), these contributed another 310 kg of mercury per year within 200 miles of Sanchez Reservoir. CF & I Steel contributed 83 percent of the mercury load from these facilities. Mercury speciation data are generally not available for these sources.

The largest non-utility emitter within 200 miles of Sanchez Reservoir in 2006 was CF & I Steel in Pueblo, CO, which recycles crushed automobiles. CF & I is approximately 80 miles from Sanchez, although separated from the watershed by high mountains. This type of facility emits mercury primarily due to mercury-containing automotive switches. CDPHE established an active mercury switch removal program for scrap yards in January 2004, which currently has about 40 participants, accounting for about 80 percent of the scrapped vehicles. This program should have significantly reduced mercury emissions

from CF & I, though an increase of 58 percent was seen from 2003 to 2006. This increase is likely due to improvements in testing methodologies and an increased percent of emissions exiting through the stack (email from Aimee Konowal, CDPHE to Alix Matos, Tetra Tech, 4/22/2008.)

Another large non-utility emitter of mercury within 200 miles of Sanchez is the Cemex, Inc. Lyons Cement Plant, which reported releases of 141.5 kg in 1999, but only 24 kg in 2006. This facility is permitted to burn tire-derived fuel, which is a potential source of mercury emissions (Reisman, 1997), but has not done so in several years, which may account for the difference between 1999 and 2006 emissions. In 2005, Cemex was applying to resume use of tire-derived fuel (personal communication, Mark McMillan, CDPHE, to Jonathan Butcher, Tetra Tech, 10/13/2005), which may account for the subsequent increase in 2006 relative to 2003, when release estimates were 5.4 kg.

Gold mining sources (such as Cripple Creek and Victor) typically have wet scrubbers without bypass on the mine roaster stacks. Tests of mercury speciation for coal utilities with no-bypass wet scrubbers showed divalent mercury emission averages of 7.8 percent (bin 10, bituminous pulverized coal boilers with cold-side electrostatic precipitator and flue gas desulfurization), 33 percent (bin 12, bituminous pulverized coal boilers with fabric filter baghouses and wet flue gas desulfurization), and 11.3 percent (bin 38, bituminous coal and coke cyclone boilers with cold-side electrostatic precipitator and wet flue gas desulfurization) (email from Dwight Atkinson, USEPA to Bruce Zander, USEPA, 9/13/2005). Similar percentages likely apply for the mine roasters.

There are also numerous smaller fixed sources (less than 5 kg/yr) shown on the TRI, many of which do not have valid locations recorded. The incremental contributions of these sources is, however, small, as all such sources in Colorado emitted only 8.5 kg to air on the 2006 TRI.

Table 3-1. Mercury Emissions to Air from Facilities within 200 Miles of Sanchez Reservoir

Table 3-1, Part A. Estimated Mercury Emissions from Coal-Fired Power Plants

Plant	Location	ORISPL	Distance to Sanchez (miles)	Bearing from Sanchez	Power Generation (MWh)[1]	Emission Control Type[2]	Total Hg Emissions 2003 (kg/yr)[3]	Total Hg Emissions 2006 (kg/yr)[3]	Reactive Hg Emissions 2006 (kg/yr)[3]
Comanche	Pueblo, CO	470	73.4	NE	4,223,847	15	29.0	67.6	60.6
Ray D. Nixon	Fountain, CO	8219	92.7	NNE	1,742,251	15	4.7	13	10.8
Martin Drake	Colorado Springs, CO	492	98.5	NNE	1,870,734	15	3.9	8.7	7.1
Arapahoe	Denver County, CO	465	138.7	NNE	1,395,220	13/15/18	21.7	28.9	9.3
San Juan	Waterflow, NM	2451	147.2	W	12,385,885	20	413.8	225	14.4
Four Corners	Fruitland, NM	2442	151.2	WSW	14,929,616	16/19	388.9	253.8	8.9
Escalante	Prewitt, NM	87	160.1	SW	1,804,546	19	35.0	3.2	0.1
Nucla	Nucla, CO	527	163.2	WNW	657,042	40	7.7	6.4	0.2
Cherokee	Denver, CO	469	174.5	NNE	15,418,208	15	4.1	85.7	71.1
Pawnee	Brush, CO	6248	187.6	NNE	3,655,268	15	33.5	62.1	51.5
Total					58,082,616		942.3	754.4	234.1

Table 3-1, Part B. Estimated Mercury Emissions from Facilities other than Coal-Fired Power Plants Emitting More than 5 kg/yr

Facility	Location	Distance to Sanchez (miles)	Bearing from Sanchez	NEI Hg Emissions 1999 (kg/year)[4]	TRI Hg Emissions 2003 (kg/year)[4]	TRI Hg Emissions 2006 (kg/year)[4]
Holcim (US) Inc. Portland Plant[5]	Florence, CO	69	N	NA	15.0[5]	3.6
CF & I Steel L.P	Pueblo, CO	74	N	39.6	162.4	256.7
Los Alamos National Laboratory	Los Alamos County, NM	83	SW	21.8	< 1	NA
Cripple Creek and Victor Gold Mining Co.	Victor, CO	90	N	NA	15.3	16.3
GCC Rio Grande, Inc. (cement)	Tijeras, NM	122	SW	NA	5.4	5.1
Colorado Refining Co. (now Suncor)	Denver County, CO	144	NNE	5.6	0	NA
Rocky Mountain Bottle Co.	Wheat Ridge, CO	146	N	NA	5.5	NA
Conoco Inc. Denver Refinery (now Suncor)	Adams County, CO	158	NNE	12.2	0.6	1.1
Giant Refining Ciniza Refinery	Jamestown, NM	162	SW	7.7	0.26	2.9
Cemex, Inc. - Lyons Cement Plant	Boulder County, CO	168	N	141.5	5.4	24.0
Holnam Inc. Fort Collins Plant	LaPorte, CO	192	N	5.2	1.5	NA
Total				233.6	211.4	309.7

Table 3-1, Part C. Notes

[1] 2000 generation from E-GRID2002PC database (Pechan, 2003).

[2] Emission Controls from National Emissions Database (RTI, 2001):

Group	Primary Fuel	Boiler/Furnace	PM Control	SO_2 Control	External NO_x Control
1	Bituminous	CONV/PC	ESP-CS	None	None
7	Bituminous	CONV/PC	BAGHOUSE	None	None
10	Bituminous	CONV/PC	ESP-CS	WETSCRUB	None
11	Bituminous	CONV/PC	ESP-HS	WETSCRUB	None
12	Bituminous	CONV/PC	BAGHOUSE	WETSCRUB	None
13	Subbituminous	CONV/PC	ESP-CS	Low Sulfur Coal	None
14	Subbituminous	CONV/PC	ESP-HS	None	None
15	Subbituminous	CONV/PC	BAGHOUSE	Low Sulfur Coal	None
16	Subbituminous	CONV/PC	PARTSCRUB	None	None
18	Subbituminous	CONV/PC	BAGHOUSE	SDA	None
19	Subbituminous	CONV/PC	ESP-CS	WETSCRUB	None
20	Subbituminous	CONV/PC	ESP-HS	UB	None
27	Waste Bituminous	FBC	BAGHOUSE	None	None
40	Subbituminous	FBC	BAGHOUSE	None	SNCR

[3] 2006 emission estimates from 2006 TRI (USEPA, 2008). Reactive mercury estimates determined from application of speciation data in BinTable.xls (http://www.epa.gov/ttn/atw/combust/utiltox/control2.zip, accessed 7/17/01). Data from individual plants used where reported; otherwise calculated from national average speciation by control type. Speciation data were applied to 2000 emissions to estimate reactive mercury emissions.

[4] Mercury emissions from the National Emissions Inventory (NEI; USEPA, 2004a) and the Toxics Release Inventory (TRI; USEPA, 2004b; 2008). NA indicates that either NEI or TRI did not contain emissions data for the facility.

[5] Has now ceased production and serves solely as a cement distribution terminal.

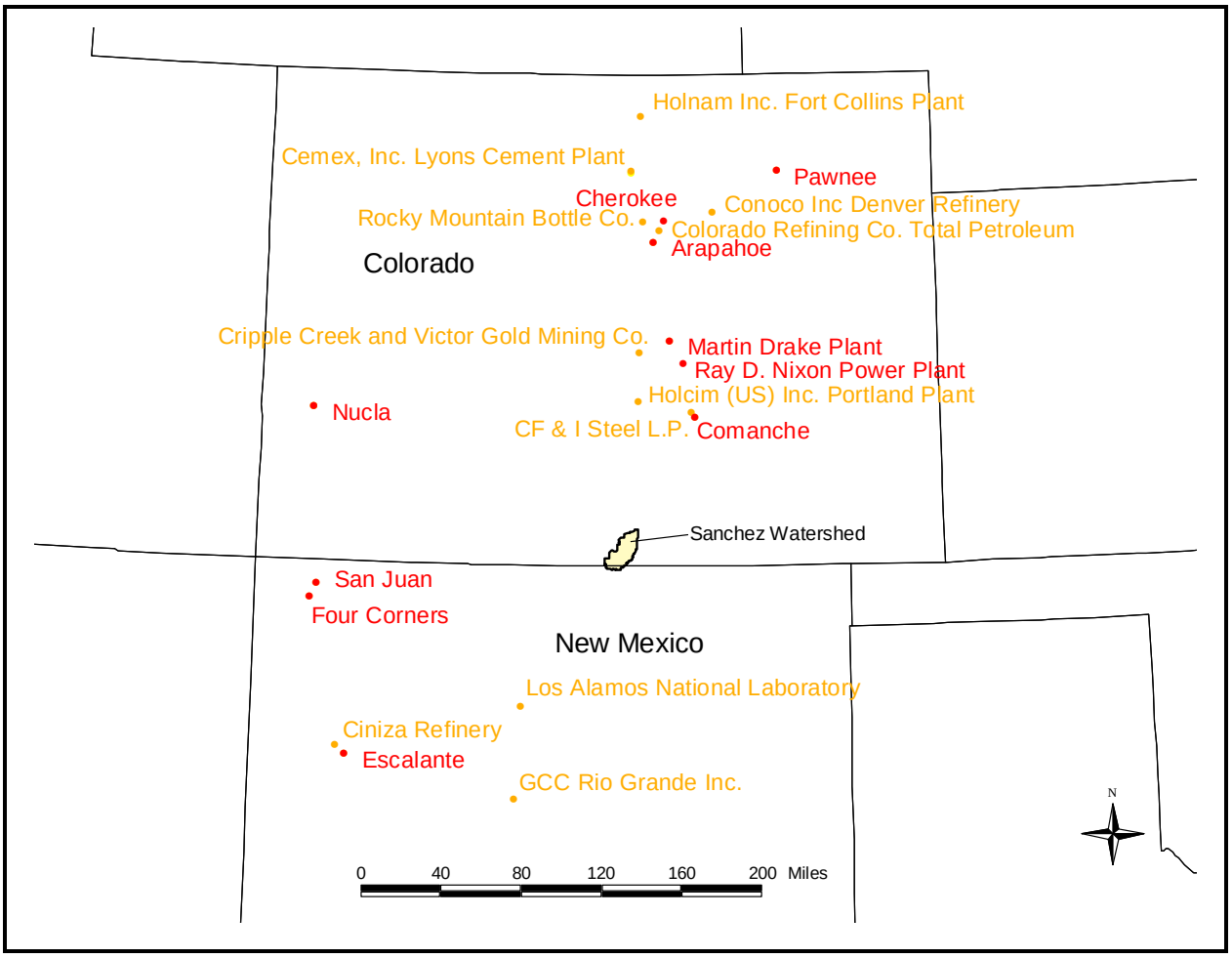

Figure 3-1. Location of Coal-Fired Electrical Generating Plants (Red) and Other Facilities (Orange) Emitting Greater than 5 kg Mercury per Year within 200 Miles of Sanchez Reservoir

3.2.2 Long-Range Atmospheric Deposition

Long-range atmospheric deposition (which creates the regional atmospheric mercury background) is a major source of mercury in many parts of the country. The long-range component is driven in large part by the transport of elemental mercury. Because of its high volatility, deposition rates of elemental mercury are low. Significant deposition occurs when elemental mercury is converted to ionic forms and also through uptake of elemental mercury by plants (see Section 3.2.4). Elemental mercury derived from both long-range and near sources determines the local concentration of elemental mercury that is available for ionization and deposition.

In a study of trace metals contamination of reservoirs in New Mexico, it was found that perhaps 80 percent of mercury found in surface waters was coming from long-range atmospheric deposition (Popp et al., 1996). In other remote areas (e.g., Wisconsin, Sweden, and Canada), atmospheric deposition has been identified as the primary (or possibly only) contributor of mercury to waterbodies (Watras et al., 1994; Burke et al., 1995; Keeler et al., 1994).

Glass et al. (1991) reported that mercury released from sources up to 2,500 km distant contributed to mercury levels in rain water deposited on remote sites in northern Minnesota. Studies of mercury contamination of soil have been correlated with regional-scale transport and deposition, with an

increasing mercury gradient from west to east in the United States associated with the degree of regional industrialization (Nater and Grigal, 1992).

In a recent application of a simplified global mercury transport model, Seigneur et al. (2004) concluded that in the area of Narraguinnep Reservoir in southwestern Colorado the largest anthropogenic contribution of mercury (27 percent) derived from South Asia, while North American direct anthropogenic emissions accounted for only 14 percent of total deposition. Most of the remainder (40 percent) is attributed to "natural" re-emissions from land and oceans. It appears, however, that the analysis presented by Seigneur et al. may underestimate the rate of dry deposition of reactive gaseous mercury (see Section 3.2.4).

USEPA has undertaken several national-scale modeling efforts to characterize mercury deposition. For the 1997 Report to Congress, EPA developed the Regional Lagrangian Model of Air Pollution (RELMAP) modeling (USEPA, 1997, Section 5.1.3) to produce gridded estimates of deposition rates. The report included comparisons between wet deposition of mercury from local anthropogenic sources and a global-scale background concentration. While the RELMAP modeling is now believed to be outdated and does not fully reflect the current state of understanding of atmospheric chemistry leading to deposition of mercury (personal communication, O. Russell Bullock, USEPA, to J. B. Butcher, Tetra Tech, 7/25/2001), these results suggested that the deposition of mercury in southwestern Colorado has a strong global or long-range component.

The RELMAP modeling had considerable uncertainty, particularly for the Southwest, where monitoring data were scarce and dry deposition of mercury may play a larger role. The broad-scale RELMAP modeling also could not take into account the effects of local topography on deposition, nor does it account for the interaction of chloride ions in power plant emissions with elemental mercury to form species such as mercuric chloride that are subject to more rapid deposition. EPA subsequently developed a more sophisticated regional mercury transport model (Community Multiscale Air Quality (CMAQ-Hg)) based on the Models-3/CMAQ system (Byun and Ching, 1999), which incorporated a more sophisticated representation of mercury chemistry. In support of the Clean Air Mercury Rule, the CMAQ-Hg model was used to predict mercury deposition for the 2001 base case on a 36x36 km model grid (USEPA, 2005). Grid-scale results of the 2001 base case application were made available to this project (personal communication, Tom Braverman, USEPA RTP to Kathryn Hernandez, USEPA Region 8, 8/29/2005). The Sanchez watershed falls within two cells of the CMAQ output (Column 56, rows 50 and 51), for which the 2001 total Hg deposition estimates are 15.41 and 14.81 g/km^2/yr, respectively, for an average of 15.11 g/km^2/yr. The CMAQ model simulates this loading as primarily occurring through dry deposition, with 2.94 g/km^2/yr wet and 12.17 g/km^2/yr dry deposition (80 percent dry deposition).

An additional run of the CMAQ model was undertaken for 2002 conditions, with alterations to the functional description of processes leading to the dry deposition of mercury. The 2002 CMAQ results were also made available for the TMDL (personal communication from O. Russell Bullock, USEPA to J.B. Butcher, Tetra Tech, 4/24/2008). The total deposition rates reported for the two CMAQ cells covering the watershed were 27.39 g/km^2/yr and 25.88 g/km^2/yr (average of 26.64 g/km^2/yr). The average wet deposition rate was 3.12 g/km^2/yr (12 percent of the total), and the average dry deposition rate was 23.52 g/km^2/yr (88 percent of the total). The two simulations predict similar rates of wet deposition, but dry deposition is nearly twice as high in the 2001 simulation.

USEPA has also sponsored national-scale mercury modeling using ICF's Regional Modeling System for Aerosols and Deposition (REMSAD). One important feature of REMSAD is source tagging, which enables attribution of the sources of mercury deposition at a site. This analysis estimated total mercury deposition in the Sanchez Reservoir watershed to range from 7.81 to 10.99 g/km^2/yr. Global background sources contributed over 97 percent of the deposition to the Sanchez Reservoir for this model run (ICF, 2006). REMSAD estimates of total deposition are lower than those from CMAQ because REMSAD simulates less dry deposition. This is believed to be due to slower deposition velocities as well as less

vertical mixing under convective conditions (personal communication from O. Russell Bullock, USEPA to J.B. Butcher, Tetra Tech, 5/8/2008).

For this project, independent estimates of wet and dry deposition were calculated based on direct and indirect measurements, prior to obtaining the CMAQ and REMSAD results. These estimates, described in the following sections, are in excellent agreement with the CMAQ 2001 base case results, which represent the mid-range of the values estimated by the three studies cited above.

3.2.3 Mercury Wet Deposition Monitoring

The National Mercury Deposition Network (MDN) monitors wet deposition of mercury at a number of locations around the U.S. Prior to late 2001 only one location was in Colorado with no others nearby. This is the Buffalo Pass station (CO97), located in northern Colorado, which has been operational only since October 1998. During the complete monitoring year of 1999, the average volatile wet mercury deposition concentration at this station was 9.75E-03 µg/L.

Because the MDN sites were not located near the southern Colorado region where several lakes have elevated fish tissue concentrations of mercury, Tetra Tech suggested installing a MDN site in Mesa Verde, Colorado to provide more accurate estimates. The new MDN site at Mesa Verde (CO99, Figure 3-2) was installed in 2001 and became operational in December 2001. Weekly observed mercury concentrations in rainfall are shown in Figure 3-2.

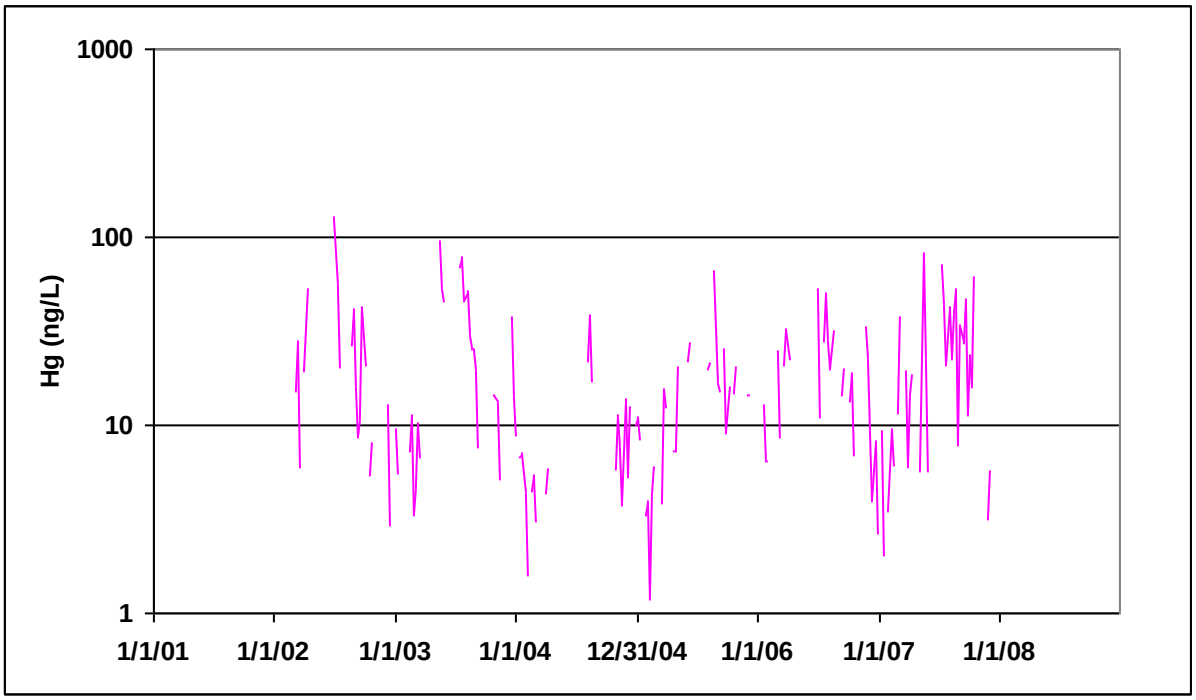

Figure 3-2. Weekly Mercury Concentrations in Rainfall at Mesa Verde, CO

Although mercury deposition data at Mesa Verde were not collected until 2001, this site has also been a National Atmospheric Deposition Program (NADP) site since 1981, collecting wet deposition data for sulfate, nitrate, and other chemicals. The NADP (http://nadp.sws.uiuc.edu/mdn/) maintains a relatively dense array of sites in Colorado, as shown in Figure 3-3. Data were obtained for seven active sites, mostly located in western Colorado (CO00, CO19, CO91, CO96, CO97, CO98, and CO99). CO97 is also

the Buffalo Pass MDN station (Figure 3-3). Records from these seven stations for 1990–1998 were previously used as surrogates to estimate general deposition rates of pollutants associated with coal-fired boilers in southwestern-southcentral Colorado (Tetra Tech, 2001).

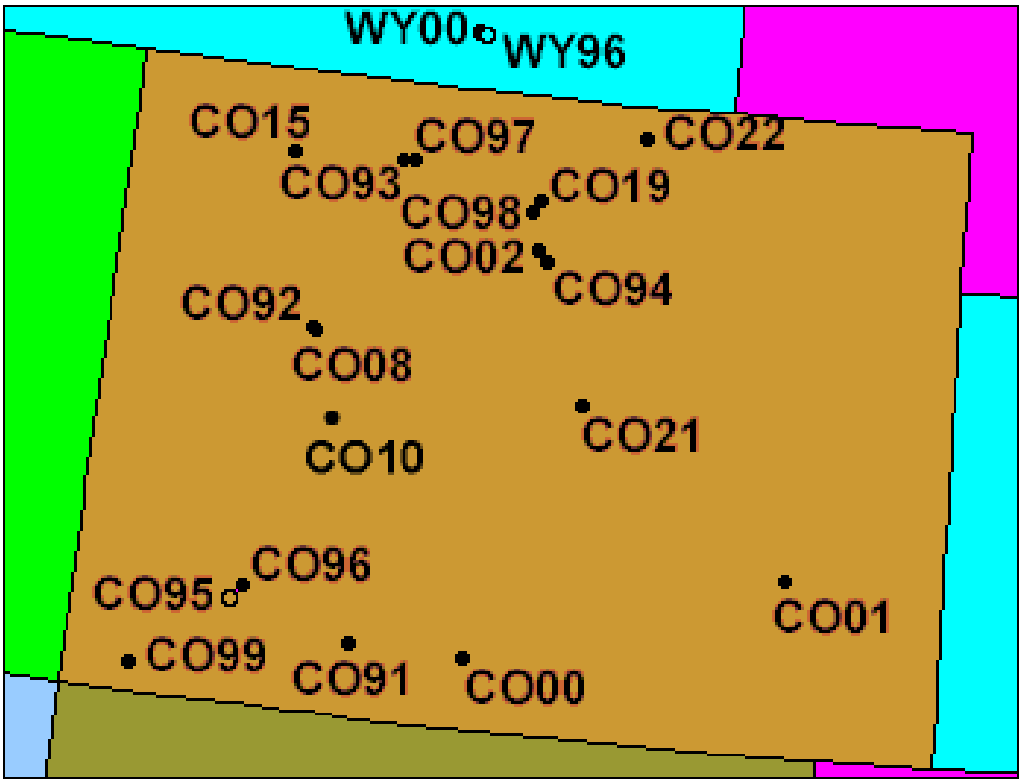

Figure 3-3. National Atmospheric Deposition Program Sites in Colorado

Sulfate and NOx deposition rates exhibit a significant elevation effect in the Rockies, with higher deposition at lower altitudes. This elevation effect must be taken into account in transferring results to other locations. In addition, there have been temporal changes reflecting emission reductions in SO_4 under Clean Air Act requirements and an increasing trend with time for NOx.

In western Colorado, the recent NADP data show a decreasing trend with time for SO_4 and an increasing trend with time for NO_3 deposition. The NADP data do not reveal a spatial gradient in Colorado that is not explained by elevation.

The following cross-sectional models were previously derived from the NADP data (Tetra Tech, 2001):

$$LN(SO_4) = 8.0934 - 1.1243 \cdot LN(Elevation) + 0.06237 \cdot LN(Year), \quad R^2 = 0.404$$

$$LN(NO_3) = 6.6828 - 0.9041 \cdot LN(Elevation) + 0.03764 \cdot LN(Year), \quad R^2 = 0.411,$$

where SO_4 and NO_3 are volume-weighted mean concentrations of sulfate and nitrate in mg/L and elevation is in meters.

Weekly sulfate and nitrate concentrations collected at Mesa Verde are shown in Figure 3-4 and Figure 3-5. Annual volume weighted mean concentrations are shown in Figure 3-6 and Figure 3-7. Sulfate concentrations at both scales appear to decrease with time while nitrate concentrations have remained fairly constant.

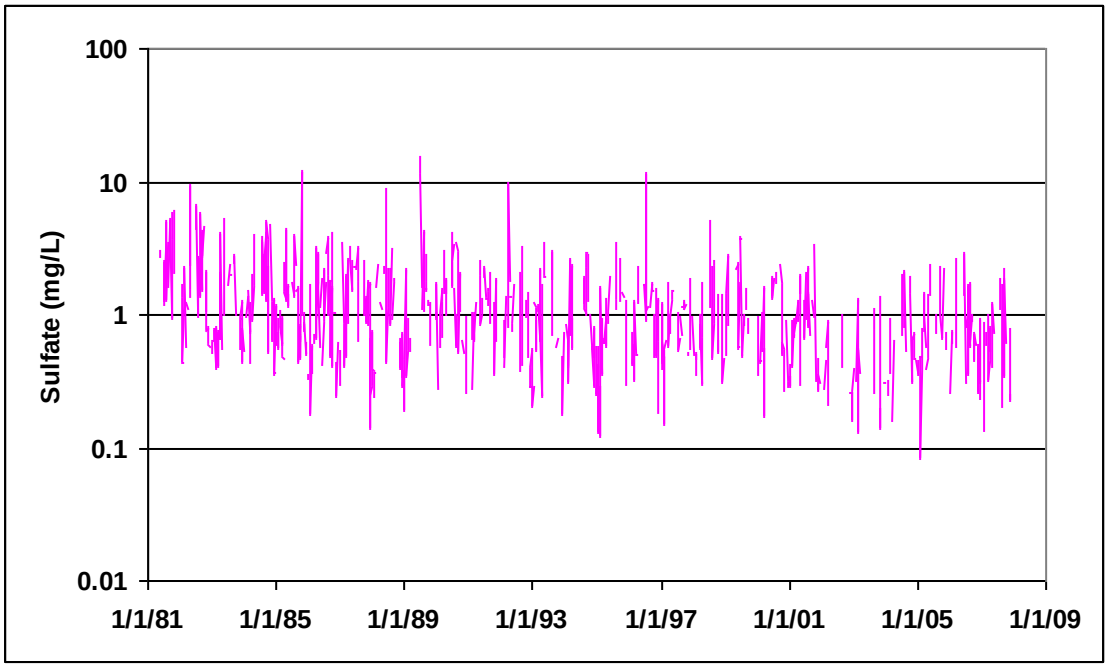

Figure 3-4. Weekly Sulfate Concentrations in Rainfall at Mesa Verde, CO

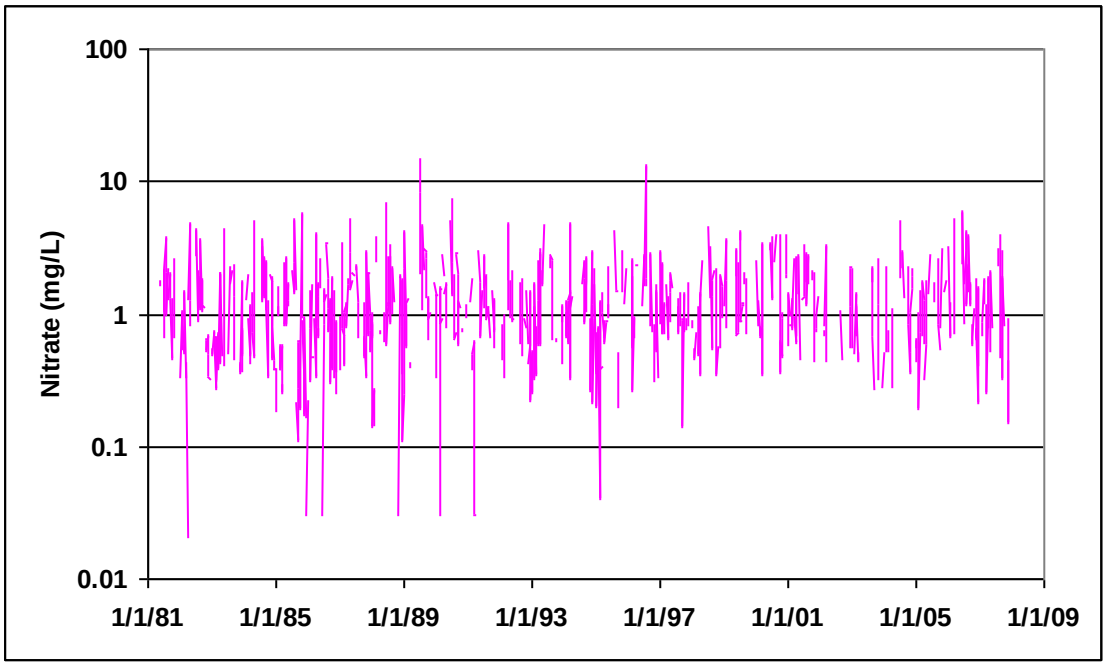

Figure 3-5. Weekly Nitrate Concentrations in Rainfall at Mesa Verde, CO

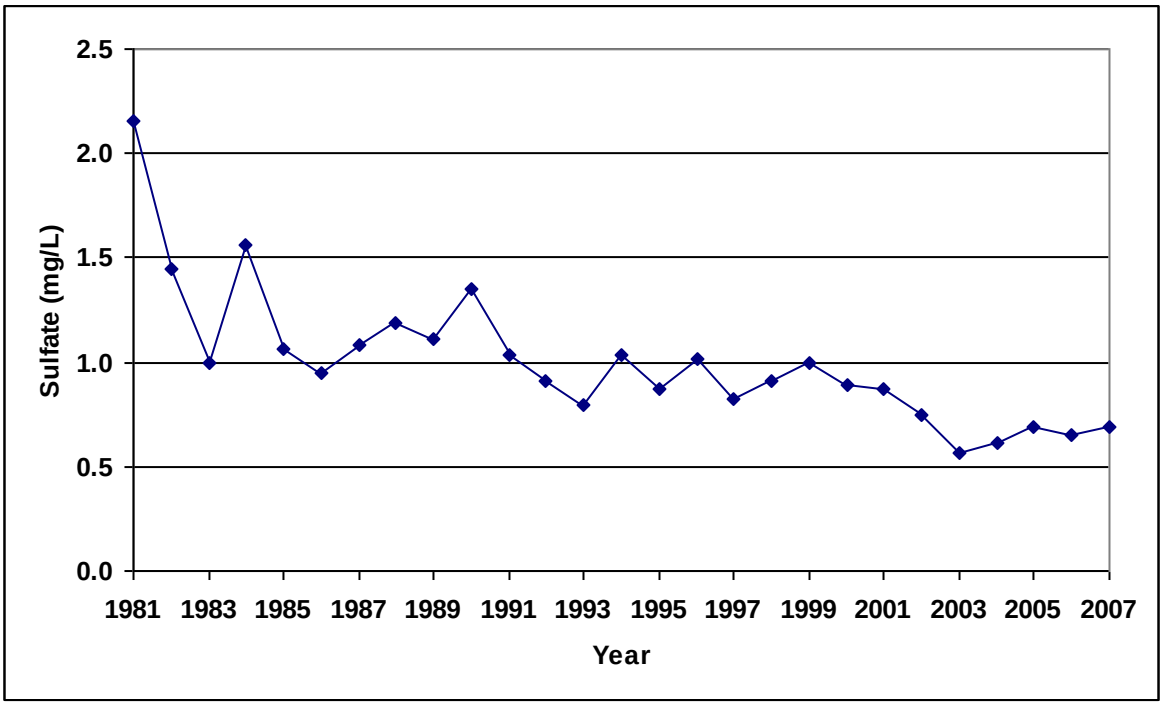

Figure 3-6. Annual Volume Weighted Mean Sulfate Concentrations at Mesa Verde

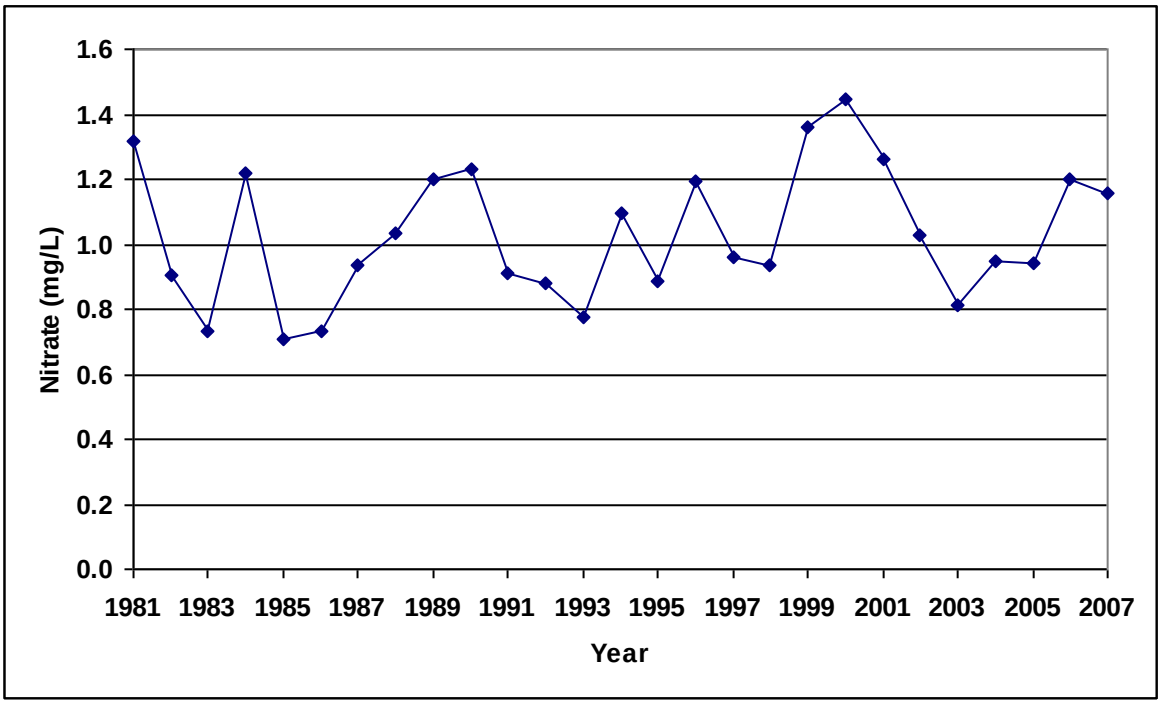

Figure 3-7. Annual Volume Weighted Mean Nitrate Concentrations at Mesa Verde

Various regressions of mercury as a function of nitrate or sulfate were compared to determine which method provided the best estimate of mercury concentrations. In an earlier analysis (Tetra Tech, 2006), mercury deposition data at Mesa Verde were only available from 2001 through 2004. Figure 3-8 shows the correlation of mercury concentration to nitrate concentration, and Figure 3-9 shows the correlation to sulfate for this period. The R^2 values for the nitrate and sulfate regressions are similar though sulfate has a better fit to observed data. The apparent strength of these regressions is largely determined by the high leverage associated with one observation with very high mercury, nitrate, and sulfate concentrations.

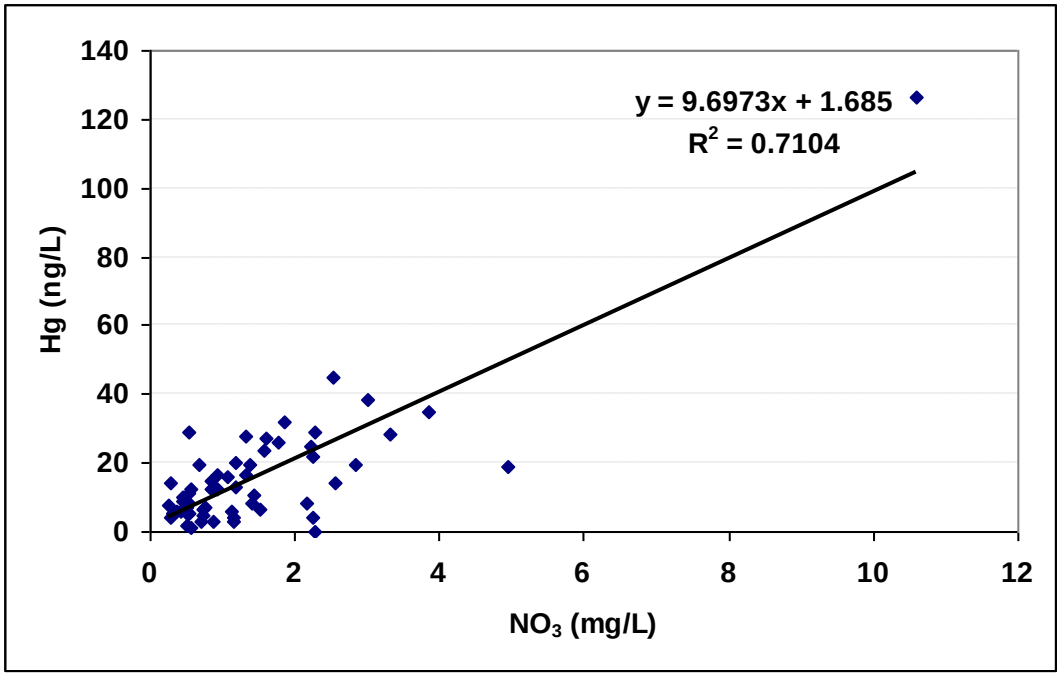

Figure 3-8. Correlation of Mercury and Nitrate Concentration in Wet Deposition at Mesa Verde MDN Site, 2001-2004

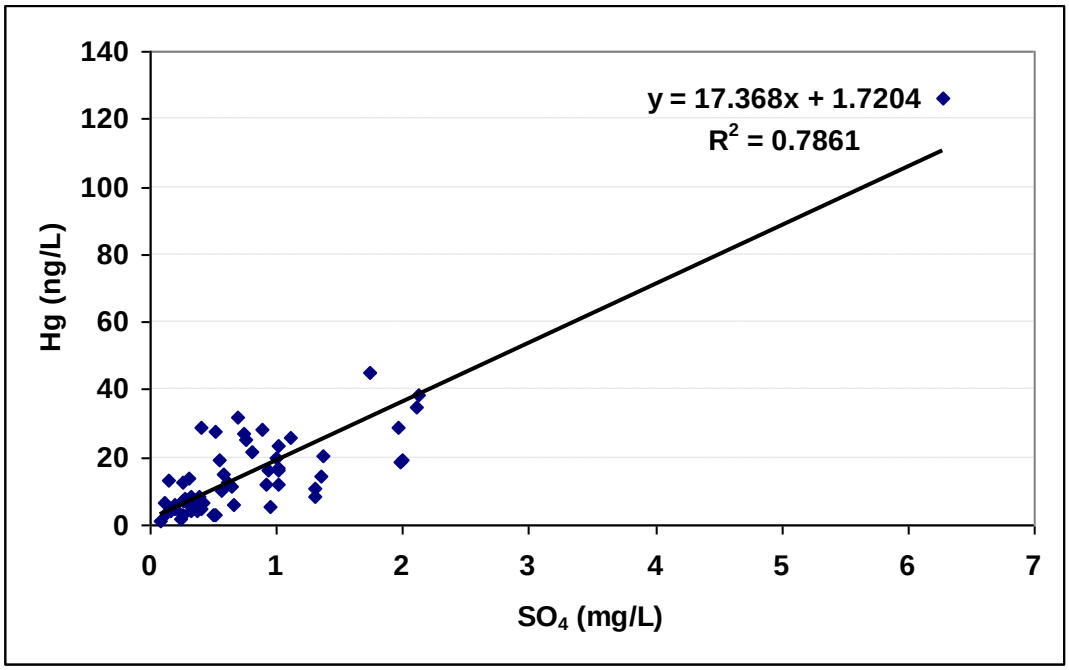

Figure 3-9. Correlation of Mercury and Sulfate Concentration in Wet Deposition at Mesa Verde MDN Site, 2001-2004

When the regression is performed with extended data collected through 2007, the R^2 decreases for both the NO_3 and SO_4 regressions because the impact of the outlier is diluted. Figure 3-10 and Figure 3-11 show the regression of mercury concentration for the period of record at Mesa Verde. Both equations have an R^2 value of approximately 0.41.

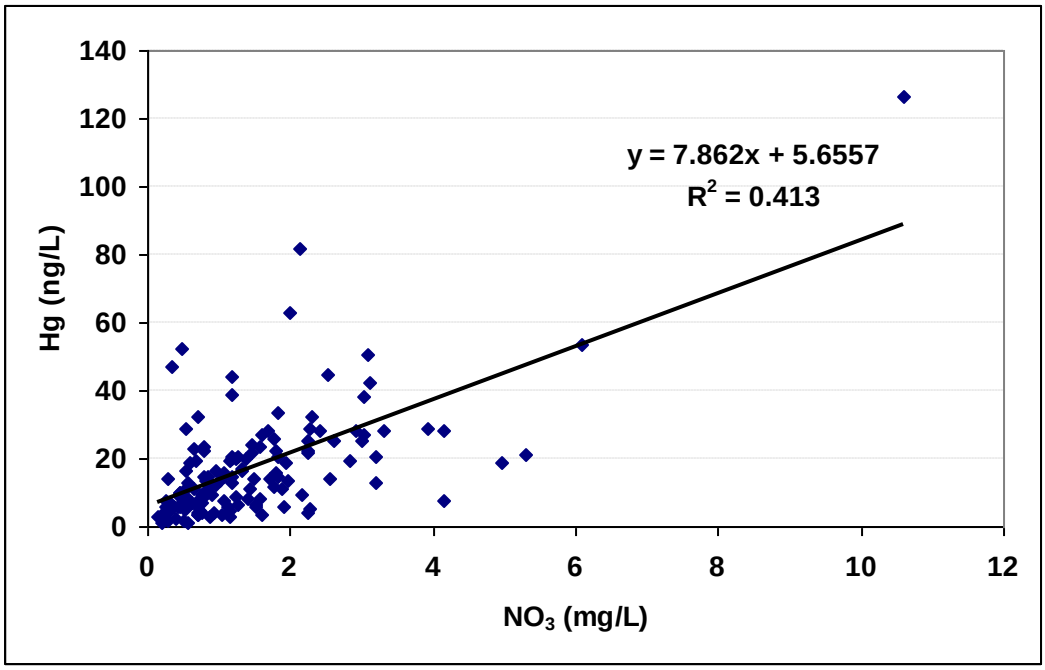

Figure 3-10. Correlation of Mercury and Nitrate Concentration in Wet Deposition at Mesa Verde MDN Site, 2001-2007

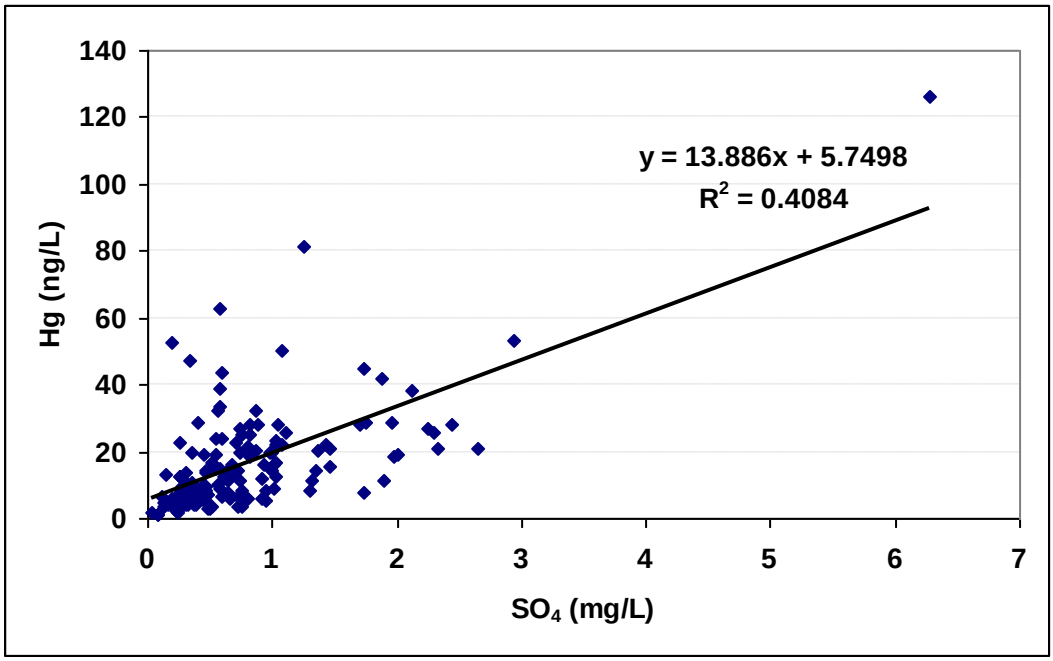

Figure 3-11. Correlation of Mercury and Sulfate Concentration in Wet Deposition at Mesa Verde MDN Site, 2001-2007

Given that NO_3 and SO_4 are near-equally significant in predicting mercury concentrations, a regression on both variables was chosen as a basis for inferring likely mercury deposition based on measured acid deposition. Based on the earlier work, a log-log regression is preferable for these data. For weeks where nitrate, sulfate, and mercury data were available at Mesa Verde, a logarithmic regression of mercury concentration on nitrate and sulfate concentration was created:

$$LOG_{10}(Hg, ng/L) = 1.175 + 0.286\ LOG_{10}(NO_3, mg/L) + 0.457\ LOG_{10}(SO_4, mg/L),\ R^2 = 42.1\%.$$

The regression was then combined with rainfall depth to predict wet mercury deposition at Mesa Verde. Figure 3-12 compares the estimated and observed weekly deposition rates.

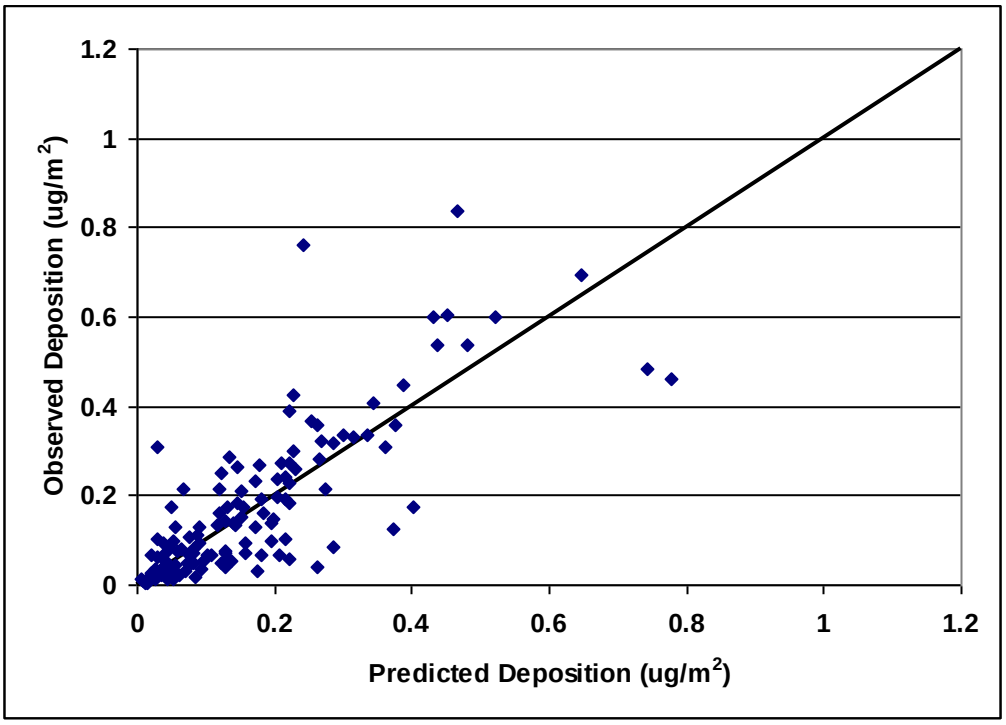

Figure 3-12. Comparison of Observed and Predicted Weekly Mercury Wet Deposition Rates at Mesa Verde (R^2 = 0.65)

The regression on nitrate and sulfate provides a reasonable basis to extend estimates of mercury concentration and deposition at Mesa Verde back in time. Annual volume weighted mean concentrations of mercury in wet deposition are shown in Figure 3-13, using the regression equation for 1982-2001 and observed MDN data for 2002-2007.

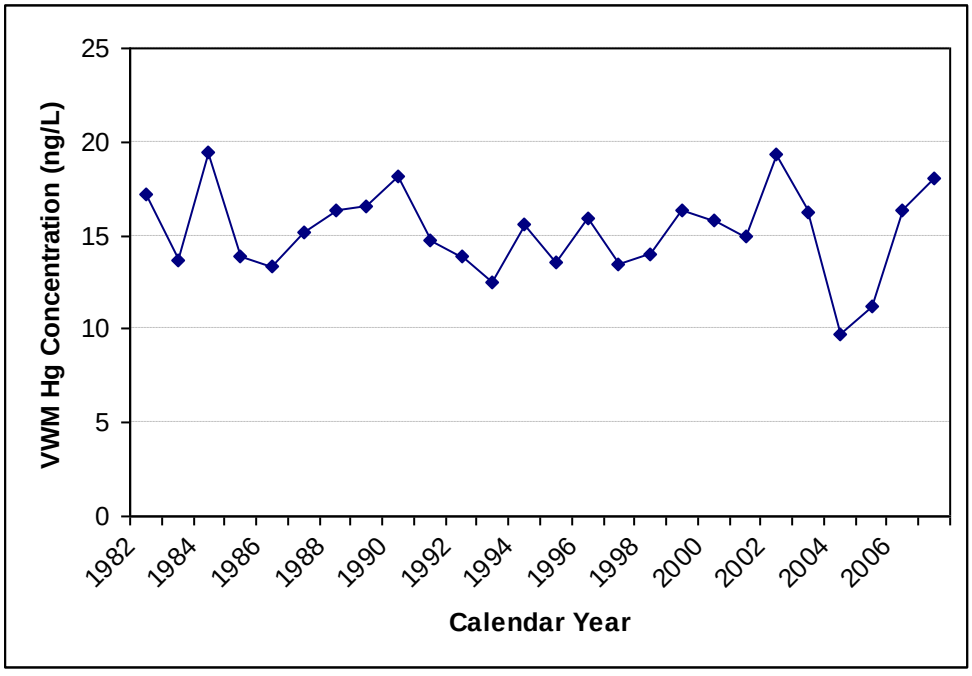

Figure 3-13. Annual Volume Weighted Mean Mercury Concentrations in Wet Deposition at Mesa Verde (MDN Data for 2002-2007, Predicted for 1982-2001)

In contrast, observed and predicted annual mercury wet deposition rates show a strong downward trend over time at Mesa Verde (Figure 3-14). This trend, however, is almost entirely due to a downward trend in annual precipitation, combined with approximately constant volume weighted mean concentrations. The average annual estimated wet deposition rate of mercury for 1990-2007 is 5.78 µg/m^2/yr.

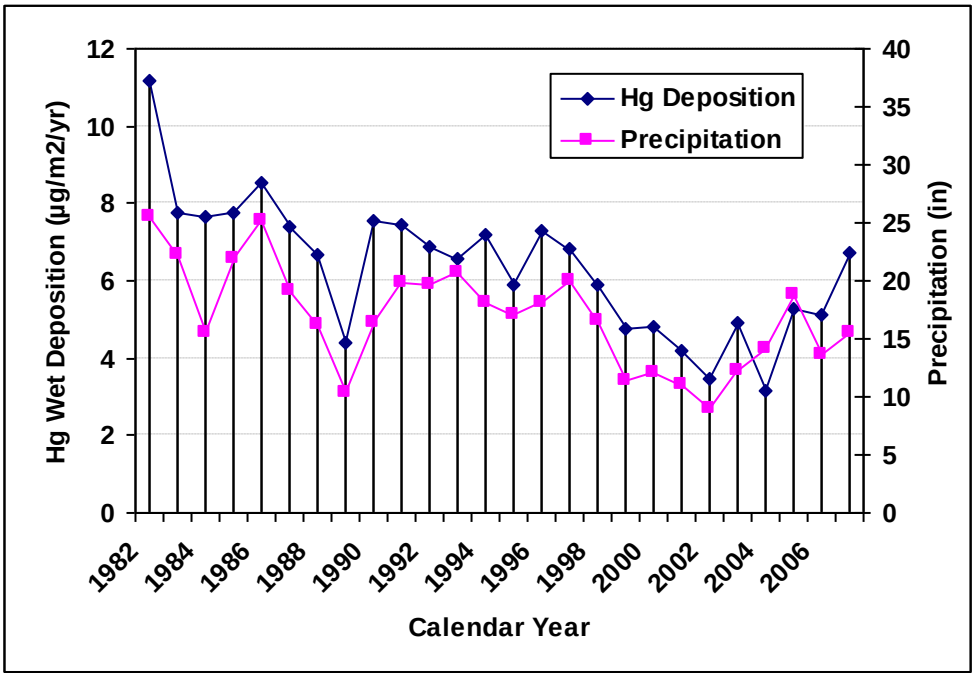

Figure 3-14. Estimated Mercury Wet Deposition Rates and Annual Precipitation at Mesa Verde (MDN Data for 2002-2007, Predicted for 1982-2001)

Based on the results for Mesa Verde, similar methods can be used to estimate mercury wet deposition rates in the area of Sanchez Reservoir. NADP data are available near Sanchez at Alamosa, Colorado (CO 00; elevation 2,298 m). These data were downloaded and corrected for the elevation at Sanchez Reservoir (elevation 2,530 m). The regression equation for Mesa Verde was then used to predict annual volume weighted concentrations of mercury in wet deposition at Sanchez Reservoir (Figure 3-15). As at Mesa Verde, nitrate, sulfate, and predicted mercury concentrations appear to have declined in the 1980s, but have been fairly stable since. The average predicted volume weighted mercury concentration for 1990-2006 is 0.011 µg/L.

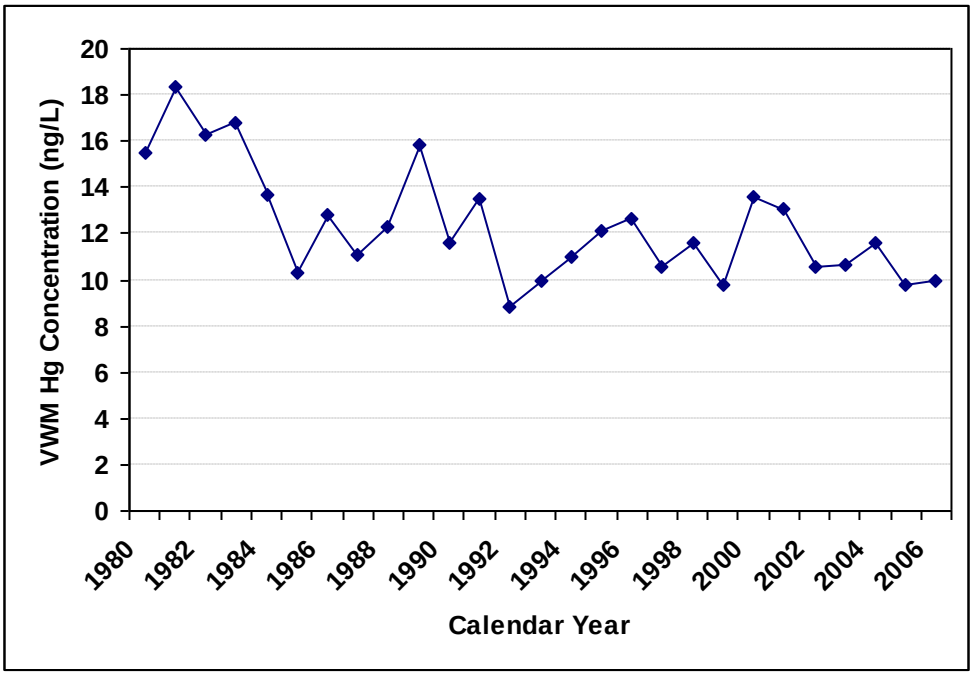

Figure 3-15. Annual Volume Weighted Mean Mercury Concentrations in Wet Deposition at Sanchez Reservoir (Predicted from Alamosa Sulfate and Nitrate Deposition Data)

The estimates of mercury concentration can be combined with measured annual precipitation at the San Luis 1 SE cooperative summary-of-the-day weather station, near Sanchez, to provide estimates of annual mercury wet deposition rates at the reservoir. Unfortunately, this weather station has significant periods of missing data, making year-by-year estimates difficult. The Western Regional Climate Center, however, estimates that the average annual rainfall at this station (based on 1971-2004 data) is 10.16 inches (258 mm). Combining this rainfall depth with the 1990-2006 average estimated volume weighted mercury concentration of 0.011 µg/L yields an estimated average mercury wet deposition rate of 2.90 $\mu g/m^2/yr$ (very close to that estimated by 2001 CMAQ results – 2.94 $\mu g/m^2/yr$). Thus, it appears likely that direct atmospheric wet deposition of mercury at Sanchez is about half that seen at Mesa Verde. It should be noted, however, that the MDN measurements record wet deposition of mercury only, and, in the more arid climate at Sanchez Reservoir, dry deposition may represent a greater fraction of the total mercury deposition load than at Narraguinnep.

The association of mercury wet deposition rates with nitrate and sulfate deposition implicitly assumes a relationship between combustion sources and atmospheric mercury load. In fact, elemental mercury may be transported globally, more or less independently of nitrate and sulfate, and be converted to reactive form by atmospheric chemical processes. While such global sources undoubtedly contribute a part of the load in the Mesa Verde area, the evidence suggests a portion of the local mercury deposition may be associated with coal fired power plants.

Partly in response to the controversies surrounding estimates of atmospheric deposition of mercury in southwest Colorado, the U.S. Geological Survey (USGS) collected and analyzed four high-resolution sediment cores from Narraguinnep Reservoir in southwestern Colorado in 2000-2002 (Gray et al., 2005). The cores were dated by ^{137}Cs methods, allowing calculation of sedimentation rates. Present day (surficial) mercury concentrations in these cores range from 0.035 to 0.050 mg/kg. All four cores appear to show an increase in concentration and mercury deposition rates during the 1970s, coincident with the increase in coal-fired power production in the Four Corners area. The authors infer: "Spatial and

temporal patterns of Hg fluxes for sediment cores collected from Narraguinnep Reservoir suggest that the most likely source of Hg to this reservoir is from atmospheric emissions from coal-fired electric power plants, the largest of which began operation in this region in the late-1960s and early 1970s."

For 1992-2002, Gray et al. estimated mercury accumulation rates in their Narraguinnep cores ranging from 28 to 57 ng/cm^2/yr (equivalent to 280 to 570 µg/m^2/yr). These accumulation rates are an order of magnitude greater than the whole-lake loading atmospheric deposition rates of 35 µg/m^2/yr estimated by Tetra Tech (2001, Table 4-11), normalized to the full lake area, and much greater than the direct atmospheric wet deposition rates for mercury measured at Mesa Verde. Deposition rates in dateable cores are not, however, equivalent to whole lake loading rates, and indeed should be greater. This is because a useful, dateable core must come from an area where sediment accumulates at a relatively consistent rate, without subsequent disturbance. Such cores thus tend to represent areas of focused sedimentation, and thus do not directly measure loading to the whole lake.

3.2.4 Dry Deposition of Mercury

Although there are few direct measurements to support well-characterized estimates, dry deposition of mercury often is assumed to be approximately equal to wet deposition (e.g., Lindberg et al., 1991; Lindqvist et al., 1991). This assumption is not always valid in the arid southwest. Dry and wet deposition were measured in the Pecos River basin of eastern New Mexico in 1993–1994 (Popp et al., 1996). Average weekly deposition rates were calculated to be 140 ng/m^2-wk of mercury from dry deposition and 160 ng/m^2-wk of mercury from wet deposition. These data demonstrate the importance of both dry and wet deposition as sources of mercury. Early throughfall studies in a coniferous forest indicate that dry deposition beneath a forest canopy could be on the order of 50 percent of the wet deposition signal (Lindqvist et al., 1991). However, the local university cooperator at the Caballo, NM MDN station (NM10) estimated dry deposition as up to six times wet deposition at this arid site (Caldwell et al., 2003).

Atmospheric dry deposition involves three groups of mercury species: reactive gaseous mercury (RGM), aerosol particulate mercury (Hg-P), and gaseous elemental mercury (Hg(0)). All three forms may deposit to land and water surfaces, but there are significant differences in chemistry and rates. Hg(0) is the dominant species in terms of ambient concentration; however, net deposition rates are much higher for the other forms (Lindberg et al., 1992).

RGM is highly reactive, and the deposition of RGM can be treated as similar to that of nitric acid (Bullock and Brehme, 2002). For the basic Regional Atmospheric Deposition Model (RADM), deposition is a simple function of a deposition velocity, V_r (Byun and Ching, 1999), while the deposition velocity is in turn a function of three resistances (Wesley, 1989):

$$Dep = C \cdot V_r = C \cdot \left(\frac{1}{R_a + R_b + R_c} \right),$$

where C is the near-surface atmospheric concentration, R_a is the aerodynamic resistance, R_b is the quasi-laminar boundary layer resistance, and R_c is the surface or canopy resistance. Models like CMAQ (Byun and Ching, 1999) update the resistances continuously based on meteorology; however, an average value can also be assumed for scoping level analyses. The Trace Element Atmospheric Model (TEAM) mercury model (Seigneur et al., 2001) assumes constant deposition velocities, while the HgCAMx model uses fixed velocities by month (Tesche et al., 2004). Re-emission of RGM and Hg-P is relatively insignificant (Cohen et al., 2004).

Various authors have reported average deposition velocities for RGM. Lindberg and Stratton (1998) reported a value of 0.4 cm/s for grass surfaces, but 5-6 cm/s for forest. The TEAM model (Seigneur et al., 2001) uses a velocity of 0.5 cm/s, similar to Lindberg and Stratton's grass value. However, work by Caldwell et al. (2003) at Caballo, NM showed that the grass deposition velocity yielded an estimate of

RGM dry deposition that was more than an order of magnitude less than direct measurements of deposition on surrogate surfaces (although it should be noted that these surrogate surface measurements are also subject to uncertainty). Results presented in the USEPA (1997) Report to Congress, cite a value of 2.9 cm/s as an average deposition velocity for RGM across various surface types. Rea et al. (2001) derived RGM deposition velocities of 2-6 cm/s for the Lake Huron watershed, using the method of Lindberg et al. (1992). Given the results reported by Caldwell et al. (2003), a value of 4 cm/s – at the middle of the range of Rea et al. and approximately 40 percent above the USEPA (1997) average appears appropriate for scoping level analysis.

Hg-P deposition can be simulated in a manner analogous to RGM, except that behavior is usually based on analogy to sulfuric acid (Bullock and Brehme, 2002). USEPA (1997) gives deposition velocities for Hg-P in the range of 0.09 to 0.45 cm/s, depending on particle size. Lindberg et al. (1992) estimated a velocity of 0.087 cm/s during the growing season and 0.003 cm/s in the dormant period for fine aerosol. Rea et al. (2001) provide an average net deposition velocity of 0.1 cm/s for the Lake Huron watershed. Given the lack of major combustion sources immediately adjacent to the Sanchez reservoir, Hg-P appears to be a minor component of the dry deposition at Sanchez, and the value given by Rea et al. is sufficient for scoping-level analysis.

Hg(0) net direct deposition to the land surface or water is typically assumed to be negligible (Bullock and Brehme, 2002; Cohen et al., 2004) because of low reactivity and ease of re-emission. The primary indirect mechanism by which net deposition of Hg(0) occurs to the land surface is through incorporation in plant leaf tissue via stomatal vapor uptake (Eriksen et al., 2003). Lindberg et al. (1992) did develop apparent deposition velocities for Hg(0) ranging from 0.06 to 0.12 cm/s, and a value of 0.01 cm/s is used in the TEAM model (Seigneur et al., 2001; Tesche et al., 2004). Use of these values tends to overestimate the direct net deposition of Hg(0), however, because it does not account for re-emission (Miller et al., 2005). Xu et al. (1999) developed a sophisticated resistance model of net exchange of Hg(0) at the land surface, including canopy re-emission; however, the necessary parameters to employ this approach are not readily attainable. For this reason, Miller et al. (2005) developed a semi-empirical approach based on a regression analysis of foliar accumulation of mercury. The end-of-growing-season foliar accumulation in deciduous species is well approximated by

$$Hg_{foliage}(ng/g) = 0.20317 \cdot AP + 4.71 \cdot (TGM - 1.37)$$

where *AP* is the accumulation period in days and *TGM* is the total gaseous mercury concentration (ng/m^3). TGM is the sum of RGM and Hg(0); however, in most cases the concentration of Hg(0) is several orders of magnitude greater than RGM, so TGM is essentially equal to Hg(0).

The accumulation period can be estimated as a function of climate as

$$AP = 83.4 + 6.2 \cdot MAT$$

in which *MAT* is the mean annual temperature in Celsius. For the Sanchez watershed, with a mean annual temperature of 6.6 ºC, *AP* is approximately 124 days.

Concentrations of mercury in evergreen foliage tend to be higher than deciduous foliage due to the longer needle lifespan of evergreens. Rasmussen (1995) found that mercury concentrations in fir and spruce needles increased by 5-10 µg/kg in the year after foliage formation. Needles may persist for four years or more, but the population is usually skewed toward the younger generation. Further, the forests in the Sanchez watershed, while predominantly evergreen, also contain a mix of deciduous species such as aspen and willow. Therefore, an adjustment factor of +10 µg/kg seems appropriate as a first approximation for the forested portions of the watershed, while no evergreen adjustment is needed for the non-forested areas.

Given foliar Hg concentration, the net contribution to the soil system can be estimated simply by multiplying by the annual leaf fall mass (or, for deciduous and annual species, the maximum annual leaf

biomass). Direct measurements of leaf fall mass are not available for the Sanchez watershed. Miller et al. (2005) report mean leaf yields up to 3.7 MT/ha/yr, but contributions are likely to be considerably less in the arid climate of southern Colorado. They will also vary by vegetation type. Measurements reported in Binkley et al. (2003) suggest that a value of 1.77 MT/ha/yr is appropriate for spruce/fir in Colorado. From Walker et al. (1994), the annual foliar production of alpine grasses is about the same order of magnitude. Lower elevation semiarid grasslands likely produce on the order of 1 MT/ha/yr (Risser and Mankin, 1986).

Data on near-surface atmospheric concentrations of mercury in the Sanchez watershed are extremely limited. Results of one week of continuous monitoring near the reservoir in August 2003 (D. Krabbenhoft, USGS, personal communication to J. Butcher, Tetra Tech, 7/25/2005) produced average values of 10.5 pg [picograms]/m^3 RGM, 9.6 pg/m^3 Hg-P, and 1.62 ng/m^3 Hg(0). Concentrations could well be very different at other times or at other locations in the watershed – but they do provide a starting point for assessing the relative magnitudes of different depositional processes. Use of these concentration values yields deposition rates (g/km^2/yr) of 13.27 for RGM, 0.30 for Hg-P, 3.63 for Hg(0) to Southwestern range cover, and 4.65 for Hg(0) to spruce-fir cover.

3.2.5 Summary of Mercury Deposition Estimates

Results of the dry deposition estimates are summarized in Table 3-2. The table also shows the wet deposition estimate from Section 3.2.3, and the resulting total deposition rates.

Table 3-2. Summary of Mercury Deposition Estimates for Sanchez Watershed

	Air Concentration (ng/m^3)	Deposition Velocity (cm/s)	Hg Loading (g/km^2/yr)
Dry Deposition by Component			
RGM	0.0105	4.0	13.27
Hg-P	0.0096	0.1	0.30
Hg(0)-spruce/fir/alpine	1.62	foliar model	4.65
Hg(0)-Southwestern range	1.62	foliar model	3.63
Hg(0)-water	1.62	~0 (net)	0.00
Total dry deposition (land), including foliar uptake			17.92
Total dry deposition (water)			13.57
Wet deposition			2.90
Total deposition (land)			20.82
Total deposition (water)			16.47

The total mercury deposition rates estimated in the table (17-21 g/km^2/yr) are in close agreement with the CMAQ model predictions for the 2001 base case of about 15 g/km^2/yr, which were generated independent of the analysis presented above. Dry deposition and wet deposition estimates are also within 2 g/km^2/yr of the CMAQ estimates for 2001.

These calculations suggest that wet deposition constitutes only a small fraction of the total Hg deposition in the Sanchez watershed – 18 percent of the direct deposition to the lake and 14 percent of the deposition to the land surface. Similarly, the CMAQ model estimates indicate that 20 percent of the deposition to the watershed occurs as wet deposition. Further, the dry deposition appears to be dominated by RGM deposition, despite its low atmospheric concentration. Caldwell et al. (2003) found similar results for the Caballo, NM site, where wet deposition was estimated to constitute 14.5 percent of the total mercury

deposition, based on direct measurements of RGM to a surrogate surface. Foliar deposition of Hg(0) accounts for about a quarter of the dry deposition and 21 percent of the total Hg deposition to land. In contrast, Miller et al. (2005) found that wet deposition, RGM dry deposition, and foliar deposition each contributed about a third of the total deposition in the much wetter and more heavily vegetated climate of the northeastern US.

Seigneur et al. (2004) published a global analysis of mercury deposition rates and source attributions using the TEAM model. His results are comparable to ours for wet deposition; however, the dry deposition estimates differ significantly despite model predictions of RGM concentrations that are similar to those observed at Sanchez (Seigneur et al. appear to estimate a flux of less than 5 g/km^2/yr dry deposition for the Sanchez area). The discrepancy is mostly due to the low estimate of RGM deposition velocity used in the TEAM model, and is similar to the discrepancy between observed RGM deposition and estimated deposition, using a deposition velocity similar to that in TEAM, reported by Caldwell et al. (2003).

The analysis of Seigneur et al. (2004) thus appears to underestimate the contribution of dry deposition of RGM in the arid southwest while increasing the relative importance of dry deposition of Hg(0). This is important to the source attribution presented by Seigneur et al., which estimates that 27 percent of the deposition in southwestern Colorado (McPhee/Narraguinnep area) is due to Asian sources, 40 percent is due to "natural" sources (including Hg(0) re-emissions), and only 14 percent is due to North American anthropogenic sources. Hg(0) has a much longer half-life in the atmosphere than RGM. Thus, underestimation of the RGM contribution to total mercury deposition would in turn lead to an underestimation of the importance of more local sources that emit RGM.

Despite the presence of some questionable assumptions in the work of Seigneur et al. (2004), the general conclusion that only a small fraction of the mercury deposition in southern Colorado is due to US power plant emissions under current conditions appears to be valid. As part of the modeling analyses for the Clean Air Mercury Rule, USEPA (2005) conducted a run with a "zero-out" of all mercury from US power plants. Results of this scenario (see also Figure 4 in USEPA, 2005) show that the resulting decrease in total mercury deposition in the Sanchez watershed for 2001 following cessation of all power plant emissions would be only about 0.1 g/km^2/yr, or less than a one percent decrease in the modeled deposition rate for Sanchez. The small difference in the two scenarios also suggests that near-field deposition from regulated emitters to the Sanchez watershed is not significant. Similarly, applications of the REMSAD model (ICF, 2006) suggest that 97 percent of the deposition of mercury to the Sanchez watershed is derived from the global atmospheric mercury pool.

3.2.6 Snowpack Monitoring

Much of the flow in the Sanchez watershed derives from the high elevation snowpack. Snow can store both wet and dry deposition of mercury, and it was speculated that snowpack storage and release of atmospheric mercury might be a significant source of mercury release during spring runoff. Mercury concentrations present in snowpack represent an integrated measure of the combined effects of net wet and dry deposition over the snow season.

USGS conducted research on snowpack chemistry across the Rocky Mountain range in 2002 (Ingersoll et al., 2004) and 2003 (personal communication, George P. Ingersoll, USGS, to Kathryn Hernandez, USEPA Region 8, 10/3/2005), including several sites in southern Colorado and northern New Mexico. Several parameters were sampled, including total mercury, nitrate, and sulfate. One of the sites in 2002 was located in the Sanchez watershed at Culebra, Colorado and had a total mercury concentration of 3.9E-03 µg/L; concentrations at two other nearby sites were 3.6E-03 µg/L and 0.012 µg/L. In 2003, total mercury concentrations at the two nearby sites ranged from 2.0E-03 µg/L to 2.5E-03 µg/L but the Culebra site was not sampled. Concentrations at six sites in southwestern Colorado sampled in 2002 and 2003 ranged from 3.6E-03 µg/L to 0.012 µg/L. Similar concentrations have been measured by the Mountain

Studies Institute at the Molas Pass station: concentrations of mercury in snowpack ranged from 3.0E-03 to 0.011 µg/L at this site (Nydick, 2008).

Long-term trends of mercury concentrations in snowpack could not be assessed since total mercury had been sampled only since 2002. However, the researchers found that total mercury concentrations in snowpack were generally comparable to weekly precipitation mercury samples taken at MDN sites. These results suggest that snowmelt is an important source of overall mercury loading to the reservoir.

Nitrate and sulfate in the 2002 snowpack data (as microequivalents per liter) were positively correlated to total mercury in the southern Colorado/northern New Mexico region. In separate regressions of total mercury on sulfate and nitrate, sulfate accounts for 46 percent of variation in total mercury (R^2 = 0.46; p <0.05) and nitrate accounts for 36 percent of variation in total mercury (R^2 = 0.36; p <0.05). In both regressions, the Culebra snowpack mercury concentration lies below the predicted concentration, as shown in Figure 3-16 and Figure 3-17. It should be noted that the Taos Ski Valley, NM site, with a snowpack mercury concentration of 0.012 µg/L, strongly influences the sulfate-mercury relationship, and when the Taos Ski Valley site is removed, the relationship is not significant (p>0.05). Similarly, the nitrate-mercury relationship is not significant when the Taos Ski Valley site and the Monarch Pass, CO site (9.6E-03 µg/L mercury) are removed.

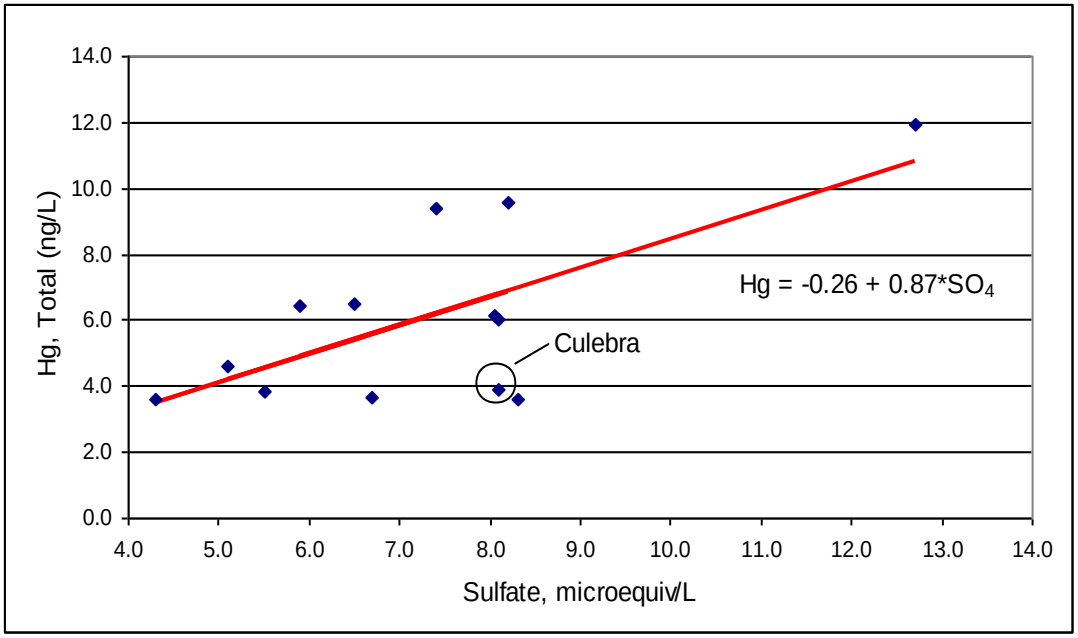

Figure 3-16. Regression of Total Mercury Concentration on Sulfate Concentration in 2002 Snowpack Data

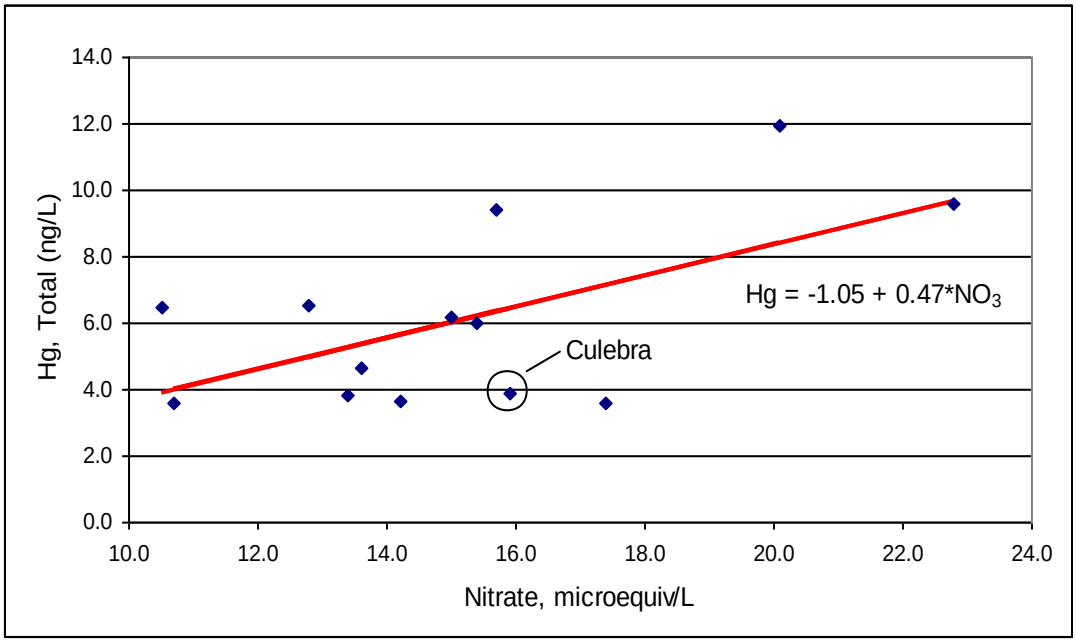

Figure 3-17. Regression of Total Mercury Concentration on Nitrate Concentration in 2002 Snowpack Data

The same regressions were performed with the 2003 snowpack data, but three of the 2002 southern Colorado sites were not sampled in 2003, reducing the sample size from 13 to 10 sites. A significant relationship between nitrate and sulfate and total mercury could not be found in the 2003 snowpack data ($p<0.05$).

The unusually high total mercury concentration of 0.012 µg/L at the Slumgullion Pass, CO site (with relatively low nitrate and sulfate concentrations) had a strong influence on the 2003 regression results. When the Slumgullion site was included in the regressions, weak negative correlations resulted, but when the Slumgullion site was removed, the 2003 regressions demonstrated weak positive correlations between nitrate and sulfate and total mercury. The unusual measurements at the Slumgullion site could indicate either a measurement error or a condition unique to that site, but sufficient information was not available to warrant excluding the site from consideration.

With the Slumgullion site included in the 2003 regressions, sulfate accounts for less than 2 percent of variation in total mercury ($R^2 = 0.02$) and nitrate accounts for 20 percent of variation in total mercury ($R^2 = 0.20$). With the Slumgullion site excluded, sulfate accounts for 15 percent of variation in total mercury ($R^2 = 0.15$) and nitrate accounts for 14 percent of variation in total mercury ($R^2 = 0.14$).

The 2002 concentration of mercury in snowpack at the Culebra site (3.9E-03 µg/L) is comparable to the range in concentration of mercury at the Sanchez stream monitoring sites during snow melt (Table 3-1). The mercury concentration at the Sanchez stream monitoring sites in June 1999 ranged from 7.0E-04 µg/L to 0.011 µg/L with an average of 3.8E-03 µg/L. The concentration in Sanchez reservoir was considerably lower, ranging from 7.0E-04 to 1.3E-03 with an average of 8.0E-04 µ g/L.

3.3 WATERSHED NONPOINT SOURCES

Mercury loads from the Sanchez Reservoir watershed are primarily driven by atmospheric deposition on land surfaces which are then delivered to the reservoir through surface runoff, erosion, and transport

processes. These processes are controlled mostly by land use characteristics. Nonpoint source loads to the Sanchez Reservoir are presented in this section.

3.3.1 Landfills/Waste Disposal

There are no permitted industrial or hazardous waste landfills in the Sanchez Reservoir watershed; however, disposal of household waste constitutes a potential source of mercury. Improperly disposed solid waste can contribute mercury loading to the reservoir from watershed based sources. Examples of solid waste that contain relatively high levels of mercury include household detergents and cleaners, particularly scrubbing powders, batteries, fluorescent light bulbs, and mercury switches commonly used in appliances and automobiles.

Nationally, the majority of household batteries, fluorescent light bulbs, and appliances are disposed in municipal solid waste landfills. However, regulations from EPA in 1994 governing collection and monitoring of leachate from landfills substantially changed solid waste services in Costilla County – nine landfills once open were closed (Doon, 2003a). The State of Colorado's proposed solution for the county's solid waste was the regional landfill outside of Del Norte, a round trip distance of approximately 150 miles from San Luis (Doon, 2003a). Due to the high fees associated with transporting solid waste to Del Norte, illegal dumping has become a widespread problem in Costilla County as trash piles up in arroyos and across the prairie as typified in Figure 3-18 and Figure 3-19. Illegal dumpsites in Costilla County continue to expand as an estimated 50 – 80 percent of all solid waste generated in the County is being improperly disposed (Doon, 2003b).

As of 2008, the solid waste disposal issue has not been resolved. There was a recent effort to create a joint landfill between Costilla and Conejos counties, though no agreement was reached (personal communication, A. Valdez, Santa Fe County to D. Pizzi, Tetra Tech, 5/6/2008). In addition, a ballot measure to enact a tax for waste management was not passed (personal communication, A. Stuebe, NRCS to D. Pizzi, Tetra Tech, 4/29/2008). The rate of waste disposal has not likely changed since 2005 (personal communication, M.K. Anderson, Santa Fe County to K.E. Browne, Tetra Tech, 4/30/2008).

Figure 3-18. Improper Disposal of Solid Waste in an Arroyo Along Vallejos Creek

Figure 3-19. Improper Disposal of Solid Waste into Torcido Creek

In rural areas such as the Sanchez Reservoir watershed, unmanaged disposal of automobiles is also a concern for mercury loading. A modern car is likely to contain three or more switches that contain a pool of about 1 g mercury each used for motion-activation of electric signals (Ecology Center, 2001). Automobile salvage yards and junked/abandoned vehicles can contribute mercury loads when mercury switches are broken. Junked/abandoned vehicles were observed in only one location during a watershed visit, and the extent to which these vehicles contribute mercury to the reservoir is unknown. As illustrated in Figure 3-20, the junked vehicles are stored in the overbank area along the lower reaches of Vallejos Creek. As of April 2008, these vehicles remain in the watershed and improper disposal is likely to continue (personal communication, A. Stuebe, NRCS to D. Pizzi, Tetra Tech, 4/29/2008).

Figure 3-20. Junked/Abandoned Vehicles Along Vallejos Creek

3.3.2 Agriculture and Silviculture

Agricultural land – particularly tilled cropland – can be a major source of sediment loading. If the soils contain mercury such sediment load can be a contributing source of mercury to reservoirs, although this loading may be mitigated by use of best management practices (BMPs). Stormwater runoff rates are generally higher compared to other rural land uses such as forest or meadow, particularly on row crop fields. The sparse ground cover during certain times of the agricultural cycle leads to higher rates of erosion. Atmospheric deposition of mercury on exposed surface soils in agricultural areas and the subsequent erosion of these soils provide another watershed-based load to Sanchez Reservoir.

According to land use data provided by the Colorado Acequia Association, only about two percent of the Sanchez Reservoir watershed is used for agriculture – 1.8 percent as pasture and 0.2 percent as alfalfa. Historically, some agricultural practices relied upon mercury-based pesticides, herbicides, fungicides, and seed treatments, however, it is unlikely that these products were used in the Sanchez Reservoir watershed because many of the individual fields are only a few acres in size and few of the farmers would have been able to use large volume cost-effective application methods (E&E, 1991). Further, the native hay and alfalfa need very little to no pesticides, and the types of seeds that are treated with mercury prior to planting probably have never been used (Edwards, personal communication, 1991, cited in E&E, 1991).

A significant portion of the pasture land in the watershed is contained within the Taylor Ranch on San Francisco Creek. A Land Use Management Plan has recently been developed for Taylor Ranch to

manage grazing lands (personal communication, A. Valdez, Santa Fe County to D. Pizzi, Tetra Tech, 5/6/2008). This plan will likely decrease erosion rates from areas previously overgrazed.

Because of the minimal amount of agriculture in the watershed, in combination with the lack of tillage associated with the primary types of agriculture, mercury loadings resulting from agricultural activities are not expected to be significant.

Similar to agricultural practices, silviculture is another potential source of increased surface soil erosion, and thus increased delivery of sediment-associated mercury. No national forest or state forest lands are located within the Sanchez Reservoir watershed, so any logging activities that occur take place on privately-owned land. As a result, the Colorado State Forest Service (CSFS) does not regulate logging activities; however, the Colorado Timber Industry Association and the CSFS recommend private logging activities abide by the Forest Stewardship Guidelines to Protect Water Quality (CSFS, 1998). The New Mexico Energy, Minerals, and Natural Resources Department (EMNRD) Forestry Division also has Commercial Timber Harvesting Requirements that are applicable to all logging activities greater than or equal to 25 acres in size (EMNRD, 2001). Based on Geographic Information System (GIS) data provided by the Colorado Acequia Association along with interpretation of aerial photography from the late 1990s, it was estimated that logging activities cover approximately 13 percent of the watershed. Thus, it is clear that silviculture has a considerable influence in the Sanchez Reservoir watershed.

Logging practices increase erosion by removing ground cover, exposing surface soils, shortening runoff pathways, increasing runoff volume by reducing infiltration and evapotranspiration, and changing the timing of runoff from snowmelt due to the removal of shade. After timber harvesting occurs, erosion and sediment-bound mercury loading from forestland is likely to increase until groundcover is restored and vegetation is established. Researchers in Finland found that mercury loads following clear cutting, mounding, and replanting were 2.5 to 5.5 times higher than before clear cutting; methylmercury loads were 4.4 to 10 times higher after (Porvari et al., 2003). Due to the lack of publicly available data on the location or timing of timber harvesting in the watershed, it is difficult to assess the direct impacts of silviculture on the Sanchez Reservoir.

3.3.3 Residential Development

In recent years, development of residential communities has begun to the west and east of Sanchez Reservoir. Both developments have recently or are currently clearing land for construction and cutting new roads (personal communication, E. Valdez, Dos Hermanos Ranch to K. Browne, Tetra Tech, 4/24/2008; personal communication, J. Lobato, NRCS to K. Browne, Tetra Tech, 5/2/2008). Tetra Tech has not been able to determine the size and layout of these developments, and it is not known if BMPs are being utilized on these sites to control erosion and sediment transport.

Land clearing and road cutting activities can generate extremely high sediment loads during construction and in the period prior to stabilization. Though it is difficult to estimate the sediment and associated mercury loads from these developments with the current level of knowledge, use of erosion control BMPs should be encouraged in any development occurring near Sanchez Reservoir.

3.4 GEOLOGICAL SOURCES

The geology underlying a watershed has the potential to both directly and indirectly contribute to mercury loadings. Geologic formations that contain mercury species, particularly quicksilver (Hg), cinnabar (HgS), amalgam (AgHg), and coloradoite (HgTe) in Colorado (Streufert and Cappa, 1994), can directly contribute to mercury loadings through weathering and erosion. Geologic formations containing low-grade deposits of precious metals (e.g., gold, silver, and copper) have also often been mined using

mercury as an amalgam to leach these metals from the ore. As a byproduct of mining activities, mercury loadings can indirectly be influenced by certain geologic formations.

3.4.1 Direct Geologic Sources of Mercury

There are no known geologic formations within the Sanchez Reservoir watershed that definitively contain significant mercury concentrations, despite the recent detailed geologic mapping of the La Valley (Kirkham et al., 2004) and Taylor Ranch (Kirkham et al., 2003) quadrangles. In general, however, mercury has a higher probability of occurrence in mineralized areas along fault lines or intrusive dikes in igneous formations. Volcanic activity has the potential to release mercury into the air, so areas with large ash deposits may contain higher concentrations of mercury. Mercury is also more likely to occur in shale and slate deposits as they are derived from clays, which have high affinities for adsorbing metals such as mercury (this affinity explains why coal burning power plants emit mercury).

More detailed descriptions of the geologic formation of the San Luis valley and the San Juan and Sangre de Cristo mountain ranges (Tetra Tech, 2000; E&E, 1991; Burroughs, 1981) reveal that the region is an active seismic and geothermal area. Due to historic volcanic mountain building, the Culebra Range to the east of the Sanchez Reservoir is underlain by Proterozoic igneous and metamorphic formations. These formations exhibit numerous and complex faults, but the paucity of outcrops inhibited the mapping of the faults (Kirkham et al., 2004). Faults that could be identified, or inferred, and intrusive dikes were identified in the following locations:

- El Poso Creek from the confluence with Culebra Creek upstream approximately seven miles (at which point the detailed mapping terminates, the fault likely continues upstream)
- El Poso Creek headwaters through approximately three miles of Jarioso Canyon
- Culebra Creek just east of Chama upstream approximately eight miles (at which point the detailed mapping terminates, the fault likely continues upstream)
- Carneros Creek from its confluence with Culebra Creek upstream for approximately two and a half miles
- El Rito de Aban in the headwaters for less than one mile
- Vallejos Creek from the confluence of North Vallejos and Vallejos Creek for approximately two miles downstream to the Sangre de Cristo fault
- North Vallejos Creek from the confluence with Vallejos Creek to the Trinchera Peak fault, located approximately four miles upstream
- Alamosito Creek for approximately three miles; a mafic intrusion is located along the north side of the creek
- Paralleling and crossing San Francisco Creek for approximately three miles
- Both headwater tributaries to the northern tributary of El Fragaso Creek
- Jaroso Creek headwaters for approximately one and one-half miles; a mafic intrusion is located in the wall of Jaroso Creek
- Cuates Creek for approximately one mile; two gabbroic dikes are located along the south side of Cuates Creek

The location of these larger faults tends to follow drainage divides along many of the named tributaries to Sanchez Reservoir. The faults that correspond with locations of intrusive dikes (e.g., Alamosito Creek, Jaroso Creek, and Cuates Creek) have the greatest likelihood of contributing to the mercury loading to the

reservoir. Instream total and dissolved mercury samples and sediment samples collected in the summer of 1999 indicate higher mercury concentrations in Alamosito, Jarosito, and Cuates Creeks (Tetra Tech, 2000).

Despite the prevalence of volcanic activity in the watershed, some in recent geologic time, only one ash bed was identified through detailed geologic mapping. A prominent bed of ash tephra located between the forks of Vallejos and North Vallejos creeks is nearly 10 feet thick and can be traced along the hillslope for a horizontal distance in excess of 1,500 feet (Kirkham et al., 2004). An unnamed tributary or possibly a gully drains this tephra bed to Vallejos Creek just upstream from the confluence with North Vallejos Creek. Due to the potential for mercury to be released to the atmosphere through volcanic activity, this ash bed may be a source of mercury to the reservoir; however, instream flow and sediment monitoring does not reveal elevated levels of mercury in Vallejos Creek downstream of the bed (Tetra Tech, 2000).

Shale and slate deposits are the third primary direct source of mercury loadings for geologic formations. Based on the statewide geologic map of Colorado (Tweto, 1979), within the Sanchez Reservoir watershed only the Beldin and Miniturn formations contain shale and these formations underlie the headwaters of El Poso Creek through Jarioso Canyon. The detailed geologic mapping of the La Valley quadrangle identified shale in western parts of the quadrangle as a component of the Santa Fe formation – a group of informal sedimentary and volcanic members consisting of a thick sequence of sedimentary strata and intercalated volcanic flows (Kirkham et al., 2004). The shale components in the Beldin, Miniturn, and Santa Fe formations are poorly mapped due to the complexity of the formations, which confounds any relationships between monitored mercury loads and spatial distributions of shale formations.

While no direct sources of mercury in geologic formations underlying the Sanchez Reservoir watershed were identified through detailed geologic mapping, indicators of areas that have higher probabilities of mercury occurrence were identified. The lack of spatial extent and location associated with the geology of the Sanchez Reservoir watershed precludes a determination of the contribution from the natural rocks and sediment to the mercury loads to the reservoir.

3.4.2 Indirect Geologic Sources of Mercury

Geologic formations containing deposits of precious metals (e.g., gold, silver, and copper) have been targets of historic and current mining activities. In cases where the desired metals are contained in ore as opposed to veins, extraction of the desired metal commonly occurs through the process of amalgamation, in which mercury is used as the amalgam. Amalgamation is an easy and inexpensive process of removing fine metal particles from ore, but when it is poorly implemented, it can lead to spillage of mercury. Thus, in relation to mining potential, the geologic formations in a watershed can indirectly influence mercury loadings, and are reviewed in this section.

No mines are known to have operated within the Sanchez Reservoir watershed (Tetra Tech, 2000). The El Plomo Gold Mine and the San Luis Project were in operation as recently as 1999, but both of these mines are located in the Rito Seco drainage – the Rito Seco River does not discharge directly or indirectly into Sanchez Reservoir so there is no potential for mine runoff or seepage from these mines to reach Sanchez Reservoir (Tetra Tech, 2000).

There are anecdotal reports of small-scale gold and silver mining operations in the early 1900s in the headwaters of the tributaries draining to Sanchez Reservoir, particularly along San Francisco Creek, where mercury amalgamation techniques may have been used (Tetra Tech, 2000). According to Bob Kirkham, no evidence of significant mining related activities was observed in over 90 percent of the La Valley quadrangle he walked for the detailed geologic mapping (personal communication, Bob Kirkham to D. Pizzi, Tetra Tech, 3/31/2005). However, he did observe a few prospector pits and a few trenches where bulldozers excavated surface soils along an unnamed tributary to San Francisco Creek that is

located on the Trinchera Peak fault. As no large-scale mining operations were associated with these test sites, it is unlikely that significant loadings of mercury associated with amalgamation contribute to the elevated levels in the reservoir.

4 Linkage Analysis

The linkage analysis defines the connection between numeric targets and identified pollutant sources and may be described as the cause-and-effect relationship between the selected indicators, the associated numeric targets, and the identified sources. This provides the basis for estimating total assimilative capacity and any needed load reductions. Specifically, models of watershed loading of mercury are combined with an estimated rate of bioaccumulation in the lake. This enables a translation between the numeric target (expressed as a fish tissue concentration of mercury) and mercury loading rates. The loading capacity is then determined via the linkage analysis as the mercury loading rate that is consistent with meeting the target fish tissue concentration.

4.1 THE MERCURY CYCLE

Development of the linkage analysis requires an understanding of how mercury cycles in the environment. Mercury chemistry in the environment is quite complex. Mercury has the properties of a metal (including great persistence due to its inability to be broken down), but also has some properties of a hydrophobic organic chemical due to its ability to be methylated through a bacterial process. Methylmercury is easily taken up by organisms and tends to bioaccumulate; it is very effectively transferred through the food web, magnifying at each trophic level. This can result in high levels of mercury in organisms high on the food chain, despite nearly unmeasurable quantities of mercury in the water column. In fish, mercury is not usually found in levels high enough to cause the fish to exhibit signs of toxicity, but wildlife that habitually eat contaminated fish are at risk of accumulating mercury at toxic levels, and the mercury in sport fish can present a potential health risk to humans.

Selected aspects of the lake and watershed mercury cycle are summarized schematically in Figure 4-1, based on the representations discussed in Hudson et al. (1994) and Tetra Tech (1999c). The boxes represent stores of mercury, and the arrows represent fluxes. The top of the diagram summarizes the various forms of mercury that may be loaded to a lake.

Lake Mercury Cycle

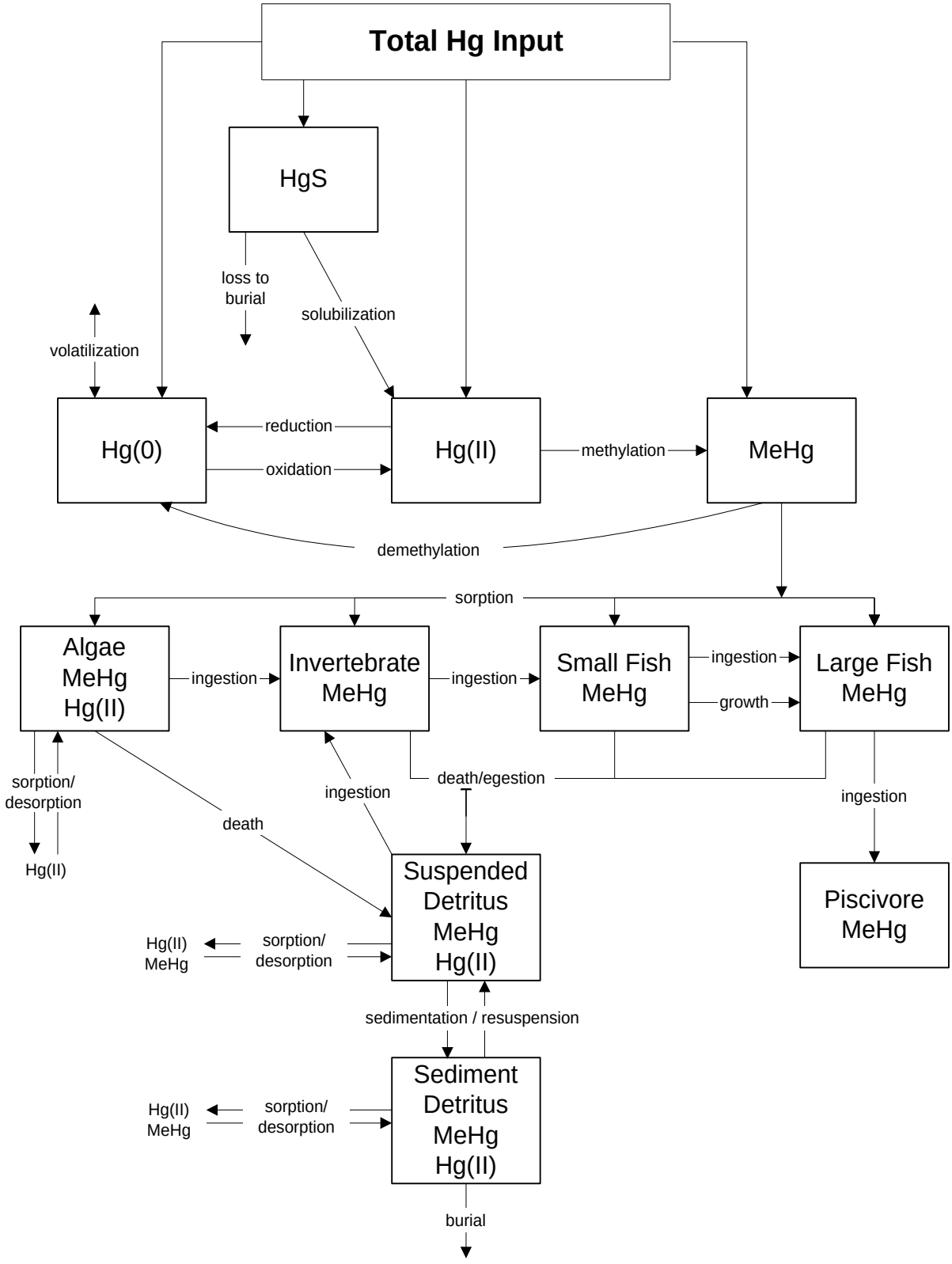

Figure 4-1. Conceptual Diagram of Lake Mercury Cycle

It is important to recognize that mercury exists in a variety of forms, including elemental mercury (Hg(0)), ionic mercury (Hg(I) and Hg(II)), and compounds in which mercury is joined to an organic molecule.

In the figure, Hg(I) is ignored because Hg(II) species generally predominate in aquatic systems. Mercuric sulfide (HgS or cinnabar) is a compound formed from Hg(II) but is shown separately because it is the predominant natural ore. Organic forms of mercury include methylmercury (CH_3Hg or "MeHg"), and other natural forms such as dimethylmercury and man-made compounds such as organic mercury pesticides. (Where sorption and desorption are indicated in Figure 4-1, "Hg(II)" and "MeHg" refer to the same common pools of water column Hg(II) and MeHg shown in the compartments at the top of the diagram.)

In the lake mercury cycle, it is critical to consider the distribution of mercury load between the various forms. The major forms reaching a lake from the watershed can have different behaviors:

- Mercuric sulfide (HgS) can be washed into the lake as a result of weathering of natural cinnabar outcrops. HgS has low solubility under typical environmental conditions and would be expected to settle out to the bottom sediments of the lake. Under aerobic conditions, however, Hg(II) may be liberated by a bacteria-mediated oxidation of the sulfide ion. This Hg(II) would then be much more bioavailable and would be available for methylation. Alternatively, under anaerobic conditions, HgS may be formed from Hg(II).
- Methylmercury (MeHg) is found in rainfall and may be found in small amounts in mine tailings or wash sediments. It is more soluble than HgS and has a strong affinity for lipids in biotic tissues.
- Elemental mercury (Hg(0)) may remain in mine tailings, as has been noted in tailings piles from recent gold mining in Brazil. Elemental mercury tends to volatilize into the atmosphere, though some can be oxidized to Hg(II).
- Other mercury compounds that contain and may easily release ionic Hg(II) are found in the fine residue left at abandoned mine sites where mercury was used to draw gold or silver out of pulverized rock.

Note that dimethylmercury (CH_3-Hg-CH_3) is ignored in the conceptual model shown in Figure 4-1, because this mercury species seems to occur in measurable quantities only in marine waters. Organic mercury pesticides also have been ignored in this TMDL study, because such pesticides are not currently used in this country and past use is probably insignificant as there is little cropland in the Sanchez watershed.

Mercury and methylmercury form strong complexes with organic substances (including humic acids) and strongly sorb onto soils and sediments. Once sorbed to organic matter, mercury can be ingested by invertebrates, thus entering the food chain. Some of the sorbed mercury will settle to the lake bottom; if buried deeply enough, mercury in bottom sediments will become unavailable to the lake mercury cycle. Burial in bottom sediments can be an important route of removal of mercury from the aquatic environment.

Methylation and demethylation play an important role in determining how mercury will accumulate through the food web. Hg(II) is methylated by a biological process that appears to involve sulfate-reducing bacteria. Rates of biological methylation of mercury can be affected by a number of factors. Methylation can occur in water, sediment, and soil solutions under anaerobic conditions, and to a lesser extent under aerobic conditions. In lakes, methylation occurs mainly at the sediment-water interface and at the oxic-anoxic boundary within the water column. The rate of methylation is affected by the concentration of available Hg(II) (which can be affected by the concentration of certain ions and ligands), the microbial concentration, pH, temperature, redox potential, and the presence of other chemical

processes. Methylation rates appear to increase at lower pH. Demethylation of mercury is also mediated by bacteria.

Both Hg(II) and methylmercury (MeHg) sorb to algae and detritus, but only the methylmercury is assumed to be passed up to the next trophic level (inorganic mercury is relatively easily egested). Invertebrates eat both algae and detritus, thereby accumulating any MeHg that has sorbed to these. Fish eat the invertebrates and either grow into larger fish (which continue to accumulate body burdens of mercury), are eaten by larger fish or other piscivores, or die and decay. At each trophic level, a bioaccumulation factor must be assumed to represent the magnification of mercury concentration that occurs as one steps up the food chain.

Typically, almost all of the mercury found in fish (greater than 95 percent) is in methylmercury form. Studies have shown that fish body burdens of mercury tend to increase concurrently with increasing size or age of the fish, under conditions of constant exposure.

Although it is important to identify external sources of mercury to the reservoir, there may be fluxes of mercury within the reservoir that would continue for some time even if all external sources of mercury load were eliminated. The most important store of mercury within the reservoir is the bed sediment. Mercury in the bed sediment may cause exposure to biota by being:

- Resuspended into the water column, where it is ingested or it adsorbs to organisms that are later ingested.
- Methylated by bacteria. The methylmercury tends to attach to organic matter, which may be ingested by invertebrates and thereby introduced to the lake food web.

4.2 STRUCTURE OF THE WATERSHED LOADING COMPONENT OF THE TMDL

While mercury load can originate from a wide variety of source types, information to characterize many of these sources is limited for the Sanchez watershed. Lake and stream water and sediment monitoring for mercury in the watershed by modern ultra-clean analytical methods consists primarily of the two sampling events conducted by Tetra Tech in June and August 1999 (Tetra Tech, 2000) plus supplementary sediment sampling from the Sanchez Canal in 2005 (Tetra Tech, 2006). These sampling events achieved good spatial coverage, but two points in time is not enough to establish reliable averages, and cannot resolve seasonal trends.

How are the limited available data best used to characterize mercury loading? Because ionic mercury is particle-reactive, much of the mercury within streams is associated with the sediment and moves through the watershed during major sediment scour events. At other times, smaller amounts of mercury move in dissolved form. Dissolved mercury associated with seeps and point sources might predominate during low flow periods. Given the available data, it is useful to consider three components of watershed transport of mercury: dissolved and suspended mercury during non-snow melt conditions; dissolved and suspended mercury derived from melt of the winter snowpack; and bedload transport of particulate mercury.

The stream sediment mercury concentration can be assumed to be relatively stable in time, although highly variable in space. Thus, the two sample rounds are likely adequate to characterize sediment concentrations. Two sampling events do not provide a very clear basis for inference regarding long-term average water column loads, since water concentrations are likely much more variable in time. A simple approach is to assume that the average of the water column samples reported in Tetra Tech (2000) provides a "best available" estimate of the (exclusively) water column transport, while observed surface sediment concentrations provide an indication of the mercury moving in sediment bedload transport. This could lead to some double counting, to the extent that some samples include particle-associated mercury

mobilized from the sediment, but the error is (1) expected to be small relative to total mercury transport, and (2) errs on the side of conservatism.

Accordingly, the watershed ("external") loading of mercury is estimated using two components, described below. Each of these components is assessed on a geographic basis, and tied to individual source areas where data allow.

1. Water column loading of dissolved and suspended particulate mercury: The non-snow melt portion of the water column transport of mercury is estimated directly from the average of total mercury concentrations in June and August Tetra Tech sampling coupled with an analysis of flow. Mercury transport is potentially enhanced during the melt of the winter snowpack, as this may release atmospheric deposition load accumulated and stored over the winter. Potential loads associated with snow melt are thus further checked against concentrations reported from snowpack.
2. Watershed sediment-associated mercury load: Much of the mercury load from the watershed likely moves in association with sediment during a few high-flow scour events. The available sampling represents this mercury in terms of concentrations in bed sediments. Sufficient data are not available to calibrate a model of sediment transport in the watersheds. An approximate approach is therefore used, based on an assumption of long-term dynamic equilibrium in stream channels. This approach, which was successfully used in the TMDL studies for Arivaca and Peña Blanca lakes in Arizona and McPhee Reservoir in Colorado (Tetra Tech, 1999a; 1999b, 2001), makes the following arguments:
    - The amount of sediment moving through the major streams is equivalent (as a long-term average) to the rate of sediment loading to those streams, as estimated by a sediment load model.
    - The concentration of mercury in sediment moving through the system is equivalent to the concentration measured in stream sediment samples.
    - Mercury may be treated as approximately conservative in the stream sediments.

Each of these assumptions is a rough approximation only; however, they may be combined to provide an order-of-magnitude estimate of sediment-associated mercury delivery. The watershed load estimates implicitly account for the net effects of atmospheric deposition onto the watershed and its snowpack.

4.3 WATERSHED HYDROLOGIC AND SEDIMENT LOADING MODEL

An analysis of watershed loading could be conducted at many different levels of complexity, ranging from simple export coefficients to a dynamic model of watershed loads. Data are not, however, available at this time to specify parameters or calibrate a detailed representation of flow and sediment delivery within the watersheds. Therefore, a relatively simple, scoping-level analysis of watershed mercury load, based on an annual mass balance of water and sediment loading from the watershed, is used for the TMDL. Uncertainty introduced in the analysis by use of a simplified watershed-loading model must be addressed in the Margin of Safety.

4.3.1 Model Selection

Watershed-scale loading of water and sediment was simulated using the Generalized Watershed Loading Functions (GWLF) model (Haith et al., 1992). The complexity of this loading function model falls between that of detailed simulation models, which attempt a mechanistic, time-dependent representation of pollutant load generation and transport, and simple export coefficient models, which do not represent temporal variability. GWLF provides a mechanistic, simplified simulation of precipitation-driven runoff and sediment delivery, yet is intended to be applicable as a scoping tool without formal calibration. Solids load, runoff, and groundwater seepage can then be used to estimate particulate and dissolved-phase pollutant delivery to a stream, based on pollutant concentrations in soil, runoff, and groundwater.

GWLF simulates runoff and streamflow by a water-balance method, based on measurements of daily precipitation and average temperature. Precipitation is partitioned into direct runoff and infiltration using a form of the Natural Resources Conservation Service's (NRCS) Curve Number method. The Curve Number determines the amount of precipitation that runs off directly, adjusted for antecedent soil moisture based on total precipitation in the preceding five days. A separate Curve Number is specified for each land use by hydrologic soil grouping. Infiltrated water is first assigned to unsaturated zone storage, where it may be lost through evapotranspiration. When storage in the unsaturated zone exceeds soil water capacity, the excess percolates to the shallow saturated zone. This zone is treated as a linear reservoir that discharges to the stream or loses moisture to deep seepage, at a rate described by the product of the zone's moisture storage and a constant rate coefficient.

Flow in rural streams may derive from surface runoff during precipitation events or from groundwater pathways. The amount of water available to the shallow groundwater zone is strongly affected by evapotranspiration, which GWLF estimates from available moisture in the unsaturated zone, potential evapotranspiration, and a cover coefficient. Potential evapotranspiration is estimated from a relationship to mean daily temperature and the number of daylight hours.

Monthly sediment delivery from each land use is computed from erosion and the transport capacity of runoff, whereas total erosion is based on the universal soil loss equation (Wischmeier and Smith, 1978), with a modified rainfall erosivity coefficient that accounts for the precipitation energy available to detach soil particles (Haith and Merrill, 1987). Thus, erosion can occur when there is precipitation, but no surface runoff to the stream; delivery of sediment, however, depends on surface runoff volume. Sediment available for delivery is accumulated over a year, although excess sediment supply is not assumed to carry over from one year to the next.

4.3.2 GWLF Model Input

The GWLF application requires information on land use distribution, meteorology, and parameters that govern runoff, erosion, and nutrient load generation. Four primary data sources were used to develop the model parameters used for the watershed simulations: 1) Digital Elevations Models (DEMs), 2) Land Use/Land Cover spatial data, 3) Soil Characteristics Databases, and 4) Meteorological Data.

4.3.3 Subbasin Delineation

The watersheds were divided into subbasins to isolate potential source areas and improve the accuracy of the GWLF simulation. Digital elevation model (DEM) coverages in a 1:100,000 30-meter resolution grid format were obtained from USGS. The watershed delineation tool provided with the ArcView Soil and Water Assessment Tool (AV SWAT) (Neitsch and DiLuzio, 1999) was used to delineate the watershed boundaries based upon the DEM coverages and Reach File 3 hydrography. A total of 11 subwatersheds were defined for the Sanchez watershed (Figure 4-2). Subbasin pour points were selected to reflect availability of sampling stations, resulting in basins of unequal sizes, with the northernmost basin (Culebra and El Poso Creek) accounting for 35 percent of the total area (Table 4-1).

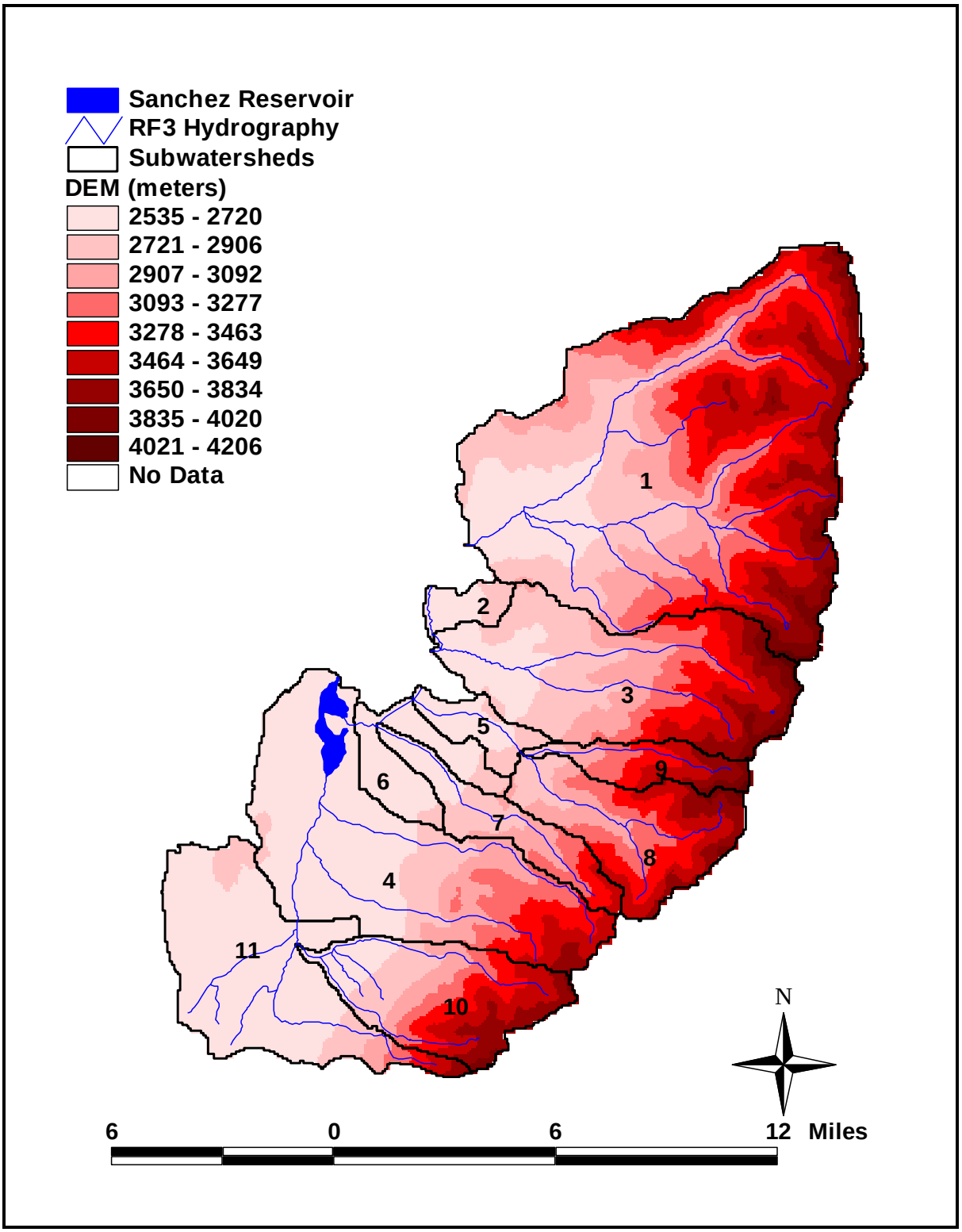

Figure 4-2. Subbasin Delineation Based on USGS Digital Elevation Model for Sanchez Reservoir, CO

Table 4-1. Sanchez Watershed Modeling Subbasins

Subbasin	Description	Area (km^2)
1	Culebra and El Poso Creek	209.0
2	Sanchez Canal Direct Drainage	6.6
3	Vallejos Creek	78.4
4	Lower Ventero, Jaroso, and Cuates Creek	96.4
5	Lower San Francisco Creek	9.8
6	Direct Drainage	17.6
7	Torcido Creek	20.4
8	Upper San Francisco Creek	38.7
9	El Fragoso Creek	14.1
10	Willow and Jarocito Creek	41.5
11	Upper Ventero Creek	62.8
Total	***Sanchez Watershed***	***595.0***

4.3.4 Land Use / Land Cover

Land cover data in the Sanchez watershed was obtained separately for the Colorado and New Mexico areas. The Colorado Acequia Association (CAA) has developed a database of vegetative cover based on 1995 satellite imagery at 25-meter resolution. Twenty-eight vegetative types are represented in the database. Land cover data for the New Mexico area were obtained from the U.S. Geological Survey (USGS) Geographic Information Retrieval and Analysis System (GIRAS) which is 1:250,000 scale quadrangle maps of the conterminous United States based on National Aeronautics and Space Administration (NASA) high altitude aerial photographs, and National High Altitude Photography (NHAP) program images.

Classifications in each dataset were translated into modeling classes according to Table 4-2 and Table 4-3. GWLF modeling classes are described in Table 4-4.

Table 4-2. Translation of CAA Vegetative Classes to GWLF Modeling Classes

CAA Land Cover	CAA Description	Percent of Watershed Area	GWLF Class
Aspen	Deciduous forest dominated by Aspen	7.86	FRSD
Cottonwood	Wooded riparian areas dominated by cottonwood	0.47	FRSD
Douglas Fir	Coniferous forest dominated by PSME	3.01	FRSE
Engelmann Spruce/Fir Mix	Coniferous forest co-dominated by PIEN and ABLA	14.97	FRSE
Pinyon-Juniper	Pinyon-Juniper woodland with mixed understory	4.15	FRSE
Ponderosa Pine	Coniferous forest dominated by PIPO	0.55	FRSE
Ponderosa Pine/Douglas Fir Mix	Mixed forest co-dominated by PIPO and PSME	5.00	FRSE

CAA Land Cover	CAA Description	Percent of Watershed Area	GWLF Class
Douglas Fir/Aspen Mix	Mixed forest co-dominated by PSME and Aspen	0.41	FRST
Spruce/Fir/Aspen Mix	Mixed forest co-dominated by PIEN, ABLA, and Aspen	11.63	FRST
Irrigated Ag	Irrigated crops and fields	0.88	RIPA
Herbaceous Riparian	Non-woody riparian areas consisting primarily of sedges	1.66	RIPA
PJ-Sagebrush Mix	Co-dominant Pinyon-Juniper and Sagebrush	1.02	RNGB
Sparse PJ/Shrub/Rock Mix	< 25% Pinyon-Juniper with sagebrush and rock	1.27	RNGB
Subalpine Shrub Community	7,000' to 11,500' tundra shrubs	3.54	RNGB
Upland Willow/Shrub Mix	High elevation shrubland dominated by willow and mixed shrubs	2.90	RNGB
Willow	Shrub riparian areas dominated by shrub willow species	0.31	RNGB
Alpine Grass Dominated	> 11,500' meadow dominated by alpine grasses	2.25	RNGE
Alpine Grass/Forb Mix	> 11,500' mixed meadow co-dominated by alpine grasses and forbs	2.49	RNGE
Subalpine Grass/Forb Mix	High elevation meadows co-dominated by grass and forbs (9,000 - 11,500)	1.51	RNGE
Rock	< 10% vegetation, rock outcrops, red sandstones, etc	6.12	ROCK
Grass Dominated	Rangeland dominated by annual and perennial grasses	4.72	SWRN
Rabbitbrush/Grass Mix	Co-dominant rabbitbrush and perennial grassland	0.35	SWRN
Sagebrush Community	Sagebrush with rabbitbrush, bitterbrush	8.09	SWRN
Sagebrush/Grass Mix	Co-dominant sagebrush shrubland and perennial grassland	13.32	SWRN
Shrub/Grass/Forb Mix	Mixed grass/forb and shrub/grass rangeland	0.14	SWRN
Xeric Mountain Shrub Mix	Deciduous woodland (or tall shrubland) dominated by Mtn. Mahogany	0.26	SWRN
Water	Lakes, reservoirs, rivers, streams	1.10	WATR

Table 4-3. Translation of GIRAS LU/LC to GWLF Modeling Classes

Land Cover	Percent NM Watershed Area	GWLF Class
Evergreen Forest Land	41%	FRSE
Shrub and Brush Rangeland	27%	RNGB
Mixed Tundra	12%	RNGB
Mixed Rangeland	10%	SWRN
Bare Ground	3%	RNGB
Mixed Forest Land	2%	FRST
Herbaceous Tundra	2%	RNGE
Shrub and Brush Tundra	1%	RNGB

Table 4-4. Description of GWLF Land Use Classes

Land Use Code	Description
FRSD	Deciduous forest, predominantly aspen
FRSE	Evergreen forest, predominantly pinyon and juniper
FRST	Mixture of evergreen and deciduous forest
LOGG	Areas recently clear cut as depicted by aerial photography; the last cutting occurred in 1996, so these areas are in a state of regrowth
RIPA	Riparian areas, irrigated pasture and alfalfa fields
RNGB	Rangeland covered predominantly by shrub and brush species
RNGE	Rangeland covered predominantly by herbaceous species
ROAD	Roads depicted by Tiger files and CAA maps, predominantly dirt surface
ROCK	Rock outcrops, red sandstones, less than 10 percent vegetative cover
SWRN	Southwest range, sparse cover, arid area, sagebrush prevalent
WATR	Lakes, reservoirs

Table 4-5 and Figure 4-3 show the distribution of GWLF classes in the watershed. The LOGG use is shown separately with underlying soil type in Section 4.3.12. LOGG areas are subtracted from the evergreen forest (FRSE) land use.

Table 4-5. Land Use Sums (acres) by Subwatershed

	1	2	3	4	5	6	7	8	9	10	11	Total
FRSD	6,986	0	1,210	0	0	0	333	0	237	0	0	8,766
FRSE	5,951	333	2,834	2,531	423	704	1,021	2,448	268	3,594	2,739	22,844
FRST	6,480	0	2,478	3,177	0	0	1,108	2,587	402	916	0	17,148
LOGG	6,691	211	2,126	1,851	231	166	615	928	256	1,402	4,809	19,287
RIPA	5,094	0	1,089	564	78	52	0	1,057	314	250	0	8,496
RNGB	4,457	0	1,863	397	0	0	0	474	493	0	0	7,684
RNGE	6,570	1,069	4,008	10,136	1,172	3,189	1,332	0	0	1,786	6,973	36,235
ROAD	0	0	0	1,370	0	0	0	0	0	0	0	1,370
ROCK	681	13	248	530	53	69	93	106	61	99	284	2,237
SWRN	7,509	0	3,307	2,642	0	0	446	1,964	1,430	2,067	501	19,864
WATR	1,220	0	198	613	454	166	83	0	19	140	211	3,104

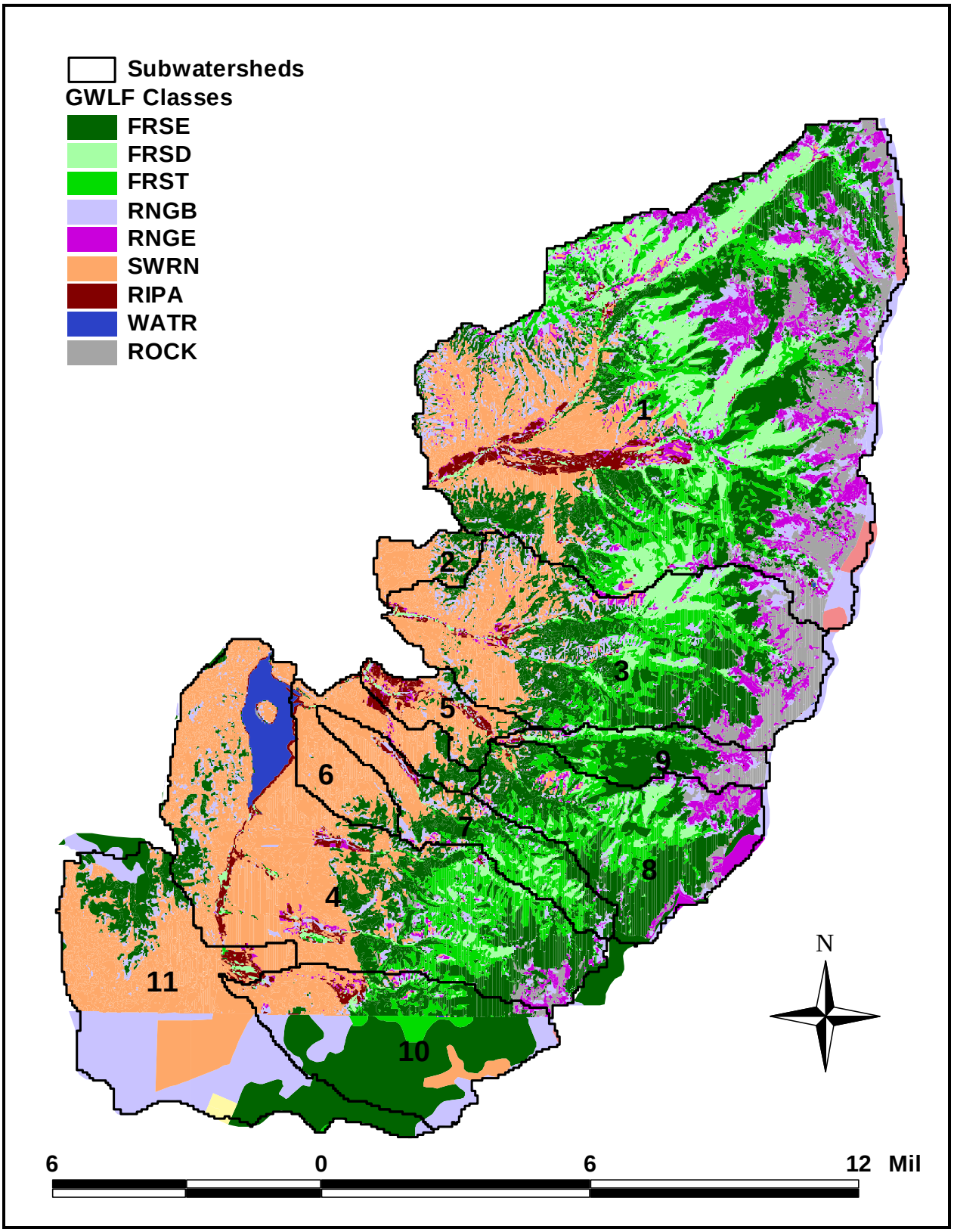

Figure 4-3. GWLF Land Classes in the Sanchez Watershed

4.3.5 Soil Properties

Soil distribution and characteristics were obtained from the U.S. Department of Agriculture State Soil Geographic Database (STATSGO) soil coverage. The STATSGO database groups similar soils together into map units. Information such as taxonomic soil groups, water capacity, soil texture, and permeability are stored within the database for each map unit within the coverage. The distribution of the major soil groups for the Sanchez watershed is presented in Figure 4-4. The union of the land use and watershed delineation themes was overlain on the STATSGO coverage to identify dominant soil groups and associated hydrologic soil classes across each land use type. Land use/ soil combinations were then input to the model as separate modeling units.

Modeling units were aggregated to represent combinations with greater than 5 percent of the area in each subwatershed. Aggregations were first assigned by land class. If the land use was not present at greater than 5 percent, aggregations were assigned to a similar land use within the same soil group. For example, in Subwatershed 1, 0.4 percent of the watershed is FRSTCO405. This area was added into the class FRSECO405, which represents 20.2 percent of the watershed area.

4.3.6 Runoff Curve Numbers

The direct runoff fraction of precipitation in GWLF is calculated using the curve number method from the U.S. Soil Conservation Service (now NRCS) TR55 method (SCS, 1986). This method is based on land use and soil hydrologic group. Curve numbers can vary from 25 for undisturbed woodland with good soils, to 100, for completely impervious surfaces. Curve numbers for each modeling unit were based on GWLF recommended values for arid/semiarid regions. The soil hydrologic group was obtained from the STATSGO database for each soil mapping unit identifier (MUID). Curve numbers are reported in Table 4-6.

4.3.7 Soil Water Capacity

Water stored in soil may evaporate, be transpired by plants, or percolate to groundwater below the rooting zone. The amount of water that can be stored in soil and is available to plants—the soil available water capacity—varies by soil type and rooting depth. Average available water capacity for each STATSGO soil type was calculated as the average of the fractional water capacities for the first two soil layers, multiplied by an assumed rooting depth of 100 cm, as recommended in the GWLF manual. Spatial weighted averages then yield available soil water capacities by model subbasin. Given the low precipitation and high temperatures in the watershed, the available soil water capacity is infrequently exceeded in most of the deeper soils, with the result that the model predicts that most streamflow occurs as surface runoff of rainfall or melting snow.

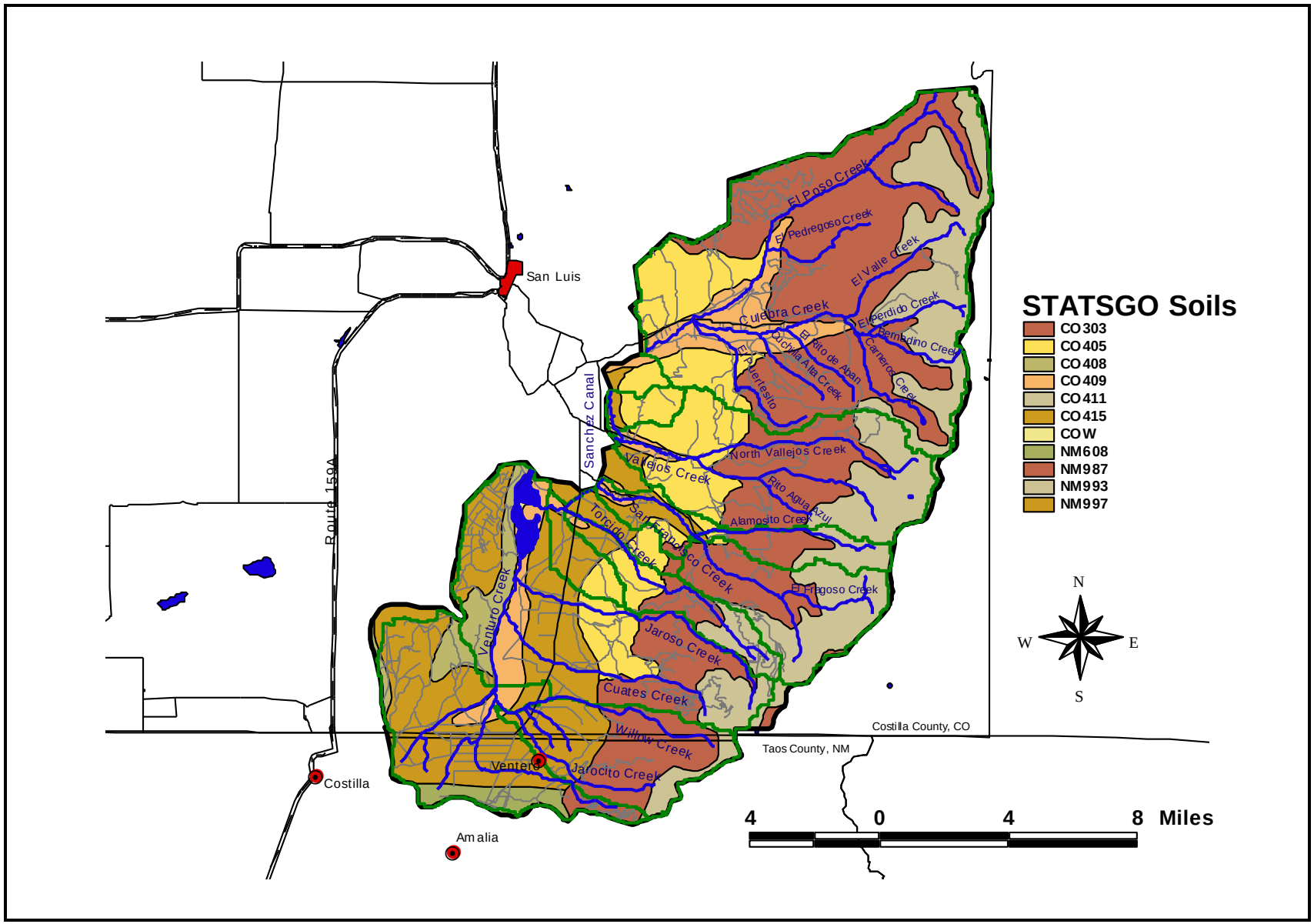

Figure 4-4. STATSGO Soil Groups in the Sanchez Watershed

Table 4-6. Curve Numbers for the GWLF-MUID Combinations in the Sanchez Watershed

GWLF Class STATSGO MUID	Soil Hydrologic Group	Assumption	CN
FRSDCO303	B	Fair cover, arid/semiarid region, oak/aspen, hyd B	48
FRSDCO411	C	Fair cover, arid/semiarid region, oak/aspen, hyd C	57
FRSECO303	B	Fair cover, arid/semiarid region, pinyon/juniper, hyd B	58
FRSECO405	C	Fair cover, arid/semiarid region, pinyon/juniper, hyd C	73
FRSECO411	C	Fair cover, arid/semiarid region, pinyon/juniper, hyd C	73
FRSECO415	B	Fair cover, arid/semiarid region, pinyon/juniper, hyd B	58
FRSENM608	C	Fair cover, arid/semiarid region, pinyon/juniper, hyd C	73
FRSTCO303	B	Fair cover, arid/semiarid region, mixed forest, hyd B, CN = average of 48 and 58	53
FRSTCO411	C	Fair cover, arid/semiarid region, mixed forest, hyd C, CN = average of 58 and 73	65
RNGBCO303	B	Fair cover, arid/semiarid region, desert scrub, hyd B	72
RNGBCO405	C	Fair cover, arid/semiarid region, desert scrub, hyd C	81
RNGBCO411	C	Fair cover, arid/semiarid region, desert scrub, hyd C	81
RNGBCO415	B	Fair cover, arid/semiarid region, desert scrub, hyd B	72
RNGBNM608	C	Fair cover, arid/semiarid region, desert scrub, hyd C	81
RNGECO303	B	Fair cover, arid/semiarid region, herbaceous, hyd B	71
RNGECO411	C	Fair cover, arid/semiarid region, herbaceous, hyd C	81
RNGECO415	B	Fair cover, arid/semiarid region, herbaceous, hyd B	71
ROCKCO411	C	Rock	98
SWRNCO405	C	Fair cover, arid/semiarid region, sagebrush with grass understory, hyd C	63
SWRNCO408	C	Fair cover, arid/semiarid region, sagebrush with grass understory, hyd C	63
SWRNCO409	C	Fair cover, arid/semiarid region, sagebrush with grass understory, hyd C	63
SWRNCO415	B	Fair cover, arid/semiarid region, sagebrush with grass understory, hyd B	51
WATRCO409	C	Water	100
ROADCO303	B	Dirt road, hyd B	82
ROADCO405	C	Dirt road, hyd C	87
ROADCO408	C	Dirt road, hyd C	87
ROADCO409	C	Dirt road, hyd C	87
ROADCO411	C	Dirt road, hyd C	87
ROADCO415	B	Dirt road, hyd B	82
ROADNM608	C	Dirt road, hyd C	87
LOGGCO303	B	Previously logged pinyon/juniper stand, poor cover, hyd B	75
LOGGCO411	C	Previously logged pinyon/juniper stand, poor cover, hyd C	85
RIPACO405	C	Good ground cover, arid/semiarid region, herbaceous cover/forage pasture, C	74
RIPACO409	C	Good ground cover, arid/semiarid region, herbaceous cover/forage pasture, C	74
RIPACO415	B	Good ground cover, arid/semiarid region, herbaceous cover/forage pasture, B	62

4.3.8 Evapotranspiration Cover Coefficients

The portion of rainfall returned to the atmosphere is determined by GWLF based on temperature, type of vegetation, and the vegetation distribution. The evapotranspiration cover coefficient for each subwatershed was estimated by calculating an area weighted value based upon cover type. Evergreen forest and perennial crops such as pasture and range are given a constant coefficient of 1.0 throughout the year. Cover coefficients for annual crops and deciduous forests were set to 1.0 for the growing season and 0.3 for the nongrowing season. Results are reported in Table 4-7. GWLF limits evapotranspiration by soil moisture content, so the model is fairly insensitive to these values in arid climates.

Table 4-7. Evapotranspiration Cover Coefficients for the Sanchez Subwatersheds

Subwatershed	ET Growing Season	ET Dormant Season
1	0.86	0.60
2	0.99	0.72
3	0.84	0.60
4	0.88	0.63
5	0.98	0.78
6	0.99	0.72
7	0.94	0.66
8	0.85	0.69
9	0.68	0.49
10	0.89	0.71
11	0.97	0.70

4.3.9 Recession and Seepage Coefficients

The GWLF model has three subsurface zones: a shallow unsaturated zone, a shallow saturated zone, and a deep aquifer zone. Behavior of the second two stores is controlled by a groundwater recession and a deep seepage coefficient. Because the model simulation yields almost no shallow groundwater flow, results are insensitive to specification of these parameters. The model used a default recession coefficient of 0.048 per day, while the deep seepage coefficient was set to 0.

4.3.10 Erosion Parameters

GWLF simulates rural soil erosion using the Universal Soil Loss Equation (USLE). This method has been applied extensively, so parameter values are well established. This computes soil loss per unit area (sheet and rill erosion) at the field scale by

$$A = RE \cdot K \cdot LS \cdot C \cdot P$$

where

A = rate of soil loss per unit area

RE = rainfall erosivity index

K = soil erodibility factor

LS = length-slope factor

C = cover and management factor

P = support practice factor

It should be noted that use of the USLE approach might underestimate total sediment yield within a watershed of this type. This is because the USLE addresses only sheet and rill erosion, whereas mass wasting (landslides) and gullying are probably significant components of the total sediment budget within the watershed. It was reasoned, however, that the mercury from the watershed that is likely to become bioavailable in the lake would be the mercury associated with the fine sediment fraction. The USLE approach should provide a reasonable approximation of the finer sediment load, even though movement of larger material by other processes is omitted, and can thus serve as a basis for evaluation of mercury loading from watershed sediments to the lake.

Soil loss or erosion at the field scale is not equivalent to sediment yield since substantial trapping may occur, particularly during overland flow or in first-order tributaries or impoundments. GWLF accounts for sediment yield by (1) computing transport capacity of overland flow, and (2) employing a sediment delivery ratio (DR) which accounts for losses to sediment redeposition.

4.3.10.1 Rainfall Erosivity (RE)

Rainfall erosivity accounts for the impact of rainfall on the ground surface, which can make soil more susceptible to erosion and subsequent transport. Precipitation-induced erosion varies with rainfall intensity, which shows different average characteristics according to geographic region. The factor is used in the USLE and is determined in the model as follows:

$$RE_t = 64.6 \cdot a_t \cdot R_t^{1.81}$$

where

RE_t = rainfall erosivity (in megajoules mm/ha-h)

a_t = location- and season-specific factor

R_t = rainfall on day t (in cm)

Erosivity was assigned a value of 0.22 for April through September, and 0.11 for October through March, based on New Mexico data reported by Selker et al. (1990).

4.3.10.2 Soil Erodibility (K) Factor

The soil erodibility factor indicates the propensity of a given soil type to erode and is a function of soil physical properties and slope. Soil erodibility factors (K) were derived from STATSGO data and weighted based on percent composition of each soil type represented in the MUID. Values for soil groups are shown in Table 4-8.

Table 4-8. Soil Erodibility Factors (K) for Predominant Soil STATSGO Types in the Sanchez Watershed

STATSGO MUID	K factor
CO303, NM 987	0.15
CO405	0.13
CO408	0.14
CO409	0.24
CO411, NM993	0.09
CO415, NM997	0.21
NM608	0.16

4.3.10.3 Length-Slope (LS) Factor

Erosion potential varies by slope as well as soil type. Length-slope factors were calculated by measuring representative slopes from topographic maps for upland and bottomland land use categories. The LS factor is calculated by AV SWAT, following Wischmeier and Smith (1978), as:

$$LS = (0.045 \cdot x_k)^{0.5} \cdot (65.41 \cdot \sin^2 \phi_k + 4.56 \cdot \sin \phi_k + 0.065)$$

where

ϕ_k = $\tan^{-1}(ps_k/100)$, where ps_k is percent slope

x_k = slope length (m)

Percent slopes were calculated separately for roads. Most land uses will follow the natural grade of the watershed, but roads are often designed with switchbacks to decrease the effective slope. SWAT was used to estimate slope lengths (x_k) and percent slope (ps_k) for each subwatershed. Slopes ranged from 5 to 27 percent in the Sanchez watershed. For subwatersheds with land slope less than 10 percent, road slope was assumed the same as land slope. For subwatersheds with greater than 10 percent slope, switch backs are likely incorporated. To estimate the slopes of roads in high gradient watersheds, the average of the land slope and perennial stream slope was calculated for each watershed. Resulting road slopes were less than 20 percent. Table 4-9 compares the land slopes and road slopes for each subwatershed.

Table 4-9. Land and Road Slopes for Each Modeling Subwatershed

Subbasin	Land Slope %	Estimated Road Slope %
1	24.0	15.2
2	8.9	8.9
3	21.4	14.3
4	11.6	10.2
5	8.1	8.1
6	5.6	5.6
7	16.9	12.2
8	27.5	17.4
9	26.7	18.5
10	22.5	17.2
11	5.5	5.5

Calculated LS values by land use varied from 0.85 to 3.88. For roads, the LS factor ranges from 0.85 to 2.24.

4.3.10.4 Cover Factors

Cover factors for each land use are based on Wischmeier and Smith (1978, Table 4-10) values reported for various types of canopy cover and percent ground cover. At the higher elevations, ground cover is sparse and C factors are set higher. STATSGO soil groups coincide with changes in elevation, so the land use/soil combinations work well to define vegetative cover factors. Vegetative cover is sparser on soil type CO411 due to low precipitation and unfavorable soil conditions. Modeling parameters for land uses on CO411 were modified to account for sparse cover.

Based on the site visit and review of detailed vegetation characteristics, estimates of both canopy and ground cover were reduced from the values used in Tetra Tech (2000). This results in significantly higher C factors and correspondingly larger estimates of erosion than were presented in the earlier document.

Cover Factor estimates are summarized in Table 4-10.

Table 4-10. Cover Factors for the GWLF Land Use Classes in the Sanchez Watershed

GWLF/MUID	Assumptions to Set Cover Coefficient	USLE Cover Coefficient
FRSDCO303	75% canopy cover, weed understory with 60% cover	0.084
FRSDCO411	75% canopy cover, weed understory with 20% cover	0.2
FRSECO303	75% canopy cover, weed understory with 60% cover	0.084
FRSECO405	75% canopy cover, weed understory with 60% cover	0.084
FRSECO411	75% canopy cover, weed understory with 20% cover	0.2
FRSECO415	75% canopy cover, weed understory with 60% cover	0.084
FRSENM608	75% canopy cover, weed understory with 60% cover	0.084
FRSTCO303	75% canopy cover, weed understory with 60% cover	0.084
FRSTCO411	75% canopy cover, weed understory with 20% cover	0.2
RNGBCO303	50% canopy cover, weed understory with 40% cover	0.11
RNGBCO405	50% canopy cover, weed understory with 40% cover	0.11
RNGBCO411	25% canopy cover, weed understory with 20% cover	0.2
RNGBCO415	50% canopy cover, weed understory with 40% cover	0.11
RNGBNM608	50% canopy cover, weed understory with 40% cover	0.11
RNGECO303	no appreciable canopy, weeds, 20% cover	0.24
RNGECO411	no appreciable canopy, weeds, 20% cover	0.24
RNGECO415	no appreciable canopy, weeds, 20% cover	0.24
ROCKCO411	assume low erodibility relative to other covers	0
SWRNCO405	no appreciable canopy, weeds, 60% cover	0.091
SWRNCO408	no appreciable canopy, weeds, 60% cover	0.091
SWRNCO409	no appreciable canopy, weeds, 60% cover	0.091
SWRNCO415	no appreciable canopy, weeds, 60% cover	0.091
WATRCO409	water	0
ROADCO303	set to zero, simulate sediment with WEPP	0
ROADCO405	set to zero, simulate sediment with WEPP	0
ROADCO408	set to zero, simulate sediment with WEPP	0
ROADCO409	set to zero, simulate sediment with WEPP	0
ROADCO411	set to zero, simulate sediment with WEPP	0
ROADCO415	set to zero, simulate sediment with WEPP	0
ROADNM608	set to zero, simulate sediment with WEPP	0
LOGGCO303	20% grass cover, logged areas in state of regrowth	0.1
LOGGCO411	10% grass cover, logged areas in state of regrowth	0.24
RIPACO405	80% grass cover	0.01
RIPACO409	80% grass cover	0.01
RIPACO415	80% grass cover	0.01

4.3.10.5 Sediment Delivery

GWLF uses the USLE equation to estimate erosion from land surfaces and then applies a sediment delivery ratio (DR) to account for trapping during overland flow. Values for DR were estimated from an empirical relationship of DR to watershed area (ASCE, 1975). The American Society of Civil Engineers' (ASCE) graphical relationship is approximated by the following empirical equation:

$$Log_{10}(DR) = -0.301 Log_{10}(Area) - 0.400$$

where area is the subwatershed area in square kilometers.

Sediment delivery ratios by subwatershed are presented in Table 4-11.

Table 4-11. Sediment Delivery Ratios in the Sanchez Watershed

Subwatershed	Area (km^2)	Sediment Delivery Ratio
1	209.0	0.08
2	6.6	0.23
3	78.4	0.11
4	96.4	0.10
5	9.8	0.20
6	17.6	0.17
7	20.4	0.16
8	38.7	0.13
9	14.1	0.18
10	41.5	0.13
11	62.8	0.11

4.3.11 Meteorology

Hydrology in GWLF is simulated by a water-balance calculation, based on daily observations of precipitation and temperature. Precipitation in south-central Colorado shows considerable local geographic variability, primarily due to orographic (elevation) effects, with higher precipitation at higher elevations. A search was made of available National Oceanic and Atmospheric Administration (NOAA) Cooperative Summary of the Day (SOD) reporting stations that were in close proximity to the watershed and had long periods of record without major data gaps. Table 4-12 presents the summary information for these stations. Figure 4-5 shows the locations of these stations. The San Luis station was selected for use; however, elevation effects were incorporated through evaluation of the Culebra SNOTBL station.

Table 4-12. Selected Meteorological Stations

Station	Latitude	Longitude	Elevation (ft)	Available Data
San Luis 2 SE, CO COOP 057430	37.11	105.25	8,031	Precipitation Temperature
Blanca, CO COOP 050776	37.26	105.31	7,748	Precipitation Temperature
Alamosa WSO, CO WMO 72462	37.26	105.51	7,530	Precipitation Temperature
Culebra #2 SNOTEL CULC2	37.12	105.12	10,200	Precipitation Snowpack

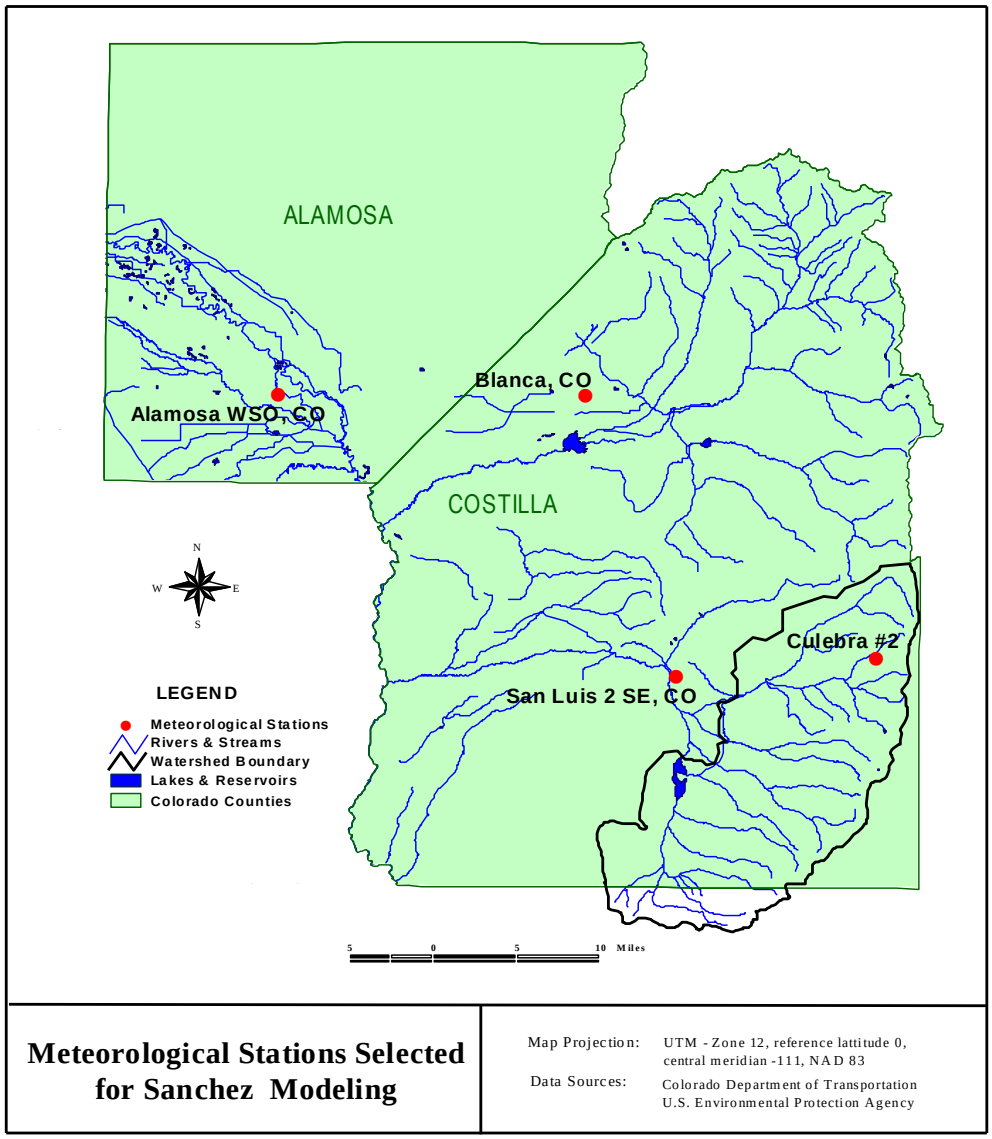

Figure 4-5. Weather Station Locations

Daily precipitation and mean temperature were obtained for the San Luis station from January 1980 to May 2005. To account for elevation differences in each subwatershed (Table 4-13), lapse rates were calculated based on elevation difference relative to San Luis 2SE (which is at 8,031 ft MSL). For precipitation, the lapse rate is +1.000642 mm per increase in elevation (m) expressed as a multiplier on San Luis precipitation. For temperature, the lapse rate is -9.26 degrees C per 1,000 m increase in elevation expressed as an additive term.

Table 4-13. Precipitation and Temperature Lapse Rates Relative to San Luis Weather Station

Subwatershed	Mean Elev (m)	Difference from San Luis (m)	Precipitation Factor	Temperature Factor
1	3,218	+776.6	1.50	-7.19
2	2,670	+228.6	1.15	-2.12
3	3,135	+693.6	1.44	-6.42
4	2,888	+446.6	1.29	-4.14
5	2,681	+239.6	1.15	-2.22
6	2,649	+207.6	1.13	-1.92
7	2,961	+519.6	1.33	-4.81
8	3,322	+880.6	1.56	-8.15
9	3,415	+973.6	1.62	-9.02
10	3,190	+748.6	1.48	-6.93
11	2,691	+249.6	1.16	-2.31

4.3.12 Logging Areas

Timber harvesting is a significant activity in the Sanchez watershed. All of the forested areas within the watershed are located on privately owned land and the Colorado State Forest Service does not require permits for harvesting activities on private land. Though a major cutting has not occurred since 1996, sediment loading from previously logged areas may be high relative to other sources.

Tetra Tech used 1999 black and white aerial photography and tiger road files in a GIS to identify areas of sparse vegetation with dense road coverage. GIS polygons were drawn around areas that exhibited evidence of logging and then overlain with an aspect grid to delete polygons on south facing slopes as these slopes generally do not contain enough moisture to support timber production.

After these logging polygons were created, Tetra Tech received additional data from the Colorado Acequia Association (CAA) that included more detailed roads (including roads/trails/paths related to logging activities), a color aerial image from August 2000, polygons delineating dense road areas, and harvested vegetation polygons. The harvested vegetation polygons were developed by intersecting dense road areas with vegetation data. These polygons were compared to the logging polygons delineated by Tetra Tech to identify areas of agreement and rectify differences. The total logged area for each subwatershed was similar between the two data sources, but each also contained unique areas. The unique areas were reviewed in more detail to determine whether they should be included in the final tally of logged areas. Aerial photos, land cover, and aspect were relied upon to confirm evidence of logging in the final polygons.

The final GIS shapefile of logged areas was then intersected with the STATSGO soil coverage (Figure 4-6). Ninety-six percent of logging has occurred on soil types CO303 and CO411. For modeling purposes, any logged areas that intersected soils CO405, CO409, CO415, or NM608 were assigned to the CO303 class, which is at a similar elevation range.

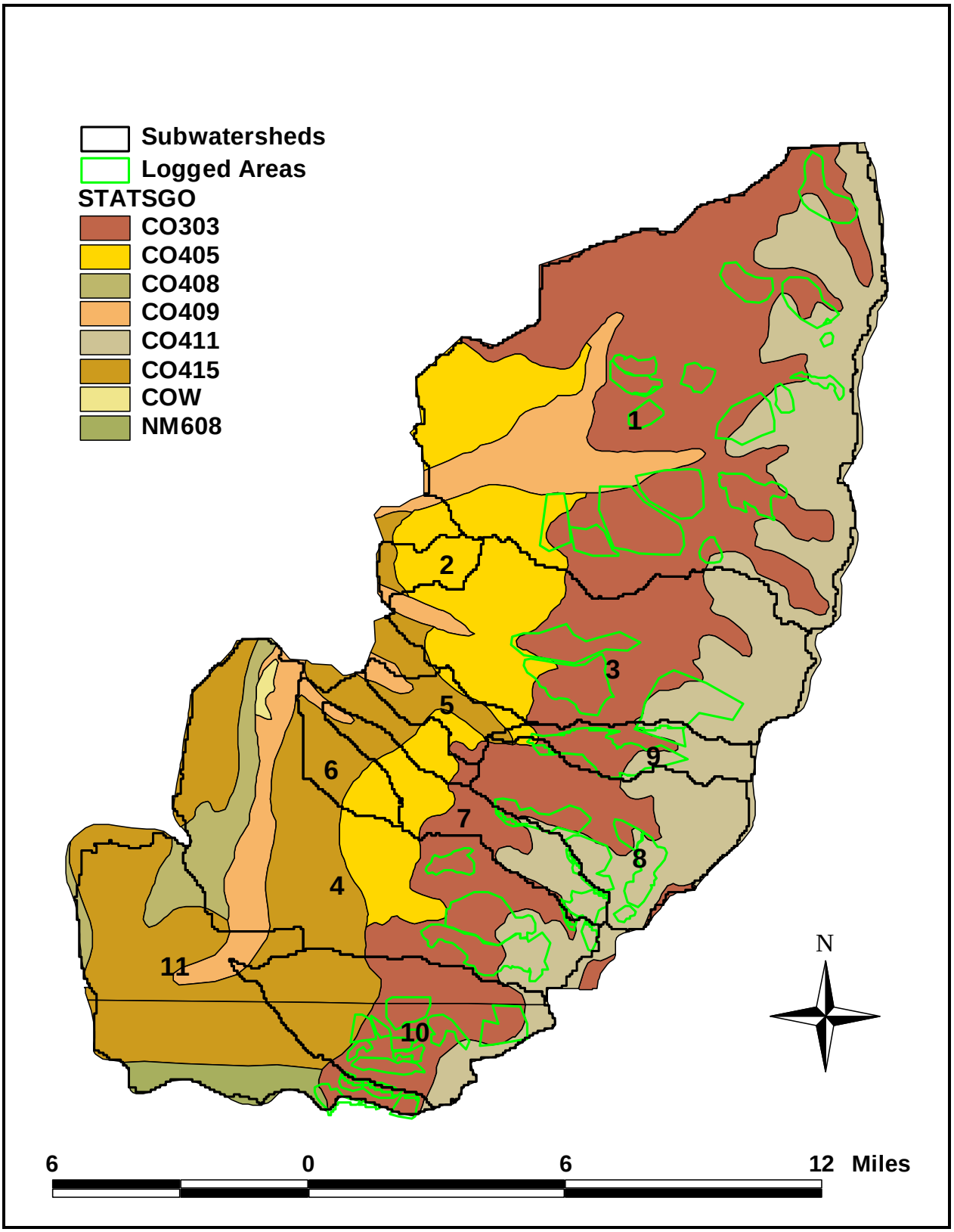

Figure 4-6. Logging Areas in the Sanchez Watershed

Logging is assumed to have occurred only in spruce/fir stands, which are represented by the FRSE (evergreen forest) land use class. Logged areas were subtracted from either FRSECO303 or FRSECO411, depending on underlying soil type. Because the resolution of the logging polygons is less accurate than the CAA vegetative cover, subtracting from FRSE sometimes resulted in small negative areas. In this case, FRSE was set to zero and excessive area was subtracted from FRST.

4.3.13 Estimates of Loading from Unpaved Roads

Roads account for less than two percent of the total land area of the Sanchez Reservoir watershed, but because nearly all are unpaved and are often located near streams, they can be a significant source of sediment to the reservoir. Sediment delivery from various types of unpaved roads (e.g., county roads, access roads, logging roads, driveways) was estimated for each subwatershed using the X-Drain program, an interface for the Road component of the Forest Service Water Erosion Prediction Project (FS WEPP) model (Elliot et al., 1999).

Because WEPP is process-based, it can be applied to a wide range of conditions where the necessary input data are known; however, WEPP is difficult to apply because of the substantial number of inputs required. Therefore, scientists at the Forest Service's Rocky Mountain Research Lab used ranges of input values from more than 130,000 combinations of topography, soil type, and climate conditions in WEPP to calculate sediment yield from various types of forest roads. The results of these model runs were collated and X-Drain serves as the interface that allows individuals to access the database to quickly evaluate erosion and sediment delivery potential from forest roads. Sediment yield in X-Drain is based on characteristics of three overland flow elements: the road surface, the fill slope, and a forested buffer. After the user inputs the road width and selects the appropriate climate conditions, soil types, and buffer characteristics (i.e., slope and length), the sediment yield from the buffer is displayed in matrix format for various combinations of road gradient and cross drain spacing. The user can then compare and select the sediment yield for the appropriate road gradient and cross drain spacing combination. The accuracy of the predicted values from X-Drain is at best within plus or minus 50 percent (USDA, 1999).

Two road data sources were used for the roads to be analyzed using X-Drain in the Sanchez Reservoir watershed. As part of the Topographically Integrated Geographic Encoding and Reference system (TIGER), the US Census Bureau generates coverages of roads derived from 1:100,000 scale USGS topographic quadrangle maps. The TIGER® roads coverage for Costilla County and Taos County, derived from 2004 Census data, were used to identify four road types: county roads, local/rural roads, four-wheel-drive vehicle trails, and driveways/service roads. Aerial photography and field verification were used to establish general road widths for each type of road, as well as the most common road design (i.e., insloped with bare ditch, insloped with vegetated/rocked ditch, outsloped and unrutted, and outsloped and rutted). The selected values are provided in Table 4-14.

The second data source for roads within the watershed was the Colorado Acequia Association (CAA). CAA staff digitized roads from custom flown aerial photography taken during the summer of 2000. The road types digitized by CAA staff primarily related to logging activities, including: access, logging, yarder, and skid roads, and skid and logging trails. According to the WEPP Road documentation, WEPP can be run to determine the erosion rate for the first year when applied to skid trails or other temporary trails. Generally, following revegetation, erosion rates rapidly decline to near zero within five years, so the recommendation for WEPP is to reduce the predicted erosion rate by 20 percent for each year after the trails are revegetated until the fifth year, at which point the erosion is taken to be zero. The logging related roads identified by CAA staff were mostly used in 1996, nearly 10 years ago. Thus, except for access roads and logging roads, which do not appear to be revegetated and sometimes overlap with the TIGER coverage, all other temporary roads/trails were assumed to contribute minimal sediment to Sanchez Reservoir. The CAA coverage included widths for access and logging roads, and the type of road was assumed to be outsloped and rutted. Representative values are provided in Table 4-14.

Table 4-14. Characteristics of Roads in the Sanchez Reservoir Watershed

Source	Road Type	Typical Width (ft)	Road Surface Condition
TIGER®	County Road	55	Half width insloped with bare ditch; half width outsloped, unrutted
TIGER®	Local/Rural Road	40	Half width insloped with bare ditch; half width outsloped, unrutted
TIGER®	4WD Trail	20	Outsloped, rutted
TIGER®	Driveway	12	Outsloped, unrutted
CAA	Access Road	20	Outsloped, rutted
CAA	Logging Road	20	Outsloped, rutted

Hermit, Colorado was selected to represent the climate for the Sanchez Reservoir watershed for the X-Drain program. Even though climate is available for Alamosa, which is closer to the watershed than Hermit, the elevation at Hermit more closely matches elevations in the watershed. In mountainous regions, the elevation is more influential than spatial distance for properly representing climate.

Preliminary queries in X-Drain revealed that regardless of road width, soil type, buffer gradient, cross drain spacing, and road gradient, the sediment load delivered from the buffer is zero when the buffer length approaches 160 feet. Therefore, all roads in excess of 160 feet from a stream were considered to have a negligible contribution to the average annual sediment load to the reservoir. This logic is based on the assumptions inherent in X-Drain that the road surface has no vegetation, the fillslope has sufficient vegetation to provide about 50 percent ground cover, and the forest buffer has a 20-year old forest with 100 percent ground cover (USDA, 1999). X-Drain provides sediment yields for five soil types. While these assumptions, in particular about the vegetation in the buffer, may not be applicable to the study area, they are parameters that cannot be adjusted through the X-Drain interface.

Within 160 feet, X Drain offers only two other buffer lengths: zero feet and 33 feet. The sediment yield with no buffer is an order of magnitude greater than either the 33-foot or 160-foot wide buffer. Therefore, two loading rates were developed. One rate, applicable to roads within 33 feet of a stream, is the average of the sediment yield for the 0-foot and 33-foot buffer lengths. The second rate, applicable to streams between 33 and 160 feet of a stream, is the average of the sediment yield for the 33-foot and 160-foot buffer lengths.

A GIS was used to buffer the streams in the study area by 33 feet and 160 feet on each side to identify the type and length of roads that could contribute to the annual sediment load. The length of the various road types shown in Table 4-14 was tallied within each buffer area by modeling subwatershed and the appropriate loading rate was applied. X-Drain offers sediment yield values for five soil types, so a GIS was used to identify which type was most similar to the STATSGO associations underlying the roads in each of the buffer areas for each subwatershed. Where the road types spanned multiple soil types, a visual estimate was used to determine the areal percentage of each type so that the loading rate could be proportionally scaled.

The sediment yield values were adjusted according to X-Drain recommendations to account for the drainage and condition of the road surface. The road gradients were estimated from slope and elevation data – frequently the loading rates for an individual subwatershed were averaged across a few of the road gradient categories if the slope and elevation data revealed a range of conditions. The sediment yield values queried from X-Drain were then multiplied by the length of road within each of the two buffer widths to provide the total annual yield within each subwatershed as shown in Table 4-15. Annual loads

for each subwatershed were apportioned into monthly values using the monthly percentages predicted by the GWLF model for that subwatershed.

Table 4-15. Average Annual Sediment Load from Road Surfaces by Subwatershed

Subbasin	Area of Contributing Road Surface (ac)	Average Annual Sediment Yield (tons/yr)
1	130	67.5
2	0	0.0
3	37	17.1
4	37	18.5
5	5	0.7
6	7	2.9
7	14	6.4
8	19	8.0
9	11	4.1
10	7	2.5
11	8	2.4

4.3.14 Watershed Model Results

The GWLF flow and sediment model was run for the period from January 1980 to May 2005 for the Sanchez watershed and combined with WEPP results for sediment loading from roads. Because no flow gage exists in the watershed, the model is not formally calibrated. The individual runoff and sediment estimates for the watersheds are shown in Table 4-16.

Table 4-16. Subwatershed Runoff and Sediment Estimates for Sanchez Watershed (Including Results from WEPP Roads)

Subbasin	Streamflow (L/yr)	Sediment (mt/yr)	Sediment (mg/km^2/yr)
1	4.13E+10	6,546	31.3
2	1.37E+08	156	23.6
3	1.37E+10	2,194	28.0
4	8.16E+09	1,631	166.4
5	1.32E+08	201	20.5
6	2.02E+08	192	10.9
7	2.11E+09	708	34.7
8	8.97E+09	2,135	55.2
9	4.14E+09	889	63.0
10	7.34E+09	2,040	49.2
11	1.04E+09	568	9.0
Total	8.72E+10	17,260	29.0

4.4 WATERSHED MERCURY LOADING ESTIMATES

Estimates of watershed mercury loading are based on the flow and sediment loading estimates generated by the watershed model through application of observed mercury concentrations. The observed concentration data were collected in 1999 and 2005, and are described in Section 1.5. Much of the mercury load from the watersheds moves in association with sediment during high flow scour events. Instream loadings were calculated by multiplying the observed mercury concentrations by estimated streamflow for the watershed area above the monitoring point. Similarly, the sediment-associated load was calculated by applying a sediment potency factor expressed as the mass of mercury per mass of sediment to the total estimated sediment load. Runoff and erosion estimates for individual watersheds were aggregated at tributary confluences to determine the total upstream load.

Ultimate sources of mercury in the watershed include release from the parent rock, mercury residue from waste disposal, and atmospheric deposition onto the watershed, including deposition and storage in snowpack. Monitoring in streams and stream sediments typically reflect the combined impact of a number of these sources. Estimated mercury loads transported in the water column were calculated by multiplying the estimated annual runoff volume by the average observed water column concentration. Sediment scour and bedload transport of mercury were calculated by multiplying sediment yield estimates by the average sediment concentration at a station.

Some watersheds and associated monitoring stations represent the net impacts of more than one upstream watershed. In these cases (watersheds 4 and 5), the load from the local watershed is calculated by differencing. The differencing procedure does produce estimates of mercury loss during transport in subbasin 4. No monitoring data are available for watersheds 2, 6, 8, and 11, accounting for 21 percent of the total area. For these watersheds, the medians of observed concentrations at all sites were applied. Subbasin loading estimates for the Sanchez watershed are shown in Table 4-17.

The 2005 sediment sampling also enables an approximate evaluation of mercury processes occurring in the Sanchez Canal. To do this, the canal is divided into two sections, the Upper Canal (above San Francisco Creek) and the Lower Canal (below San Francisco Creek). (Estimates from the canal are approximate, as the sediment transport processes have not been simulated. Calculations in Table 4-17 are based on steady-state assumptions of no net trapping of sediment; however, periodic dredging of the canal does remove sediment from the system. As this is not accounted for in the analysis, the sediment mercury load calculations in the canal, particularly the upper canal, should be viewed as an upper bound.)

Table 4-17. Estimated Watershed Mercury Loads to Sanchez Reservoir, 1999 and 2005 Data

Watershed	Station	Water Column Mercury Load (g/yr)	Sediment Mercury Load (g/yr)	Total Mercury Load (g/yr)	Total Mercury Areal Loading (mg/km^2/yr)	Areal Water Column Loading (mg/km^2/yr)	Areal Sediment Mercury Loading (mg/km^2/yr)
1	San-10	69.6	19.8	89.4	427.8	333.2	94.6
2	Median[2]	0.3	1.6	1.9	294.4	49.2	245.1
3	San-9	28.1	2.0	30.1	384.4	358.5	25.9
4	Difference[1] (SAN-11)	-20.8	91.8	71.0	736.6	-215.8	952.3
5	Difference[1] (SAN-7B)	10.9	9.9	20.8	2,133.0	1,115.8	1,017.2
6	Median[2]	0.5	2.0	2.5	140.1	27.2	112.9
7	San-6A	9.2	1.5	10.7	523.9	451.4	72.5
8	Median	21.2	22.0	43.3	1,118.6	548.9	569.7
9	San-7A	25.1	1.3	26.5	1,879.8	1,784.8	95.0
10	San-3	40.3	34.7	75.1	1,808.6	972.0	836.6
11	Median	2.5	5.9	8.3	132.6	39.3	93.3
Total from Watershed		187.0	192.5	379.5	637.8	314.2	323.5
Upper Canal	Difference[1] (SAN-8, 2005-1)	3.5	83.5	87.0			
Lower Canal	Difference[1] (SAN-SC, 2005-2,3,4)	-47.1	-30.6	-77.7			
Total to Reservoir		143.4	245.4	388.8	653.4	241.0	412.5

[1] Watershed estimate obtained by differencing cumulative estimates.

[2] No monitoring data are available for this watershed. Median of sample values was used to estimate mercury loadings.

It should be cautioned that the results shown in Table 4-17 are based on limited mercury data from two sampling rounds conducted during the summer of 1999, plus additional sediment sampling in Sanchez Canal in 2005. Some of the estimated differences between stations thus likely reflect random variability, rather than systematic differences. These uncertainties can only be remedied by conducting additional sampling.

Mercury loading estimates for subbasins 2, 6, 8, and 11 are based on medians rather than actual monitoring, so loading rates estimated for these basins should be considered highly uncertain. Subbasins 2 and 6 are small local drainages, without evident sources of elevated mercury load relative to the remainder of the watershed (except perhaps for mercury dredged out of the canal that is derived from elsewhere in the watershed), so the use of a median assumption in these subbasins should have little impact. The other two subbasins are constrained by estimates from downstream subbasins, as subbasin 8

is upstream of subbasin 5, while subbasin 11 is upstream of subbasin 4. Because subbasins 5 and 4 have been monitored, the net estimated loading from the 8+5 pair and the 11+4 pair should be reasonable, even if the partitioning to individual subbasins is suspect.

In terms of areal mercury loading, the loading rates from San Francisco Creek (subbasins 5, 8, and 9) and from Willow and Jarocito Creeks (subbasin 10) appear to be elevated relative to the remainder of the watershed. The San Francisco Creek estimated loads are high primarily due to estimated higher rates of erosion, while the Willow/Jarocito Creek estimated loads are high primarily due to elevated concentrations of mercury on sediment. In contrast, the small loading rate predicted for subbasin 11 is primarily due to a low predicted sediment yield. If, as appears likely, the watershed mercury is derived primarily from atmospheric deposition, sediment yield is likely to be the major determining factor in mercury delivery to the reservoir. See Section 4.6.4 for discussion of the probable contribution of atmospheric deposition to watershed mercury loads.

The results for the Sanchez Canal suggest that there is a net gain in mercury load in the Upper Canal (above San Francisco Creek). This inference is driven by the high sediment mercury concentration observed at station 2005-1, just downstream of the Culebra Creek diversion. The upper part of the Canal is dredged on an approximately annual basis, and much of the dredge spoil is placed on the berm immediately adjacent to the canal (Figure 4-7). It is possible that sediment mercury concentrations in this area are enriched by the process of removing sediment from the canal and placing it on adjacent berms, from which sediment fines and mercury may erode and leach back into the canal. The 2005 sampling of sediment from the berm in this area showed elevated concentrations of both total mercury and methylmercury (although not as high as in the channel). A simple management practice to reduce the recycling of mercury from the berms back into the canal would be to ensure that dredge spoils are placed beyond the berm and down-gradient from the canal, and thus disconnected from the Sanchez inflow. According to an employee of the Sanchez Ditch and Reservoir Company, no changes have been made to the placement of spoil material along the canal, and the canal continues to be dredged approximately once per year (personal communication, J. Lorenz, Sanchez Ditch and Reservoir Company to D. Pizzi, Tetra Tech, 5/2/2008).

Figure 4-7. Upstream view of Sanchez Canal at the J8 Road Crossing, Showing Dredge Spoil Placed along the Berm

The lower part of Culebra Creek above the diversion structure for Sanchez Canal is also dredged periodically, and could experience similar problems. However, the substrate in this area is mostly sand, gravel and cobble, which have relatively low capacity to sorb mercury.

In contrast to the Upper Canal, the Lower Canal appears to be a net sink of mercury, consistent with the presence of large areas of alluvial deposit near the mouth of the canal (Figure 4-8). However, the canal discharge is evidently reworking and eroding the alluvial fan with time, so long-term sequestration cannot be assured.

Figure 4-8. Upstream View of Sanchez Canal as it Incises Through its Historic Alluvial Fan in Sanchez Reservoir

4.5 DIRECT ATMOSPHERIC DEPOSITION

As described in Section 3.2, atmospheric deposition of mercury occurs both to the Sanchez watershed and direct to the lake surface. The net impacts of deposition onto the watershed are included in the watershed loading estimates, which are based on measured concentration data. An estimate of the direct deposition to the lake surface can be obtained by multiplying the total (wet and dry) deposition rate (Table 3-2) times the lake surface area. The surface area of Sanchez Reservoir is highly variable, and rarely approaches the nominal full pool area of 3,145 acres. To obtain an average estimate of the effects of direct atmospheric deposition, the calculation is performed with a typical surface area of about 1,600 acres. This yields an estimate of 106 g-Hg/yr direct deposition to the lake.

4.6 SUMMARY OF LOADS

4.6.1 Total Mercury Loads

The previous sections provide estimates of mercury loads transported in the water column, transported with scour and bedload of sediment, and in direct atmospheric deposition. The loads to Sanchez are compared to those to McPhee and Narraguinnep reservoirs in southwest Colorado, both of which have fish consumption advisories for mercury (Tetra Tech, 2001) in Table 4-18. In addition to loading rates,

this table also summarizes load per volume. Highest volumetric and areal loading rates are seen for Sanchez, followed by McPhee, and then Narraguinnep.

Table 4-18. Summary of Mercury Load Estimates for McPhee, Narraguinnep, and Sanchez Reservoirs

Reservoir	Watershed Runoff (g/yr)	Watershed Sediment (g/yr)	Interbasin Transfer (g/yr)	Direct Atmos. Deposition (g/yr)	Total (g/yr)	Load per Volume (mg/ac-ft)
McPhee	2,576	222	0	251	3,049	9.6
Narraguinnep	2.7	22.7	15.9	36.8	78.1	4.6
Sanchez	143.4	245.4	0	106	494.8	12.4

Notes: McPhee and Narraguinnep loads from Tetra Tech (2001) volumetric loads to Sanchez calculated at a typical volume of 40,000 ac-ft.

Table 4-19 re-expresses the loads on a percentage basis. Loading to McPhee appears to be dominated by water column loads derived from watershed runoff. This likely reflects the significance of mercury loading in dissolved and suspended form from mine seeps. Atmospheric deposition to the lake surface accounts for less than 10 percent of the total load. Loads to Narraguinnep are dominated by direct atmospheric deposition.

For Sanchez Reservoir, direct atmospheric deposition as a percentage falls between McPhee and Narraguinnep, but the movement of mercury with sediment from the watershed appears to be the most significant source. Of course, much of this load may ultimately derive from atmospheric deposition.

Table 4-19. Mercury Load Source Percent Contributions for Sanchez, McPhee, and Narraguinnep Reservoirs

Reservoir	Watershed Runoff	Watershed Sediment	Interbasin Transfer	Direct Atmospheric Deposition
McPhee	84.5%	7.3%	0.0%	8.2%
Narraguinnep	3.5%	29.1%	20.4%	47.1%
Sanchez	29.0%	49.6%	0.0%	21.4%

Sanchez also shows a greater importance of sediment-associated loads relative to water column loads when compared to McPhee Reservoir. This reflects the drier climate and smaller summer flows present at Sanchez. In addition, McPhee receives mine seep discharges to water. Discharges of this type do not appear to be present in the Sanchez watershed.

4.6.2 Methylmercury Loads

The responses of biota are determined by MeHg concentrations, not total Hg. These concentrations reflect both methylation within the lake and external loading of MeHg. That some methylation occurs in the watershed is shown by measured MeHg concentrations in Sanchez tributary streams, which range up to 11 percent of total Hg. Potential sources of watershed methylation are discussed in Section 4.6.3.

In midwestern and eastern lakes, methylation in lake sediments is often the predominant source of MeHg in the water column. However, in western lakes with high sedimentation rates, rapid burial tends to depress the relative importance of regeneration of MeHg from lake sediments. For instance, in McPhee Reservoir (Tetra Tech, 2001), 71 percent of the MeHg present in the water column was estimated to derive from watershed inflows.

The percentage of MeHg relative to total mercury concentrations in the water column for Sanchez monitoring stations is shown in Figure 4-9. In the majority of cases, the methyl fraction was higher in August than in June (particularly at station SAN-7, a seep on San Francisco Creek, and at SAN-4, on Cuates Creek), likely reflecting greater biological methylation activity during warmer weather. Otherwise there seems to be little distinct pattern.

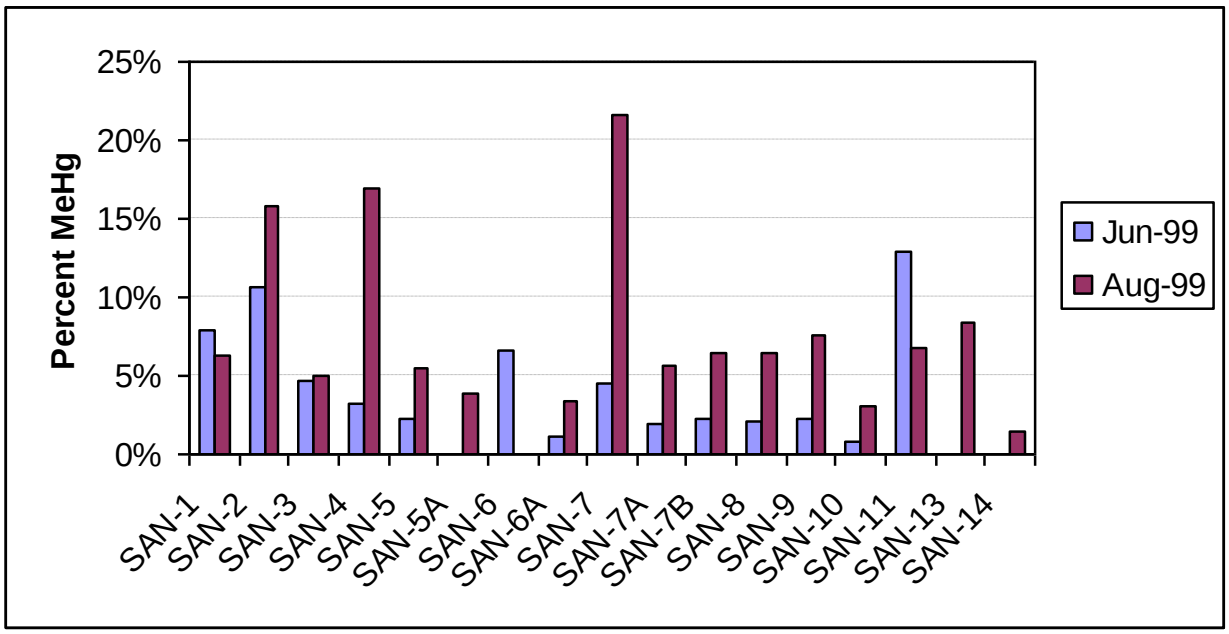

Figure 4-9. Methylmercury Fraction in Water, Sanchez Watershed Samples

A comparison of MeHg in Sanchez, McPhee, and Narraguinnep is provided in Table 4-20, based on the two sampling rounds conducted in June and August 1999. While Sanchez receives less mercury loading than McPhee on a volumetric basis, the reported inlake MeHg concentration and the fraction of mercury that is MeHg are higher. Further, the fraction of MeHg in inflow is similarly elevated. The inflow MeHg fraction for Narraguinnep is also similar to the in-lake fraction when the direct watershed and interbasin components are combined, but lower than the MeHg fraction for Sanchez.

Table 4-20. Methylmercury Comparison for Sanchez, McPhee, and Narraguinnep Reservoirs

Lake	Lake MeHg (µg/L)	Lake MeHg Fraction	Inflow MeHg (µg/L)	Inflow MeHg Fraction
Sanchez	6.1E-05	6.9 %	1.4E-04	7.3 %
McPhee	2.7E-05	1.9 %	3.9E-05	1.9 %
Narraguinnep	2.5E-05	3.1 %	1.29E-04 (watershed) 6.1E-05 (interbasin)	3.1 %

Notes: Inflow for McPhee is based on station MCP-17 (Tetra Tech, 2001); inflow for Sanchez and Narraguinnep is based on all stream stations. MeHg fractions are unfiltered MeHg divided by unfiltered total Hg in water.

For all three reservoirs, the MeHg fraction in-lake is similar to that measured in the inflow, suggesting that in-lake MeHg may be largely determined by watershed loads. For McPhee, this result is consistent with the lake model (Tetra Tech, 2001), which showed that the majority of lake MeHg was derived from inflow, rather than being created in the lake. In all three lakes, high sedimentation rates appear to result in a situation in which the sediment is a net sink for MeHg, and input of MeHg from the watershed is a major controlling factor on in-lake exposure concentrations.

4.6.3 Watershed Methylation

The results in Table 4-17 through Table 4-20 suggest that observed impacts in Sanchez Reservoir are due in part to high watershed methylation rates, which "amplify" the effects of the total mercury load. Sanchez contains significant wetland areas around the south and east boundaries of the lake, and also a variety of small wetlands associated with beaver ponds higher in the watershed. Note that the inflow data shown in Table 4-20 is for stations upstream of the near-shore wetlands, for which no water column mercury sampling data are available.

A single sediment sample from August 1999 from the wetlands at the south end of the lake showed total Hg and MeHg concentrations in the range of those seen in other stream sediment samples. Two samples in 2005 were collected from berms in the wetland area, rather than directly from reducing wetland sediments, and showed only moderately elevated MeHg concentrations (3.32E-04 and 3.89E-04 mg/kg). However, five samples of porewater from Sanchez wetlands were also analyzed in 1999 (Tetra Tech, 2000). These had average concentrations of 0.019 µg/L total Hg and 6.24E-04 µg/L MeHg, which is more than 10 times the lake concentration.

Methylation of mercury occurs under oxygen-poor, reducing conditions. Wetland areas are particularly likely sites for methylation in the watershed. Other likely sites include shallow riparian groundwater and the bottom waters and sediment of small impoundments that stratify and go anoxic.

Small beaver ponds are found at various locations in the Sanchez watershed. The associated wetlands may facilitate methylation of mercury contained in upstream runoff.

Total mercury concentration has not been found to be a good predictor of mercury methylation rates in wetlands systems (Choe et al., 2004; Bonzongo and Lyons, 2003; Bowles et al., 2003; Heim et al., 2003). Rather, production, in the presence of an available mercury pool, depends on rates of bacterial sulfate reduction.

Wetlands and beaver ponds are sources of methylmercury because they support the activity of known methylators (primarily sulfate reducing bacteria) by supplying ample organic matter under anoxic conditions. Branfireun et al. (2005) used additions of stable mercury isotopes to show conversion of

added Hg(II) to MeHg in wetland soils within one day of addition. Several recent studies report methylation rates observed in wetlands (Table 4-21).

Table 4-21. Wetland Methylation Rates Reported in the Literature

Methylation Rate ($\mu g/m^2/yr$)	Description	Reference
0.18	Wetland in Southern Ontario, Canada	Galloway and Branfireun (2004)
0.17	Riparian wetland in Adirondack region, NY	Driscoll et al. (1998)
0.45	Beaver pond in Adirondack region, NY	Driscoll et al. (1998)
0.17	Wetland surrounded by peatland, Northwestern Ontario	St. Louis et al. (2004)
7.0	First year after flooding the surrounding peatland	St. Louis et al. (2004)
1 to 5	Several years after flooding the surrounding peatland	St. Louis et al. (2004)
270	Local methylation rate of the peatland area	St. Louis et al. (2004)
0.7 to 1.4	Northern Wisconsin wetland	Cited in Hurley et al. (1995)

Wetlands release methylated mercury during storm events when pore water is flushed out (Balogh et al., 2004, St. Louis et al., 2004). Prior to a storm event in a Minnesota stream (Balogh et al., 2004), the ratio of MeHg to Total Hg in-stream ranged from 0.08 to 0.17; during the storm it ranged from 0.44 to 0.46. In the Ontario Experimental Lakes wetland study (St. Louis et al., 2004), surface water ratios of MeHg to Total Hg were 5 to 10 percent prior to flooding; after flooding they were 60 to 80 percent. The percent of Total Hg that was methylated was 1 to 2 percent before flooding, 20 percent two years after flooding, and 3.5 percent four years after flooding.

Studies indicate the importance of recently flooded terrestrial environments as initial hot spots of methylmercury production (St. Louis et al., 2004; Driscoll et al., 1998). Elevated MeHg production rates are documented soon after flooding. Within a few years, the production rates decrease as stores of mercury are depleted, but rates remain elevated compared to pre-flood conditions. Constant mercury inputs from upland areas and atmospheric deposition continue to be methylated under the favorable conditions of a wetland.

In the Experimental Lakes study (St. Louis et al., 2004), prior to flooding the wetland area produced methylmercury at a rate of 0.17 $\mu g/m^2/yr$. The surrounding peatland was then inundated and during the first year, methylation rates increased to 7 $\mu g/m^2/yr$ for the entire system. Methylation rates in the peatland areas were 270 $\mu g/m^2/yr$, but the overall rates were lower when averaged over the entire area of the pond, wetland, and peatland system. During the third through ninth years of flooding, methylation rates ranged from 1 to 5 $\mu g/m^2/yr$.

In addition to measuring methylation rates in a riparian wetland and downstream beaver pond, Driscoll et al. (1998) reported literature values for methylation rates observed in wetlands (0.3 $\mu g/m^2/yr$), lakes (0.5 to 3 $\mu g/m^2/yr$), and recently flooded areas (13 $\mu g/m^2/yr$). Methylation rates observed in the beaver pond (0.45 $\mu g/m^2/yr$) were much lower than those reported for recently flooded areas (13 $\mu g/m^2/yr$) but were near the rates observed in other wetlands. The authors do not state the exact age of the beaver pond, but do indicate that it is relatively old and expected to exhibit methylation rates typical of a wetland rather than a recently flooded area. They suggest ball-park estimates for methylation rates in initially flooded areas (whether by beaver or human impoundment) of 10 $\mu g/m^2/yr$ and for subsequent years at 0.5 $\mu g/m^2/yr$.

Researchers studying the impacts of wildfires on mercury transport have also shown increased rates of methylation. Fires not only volatize elemental mercury and add to the atmospheric pool available for

transport and deposition, but they also result in decreased stability of the forest floor. Fires liberate mercury stored in above ground biomass, and more intense fires may volatilize much of the mercury stored in surface soils. After burning, forest fires appear to increase the mobility of mercury in arid watersheds (Caldwell et al., 2000), in large part by increasing erosion potential (both by water and wind). Precipitation events on burned areas transport large amounts of sediment and charred material to surface waters (PRWG, 2007) which contain both mercury and organic carbon needed for methylation.

Caldwell et al. (2000) showed that a fire followed by storm events in south-central New Mexico resulted in increased concentrations of total mercury and methylmercury. Sediment concentrations of total mercury at the mouth of the creek draining the burned area increased from 7.5 µg/kg to 46.1 µg/kg following the fire and storm event; methylmercury concentrations in those sediments increased from 0.428 µg/kg to 12.46 µg/kg. Other sites in the watershed not impacted by upland fires showed similar concentrations of both mercury species throughout the study period.

Researchers in Washington State measured total gaseous mercury in smoke plumes from a fire that occurred in August 2001 in the Cascade Mountains. Gaseous concentrations measured 7.5 ng/m^3, six times higher than background. Ninety-five percent of the gaseous mercury was in elemental form; the remaining five percent was in particulate form (Friedli et al., 2003).

Fires that occur in wetland areas are a worst-case scenario in terms of mercury release. Atmospheric emissions of mercury from burned, boreal wetland areas in Canada were found to be 15 times higher than those from burns occurring in non-peat soil areas (Turetsky et al., 2006).

According to the US Forest Service Fire News Archives, wildfires have not occurred in the Sanchez Reservoir watershed in recent years (2004 through 2008). Several moderate-size fires occurred in the San Juan National Forest during this time, ranging in size from 1,000 ac to 14,000 ac. A large fire (92,000 ac) occurred near Phoenix, AZ. Though present loading to the reservoir is likely not impacted by wildfires, fires that occur in the future within this watershed could result in large loads of mercury to the reservoir.

4.6.4 Contribution of Atmospheric Deposition to Watershed Loads

Mercury loading to Sanchez derives primarily from the watershed, and MeHg concentrations in the lake also appear to be significantly affected by MeHg loads from the watershed. No significant anthropogenic sources of mercury have been documented. Diffuse sources of watershed mercury loading are the underlying geology and atmospheric deposition to watershed soils. A survey of the geology (Section 3.4.1) indicates very little in the way of elevated geological sources of mercury. Further, the concentrations of mercury in Sanchez snowpack (which reflect atmospheric deposition input, but not geology) are similar to those observed in-stream. These lines of evidence suggest that atmospheric deposition to soils in the watershed may be the major source of mercury loading to Sanchez.

The total estimated watershed mercury load (389 g/yr) may be due largely to atmospheric deposition. The atmospheric deposition rate to land of 20.8 g/km^2/yr (Table 3-2) could account for up to 12,230 g/yr over the watershed area of 227 mi^2 (588 km^2). Estimated watershed Hg loads delivered to the reservoir are thus only about 3 percent of the annual atmospheric input.

Concentration of mercury in surficial soils represents a long-term equilibration process with atmospheric inputs. The Indirect Exposure Methodology Model (IEM-2M) employed in the Mercury Study Report to Congress (USEPA, 1997) can be used to approximate the time course of surficial soil concentrations under conditions of constant atmospheric input. There are, however, two major problems in applying this method: (1) it requires an estimate of pre-anthropogenic soil concentration, which is generally not directly available, and (2) it assumes constant deposition. Not only is the latter assumption likely untrue, but the actual time history of deposition prior to the last few decades is largely unknown. Further, the concentration of mercury in soils of the Sanchez watershed has not been measured.

Estimates of "background" metals concentrations often rely on the work of Shacklette and Boerngren (1984). This work, however, is based on rather sparse data and does not directly account for the influence of soil type (Burt et al., 2003). More importantly for mercury, the observed data on which the analyses are based are "background" only relative to local sources, as available observations may include the impacts of 150 years or more of anthropogenic contributions to the global mercury background and associated global deposition. Newer analyses of the Shacklette and Boerngren data by USGS (Gustavsson et al., 2003) suggest that the recent concentrations of Hg in surficial soils in the Sanchez area are likely around 40 µg/kg – but stream sediment analyses from the watershed are consistently less than this value. USEPA (1997) estimated that the average pre-industrial soil mercury concentration in the western United States was on the order of 4 µg/kg.

While data are insufficient to estimate the trajectory of changes in soil mercury concentrations in Sanchez watershed (or even to estimate the current soil mercury concentration), the IEM model can be applied to provide a rough estimate of the likely responses of soils in the Sanchez watershed to atmospheric deposition loads of the magnitude described above (20.82 g/km^2/yr wet and dry deposition). Example calculations are summarized in Figure 4-10, beginning with the USEPA (1997) default of 4 µg/kg pre-industrial background for the western United States. As shown in this figure, estimated current atmospheric input rates would result in a continued increase in soil concentrations even after 160 years. The predicted long-term equilibrium concentration under these conditions would be about 170 µg/kg.

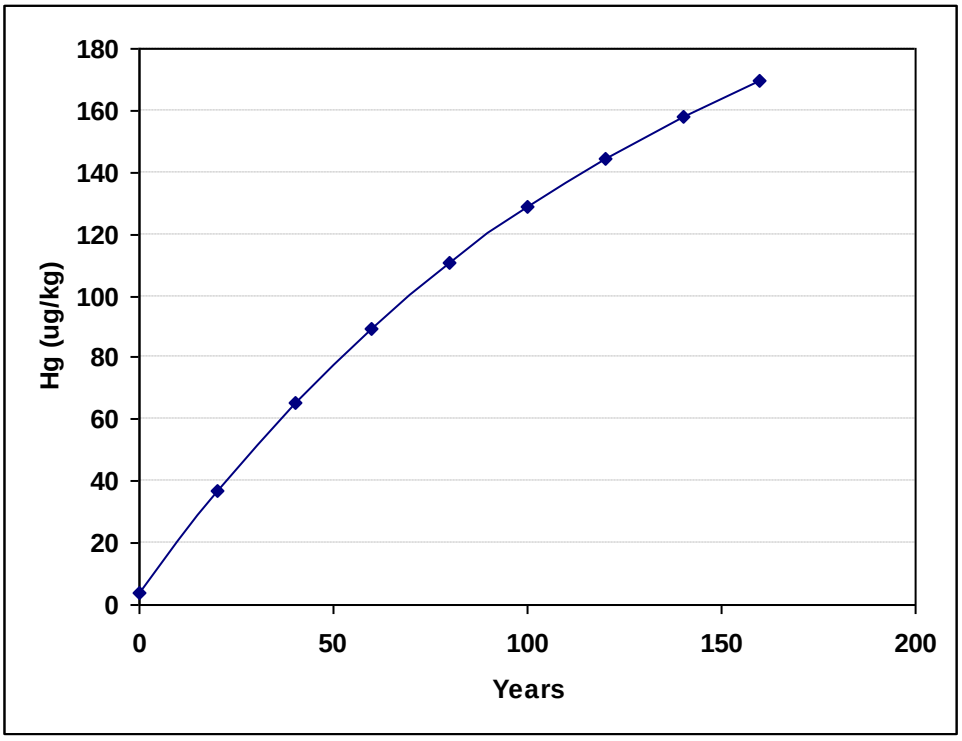

Figure 4-10. Example IEM Model Progression of Surface Soil Concentration Response to Estimated Current Atmospheric Deposition on Sanchez Watershed

4.7 LAKE RESPONSE

Neither data nor resources are available at this time to create and calibrate a detailed lake response model for Sanchez Reservoir. The key to the TMDL target is achieving acceptable concentrations in fish. As was seen in Section 1.5.2, the distribution of mercury tissue concentrations in fish in Sanchez is similar to that in Narraguinnep Reservoir (Tetra Tech, 2001), despite differences in estimated loads.

In western reservoirs with high sedimentation rates, MeHg is removed from the water column by sedimentation, and the generation of methylmercury from inorganic mercury in the sediment is limited by burial. Such lakes are therefore likely to respond approximately linearly to reductions in the watershed MeHg and total Hg load – although there may well be a delay in the response to load reductions, as found for McPhee (Tetra Tech, 2001). Nationally, authors such as Brumbaugh et al. (2001) have shown a log-log linear relationship between MeHg in water and MeHg in fish tissue normalized to length. However, this relationship is well-approximated by a linear relationship for the ranges of fish tissue concentration of concern here.

Until such time as a lake response model is constructed, and sufficient calibration data collected to develop it, an assumption of an approximately linear response of fish tissue concentrations to changes in external loads is sufficient for the development of a TMDL.

5 TMDL, Load Allocations, and Wasteload Allocations

The linkage analysis provides the quantitative basis for determining the loading capacity of Sanchez Reservoir. This in turn allows estimation of the Total Maximum Daily Load (TMDL), and allocation of that load to point sources (wasteload allocations) and nonpoint sources (load allocations). The TMDL also contains a Margin of Safety, which is described in detail in Section 6.2.

5.1 DETERMINATION OF LOADING CAPACITY

A waterbody's loading capacity represents the maximum rate of loading of a pollutant that can be assimilated without violating water quality standards (40 CFR 130.2(f)). This is the maximum rate of loading consistent with meeting the numeric target of 0.3 mg/kg for mercury in 20-in walleye.

For Sanchez, a model of lake response and fish bioaccumulation has not been created at this time. Rather, it is assumed that, in the long term, fish tissue concentrations will respond approximately linearly to reductions in mercury load. This assumption has been found to be a reasonable first-order approximation in other systems with high burial rates, such as McPhee and Narraguinnep reservoirs.

Estimating the loading capacity first requires an estimate of the existing mercury concentration in walleye. To do this, a linear regression analysis was performed on tissue concentrations versus length. The resulting regression equation is

$$Hg(fish) = -1.83844 + 0.005516 \cdot Len, \quad R^2 = 0.489$$

where *Hg(fish)* is the total mercury concentration in walleye (mg/kg) and *Len* is length in mm. The regression analysis is shown in Figure 5-1, along with the 95 percent upper confidence limit on mean predictions about the regression line (95 percent UCL) and the 95 percent upper prediction interval on individual observations (95 percent UPI). The regression has a non-zero intercept and should not be considered valid for a length less than 333 mm.

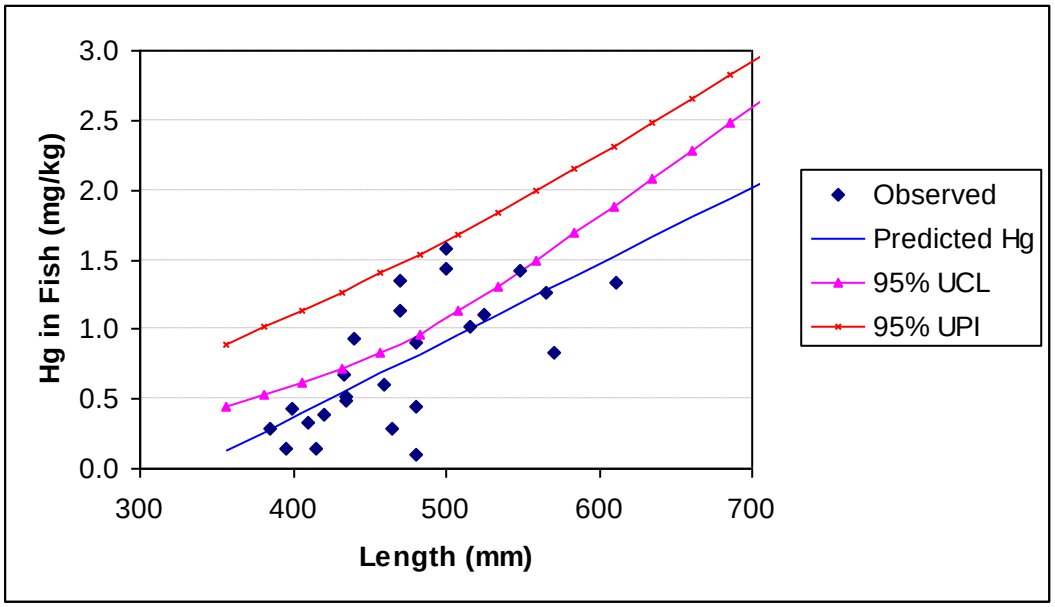

Figure 5-1. Regression Analysis of Mercury in Sanchez Walleye

For mercury, long-term cumulative exposure is the primary concern. Therefore, it is appropriate to use the 95 percent UCL to provide a Margin of Safety on the appropriate age class.

The 95 percent UCL is given by

$$UCL_{0.95} = \mu_{y|x_0} + t_{0.05,n-1} \cdot s_{\mu_y|x_0}$$

where $\mu_{y|x}$ is the predicted value of y given $x=x_0$, t is the Student's t-statistic with n-1 degrees of freedom, n is the number of observations used in the regression, and the variance on the prediction is given by

$$s^2_{\mu_y|x_0} = s^2_{y|x} \cdot \left[1/n + \left(x_0 - \bar{x}\right)^2 / \sum \left(x_i - \bar{x}\right)^2 \right],$$

where $s^2_{y|x}$ is the standard error of the model estimates. For the Sanchez walleye data, this yields

$$UCL_{0.95} - Hg(fish) = -1.83844 + 0.005516 \cdot Len + 0.7027 \cdot \sqrt{1/25 + \left(Len - 472.3\right)^2 / 83815.5}$$

The TMDL target is established in 20-in (508 mm) walleye. At this length, the prediction from the regression equation is 0.963 mg/kg and the 95 percent UCL is 1.129 mg/kg total mercury. Existing mercury loading is estimated at 495 g/yr (see Table 4-17). The fraction of existing load consistent with attaining the target (the loading capacity) is then the ratio of the target (0.3) to the best estimate of current average concentrations in the target fish population (0.963), or 0.312. The difference between the direct regression estimate and the 95 percent UCL provides the Margin of Safety. Therefore, the allocatable fraction of the existing load (the loading capacity less the Margin of Safety) is the ratio of the target to 1.129 (0.3 divided by 1.129 equals 0.266). Resulting loading capacity and allocatable load estimates for the target level of 0.3 mg/kg are summarized in Table 5-1.

Table 5-1. Estimated Total Mercury Loading Capacity, Allocatable Load, and Margin of Safety for Sanchez Reservoir

Target (mg-Hg/kg – 20" walleye)	Loading Capacity Fraction of Existing Load	Loading Capacity (g/yr)	Allocatable Fraction of Existing Load	Allocatable Load (g/yr)	Margin of Safety (g/yr)	Percent Reduction
0.3	0.312	154	0.266	132	22	73.3%

It should also be noted that the loading capacity for total mercury is not necessarily a fixed number. The numeric target for the TMDL is expressed as a mercury concentration in fish tissue. This numeric target is linked to external mercury load through a complex series of processes, including methylation/ demethylation of mercury and burial of mercury in lake sediments. Any alterations in rates of methylation or in rates of mercury loss to deep sediments will change the relationship between external mercury load and fish tissue concentration and would thus result in a change in the loading capacity for external mercury loads.

5.2 TOTAL MAXIMUM DAILY LOAD

The TMDL represents the sum of all individual allocations of portions of the waterbody's loading capacity. Allocations are made to all point sources (wasteload allocations) and nonpoint sources or natural background (load allocations). The TMDL (sum of allocations) must be less than or equal to the

loading capacity; it is equal to the loading capacity only if the entire loading capacity is allocated. In many cases it is appropriate to hold in reserve a portion of the loading capacity to provide a Margin of Safety (MOS), as provided for in the TMDL regulation.

Knowledge of mercury sources and the linkage between mercury sources and fish tissue concentrations in Sanchez Reservoir is subject to many uncertainties. (These uncertainties are discussed in more detail in Section 6.2.) There do not, however, appear to be any significant concentrated sources of mercury in the Sanchez watershed, and a majority of the mercury that is loaded likely derives from diffuse atmospheric deposition onto the watershed. The MOS is addressed implicitly through the use of an upper confidence limit in the target calculation, which results in a MOS of 22 g/yr. Therefore, the TMDL is equivalent to the estimated loading capacity minus the MOS, or 132 g/yr.

5.3 WASTELOAD ALLOCATIONS

Wasteload allocations constitute an assignment of a portion of the TMDL to permitted point sources. There are no permitted point source discharges within the Sanchez watershed. Therefore, no wasteload allocations are included in the TMDL.

5.4 LOAD ALLOCATIONS

Load allocations represent assignment of a portion of the TMDL to nonpoint sources. These allocations must be made even where there is considerable uncertainty about nonpoint loading rates. Federal regulations (40 CFR 130.2(g)) define a load allocation as follows:

> The portion of a receiving water's loading capacity that is attributed either to one of its existing or future nonpoint sources of pollution or to natural background sources. Load allocations are best estimates of the loading, which may range from reasonably accurate estimates to gross allotments, depending on the availability of data and appropriate techniques for predicting loading. Wherever possible, natural and nonpoint source loads should be distinguished.

Mercury loading to Sanchez Reservoir does not appear to be driven by any dominant local source. The natural geology presents only a minor risk of mercury loading, there has been little mining activity in the watershed, and other diffuse sources (such as private dumps and automobile junkyards) seem unlikely to contribute a major portion of the mercury load, which is spread throughout the watershed. Atmospheric deposition appears to be the main source of mercury input to the watershed. The atmospheric deposition does not, however, appear to be solely attributable to nearby sources such as coal-fired power plants, but rather represents the regional and global background. While the estimates of Seigneur et al. (2004) that the major anthropogenic source of atmospheric mercury in this part of the country derives from southeast Asia may be an overestimate due to underaccounting for dry deposition, it does appear that atmospheric mercury loading at Sanchez is driven by multiple atmospheric sources across a wide geographic area.

Estimating a TMDL that will result in attainment of uses (specifically, acceptable concentrations of mercury in fish tissue) in Sanchez Reservoir requires a reduction in the MeHg exposure concentrations in the lake. There are two general ways in which this can be achieved. The first is through a reduction in the total watershed mercury load; the second is through a reduction in the MeHg concentration through reduction of MeHg production and transport in the watershed. MeHg is produced both within the reservoir and in the watershed. It appears that the methylated fraction of mercury load in Sanchez watershed is relatively high and similar to the fraction found in the reservoir – suggesting that control of MeHg load from the watershed may be a potential option for attaining standards. It is not possible, however, to fully investigate this option without a better understanding of mercury cycling and methylation processes within the reservoir, for which a lake mercury model (not included within the

scope of the current work) would be needed. Therefore, load allocations are focused on total mercury loading in this TMDL, recognizing that a more refined approach to implementation may be possible if additional understanding of mercury cycling in the watershed is obtained.

The current state of knowledge of mercury sources in the watershed and transport to Sanchez Reservoir requires use of a "gross allotment" approach to the watershed as a whole, rather than assigning individual load allocations to specific tracts or land areas within the watershed. Loading from geologic sources has also not been separated from the net impacts of atmospheric deposition onto the watershed. Information is currently available to separate sources for load allocations into two components:

1. Direct atmospheric deposition onto the lake surface.
2. Generalized geologic background watershed loading including the impact of atmospheric deposition on the watershed.

Most of the mercury loading contained in either source appears to ultimately derive from atmospheric deposition. However, the two sources differ in that direct atmospheric deposition onto the lake surface reflects only present-day sources, whereas background loading from the watershed reflects both ongoing and historic atmospheric deposition loads to the watershed, in addition to geologic background. For this TMDL, needed load reductions are assigned proportionately to both direct atmospheric deposition and watershed background sources.

Fully implementing the needed load allocations may be difficult, as the load appears to be driven by diffuse sources, including regional and global mercury transport. These atmospheric sources can only be managed in a regional and global context. USEPA (2005) indicates that the preferred option under the Clean Air Mercury Rule (CAMR Option 1) would result in only a 2.2 percent reduction in mercury deposition rates to Sanchez watershed, whereas the needed reductions identified in Table 5-1 are approximately 73 percent.

Much of the transport of mercury from the watershed is associated with the movement of sediment. Therefore, management practices that reduce erosion and sedimentation would yield a net benefit to the management of mercury loading to the lake. One area in which progress could be made is in the management of the Sanchez Canal. Recent sampling suggests that the upper portion of the Sanchez Canal is a net source of mercury load. The canal is dredged annually, and the spoils placed adjacent, from where sediment fines and mercury may return to the canal. Placement of this material down-gradient from the canal would limit such recontamination.

In addition, efforts to mitigate impacts from illicit dumping of household waste and management of potential mercury sources from automobile junkyards would yield a net reduction, although probably small, in the mercury load to the reservoir.

5.5 ALLOCATION SUMMARY

Allocations for the Sanchez mercury TMDL are summarized in Table 5-2, based on the 0.3 mg/kg target.

Table 5-2. Summary of TMDL Allocations and Needed Load Reductions (in g-Hg/yr) for Sanchez Reservoir (0.3 mg/kg Fish Tissue Target)

Source	Allocation	Existing Load	Needed Reduction
Wasteload Allocations	~0	~0	0
Load Allocations			
Direct Atmospheric Deposition	28	106	78
Watershed Background	104	389	285
Total	132	495	363
Margin of Safety	22		
Loading Capacity	154		

Although estimates of the loading capacity and load allocations are based on best available data and incorporate a Margin of Safety, these estimates may potentially need to be revised as additional data are obtained. To provide reasonable assurances that the assigned load allocations will indeed result in compliance with the fish tissue criterion, a commitment to continued monitoring and assessment is warranted. The purposes of such monitoring will be (1) to evaluate the efficacy of control measures instituted to achieve the needed load reductions, (2) to document trends over time in mercury loading, and (3) to determine if the load reductions proposed for the TMDL lead to attainment of water quality standards. It is recommended that a detailed plan for continued monitoring be incorporated as part of the implementation plan for this TMDL.

(This page left intentionally blank.)

6 Margin of Safety, Seasonal Variations, and Critical Conditions

6.1 SOURCES OF UNCERTAINTY

The analysis for this TMDL contains numerous sources of uncertainty, and load allocations must be proposed as best estimate "gross allotments" in keeping with the TMDL regulation at 40 CFR 130.2(g). Key areas of uncertainty have been highlighted in the Source Assessment and Linkage Analysis sections and are summarized below.

The sources of uncertainty can be divided into two groups. The first group consists of sources of uncertainty that directly affect the ability of the linkage analysis to relate the numeric target fish tissue concentration to environmental mercury exposure concentrations in the lakes. These sources of uncertainty propagate directly to uncertainty in estimation of the loading capacity and TMDL. The second group consists of uncertainty in the estimation of external loads. These have their primary impact on allocations. The loading capacity estimate (when expressed as a fraction of existing loads) is much more sensitive to uncertainty in the first group and relatively robust to uncertainty in the second group.

The first group includes the following:

- Fish data from the reservoir is sparse. While the presence of problem concentrations of mercury in fish has been confirmed, the limited number of samples and limited number of collection times leads to uncertainty regarding the average population response as a function of fish weight/age.
- Even less data are available on small forage fish and invertebrates, which drive the food chain pathways leading to bioaccumulation in sport fish.
- Sediment mercury concentrations are characterized by a limited number of samples.
- Information on the vertical distribution of mercury in the water column and associated water chemistry is available for only two points in time, in June and August 1999. Without additional sampling it is not possible to determine the extent to which these two times characterize the annual mercury cycle, or whether 1999 conditions are representative of conditions in other years.
- Neither available resources nor available data allowed the development and calibration of a detailed lake mercury cycling model for Sanchez Reservoir. Instead, the estimates of loading capacity for Sanchez are based on the assumption of an approximately linear relationship between mercury loading and MeHg exposure concentrations in the reservoir. This assumption was found to be reasonable in the lake modeling for McPhee Reservoir (Tetra Tech, 2001) due to the high sedimentation rates characteristic of southwestern reservoirs, but cannot be explicitly evaluated in Sanchez without creation of a lake model.

The second group includes the following:

- Watershed background loading of mercury is estimated using a simple water balance/sediment yield model. While the concentrations in tributary sediments are based on measured data, the estimated actual rates of movement of this sediment to the lake are not validated by field measurements at this time.
- Estimates of atmospheric wet deposition of mercury are based on a limited period of mercury monitoring at the Mesa Verde MDN station along with interpretation based on acid deposition monitoring at Alamosa and EPA air modeling. Actual deposition of mercury at or near the reservoir has not been measured and may well differ significantly from the estimates used.

- While atmospheric deposition appears to be the major source of mercury in the Sanchez watershed, the extent to which mercury loads are due to past (as opposed to ongoing) mercury deposition is not known.

There are thus many sources of uncertainty in the estimation of the mercury TMDL for Sanchez Reservoir. It is evident, however, that existing loads of mercury are too high to support designated uses, as shown by the tissue concentrations measured in fish.

The TMDL regulation requires that estimates of loading capacity be made even where there is uncertainty in load estimates, and only "gross allotments" are possible for nonpoint loads. The present TMDL provides a best estimate of the loading capacity for mercury, and the needed load reductions, for Sanchez Reservoir–but the uncertainty in these estimates is high. This uncertainty is addressed in part through use of a Margin of Safety (Section 6.2). The level of uncertainty, however, suggests the need for ongoing, adaptive management to meet water quality standards. In particular, a monitoring program should be part of any implementation plan. Such a monitoring program would allow tracking of progress in attaining acceptable fish tissue concentrations in response to management actions. It would also provide the basis for potential revision (upward or downward) of the estimated load allocations consistent with attaining the standard in the reservoir.

6.2 MARGIN OF SAFETY

All TMDLs are required to include a Margin of Safety to account for uncertainty in the understanding of the relationships between pollutant sources and impacts on beneficial uses. The Margin of Safety may be provided explicitly through an unallocated reserve or implicitly through use of conservative assumptions in the analysis.

The TMDL presented in this document incorporates an explicit Margin of Safety through use of the upper 95th percentile confidence limit on the predicted response of target sport fish tissue concentrations to mercury loads. This explicit Margin of Safety is equal to about 14 percent of the loading capacity (see Table 5-1).

6.3 SEASONAL VARIATIONS AND CRITICAL CONDITIONS

A TMDL is required to address fish tissue concentrations associated with bioaccumulation of mercury within Sanchez Reservoir. There is no evidence of excursions of water quality standards for mercury. Because methylmercury is a bioaccumulating toxin, concentrations in tissue of game fish integrate exposure over a number of years. As a result, annual mercury loading is more important for the attainment of standards than instantaneous or daily concentrations, and the TMDL is proposed in terms of annual loads. It is not necessary to address standard wasteload allocation critical conditions, such as concentrations under 7Q10 flow, because it is loading, rather than instantaneous concentration that is linked to impairment. However, because mercury load is primarily delivered to the reservoir during storm washoff events, high flows do represent a critical condition. This is addressed in Section 6.4.

The impact of seasonal and other short-term variability in loading is damped out by the biotic response. The numeric target selected is tissue concentration in piscivorous game fish of edible size, which represents an integration over several years of exposure, suggesting that annual rather than seasonal limits are appropriate. Nonetheless, the occurrence of loading that impacts fish does involve seasonal components. First, watershed mercury loading, which is caused by infrequent major washoff events in the watershed, is highly seasonal in nature, with most loading occurring during the early summer snowmelt period. Second, bacterially mediated methylation of mercury is also likely to vary seasonally. The timing of washoff events is not amenable to management intervention. Therefore, it is most

important to control average net annual loading, rather than establishing seasonal limits, in calculating the TMDL consistent with the existing loading capacity.

6.4 DAILY LOAD EXPRESSION

USEPA recommends inclusion of a daily load expression for all TMDLs to comply with the 2006 D.C. Circuit Court of Appeals decision for the Anacostia River. Though it is long-term cumulative load rather than daily loads of mercury that are driving the bioaccumulation of mercury in fish in the Sanchez Reservoir, this TMDL does present a maximum daily load according to the guidelines provided by USEPA (2007). The daily maximum allowable load of mercury to Sanchez Reservoir is calculated from the estimated 90th percentile flow to the reservoir multiplied by the event mean concentration for mercury consistent with achieving the long-term loading target.

There was a USGS gage in the Sanchez Reservoir watershed active from 1967 to 1970. A three-year period of record is not sufficient for statistical analysis. A gage north of the watershed on Trinchera Creek (USGS 08240500) was chosen as a surrogate. This gage has 59 years of data (1923 to 1981), a drainage area of 45.0 square miles, and is approximately 15 miles north of the watershed. The 90th percentile flow (54 cfs) was chosen to represent the peak flow for this drainage. Choosing the 90th percentile flow eliminates errors due to outliers and is likely more representative of peak flows in the Sanchez watershed which may not experience snow melt peak flows to the same extent as Trinchera Creek.

To estimate the peak flow to the Sanchez Reservoir, the 90th percentile flow for Trinchera Creek was scaled up by the ratio of drainage areas (226.6/45.0). The resulting peak flow estimate for Sanchez Reservoir is 272 cfs.

The event mean concentration for mercury was calculated from the allowable load (132 g-Hg/yr) and the average annual simulated stream flow generated by GWLF. The resulting concentration (1.56E-03 µg/L) times the peak flow to Sanchez Reservoir (272 cfs) yields a total maximum daily load of 1.04 g-Hg/d.

(This page left intentionally blank.)

7 References

ASCE. 1975. *Sedimentation Engineering*, ed. V.A. Vanoni. American Society of Civil Engineers, New York.

Balogh, S.J., Y. Nollet, E.B. Swain. 2004. Redox Chemistry in Minnesota Streams during Episodes of Increased Methylmercury Discharge. Environ. Sci. Technol. 2004, 38, 4921-4927.

Binkley, D., U. Olsson, R. Rochelle, T. Stohlgren, and N. Nikolov. 2003. Structure, production and resource use in some old-growth spruce/fir forests in the Front Range of the Rocky Mountains, USA. *Forest Ecology and Management*, 72: 271-279.

Bonzongo, J.C.J. and W.B. Lyons. 2003. Impact of Land Use and Physicochemical Settings on Aqueous Methylmercury Levels in the Mobile-Alabama River System. A Journal of the Human Environment: Vol. 33, No. 6, pp. 328-333.

Bowles, K.C., S.C. Apte, W.A. Maher, and D.R. Blühdorn. 2003. Mercury cycling in Lake Gordon and Lake Pedder, Tasmania (Australia). I: In-lake processes. *Water, Air, and Soil Pollution* 147: 3-23, 2003.

Branfireun, B.A., D.P. Krabbenhoft, H. Hintelmann, R.J. Hunt, J.P. Hurley, and J.W.M. Rudd. 2005. Speciation and transport of newly deposited mercury in a boreal forest: a stable mercury isotope approach. *Water Resources Research*, 41, WU6016.

Brumbaugh, W.G., D.P. Krabbenhoft, D.R. Helsel, J.G. Wisner, and K.R. Echols. 2001. A National Pilot Study of Mercury Contamination of Aquatic Ecosystems Along Multiple Gradients: Bioaccumulation in Fish. Biological Science Report USGS/BRD/DSR-2001-0009. U.S. Geological Survey, Reston, VA.

Bullock, O.R. Jr. and K.A. Brehme. 2002. Atmospheric mercury simulation using the CMAQ model: formulation description and analysis of wet deposition results. *Atmospheric Environment*, 36:2135-2146.

Burke, J., M. Hoyer, G. Keeler, and T. Scherbatskoy. 1995. Wet deposition of mercury and ambient mercury concentrations at a site in the Lake Champlain basin. *Water, Air, and Soil Pollution* 80:353-362.

Burroughs, R.L. 1981. A Summary of the Geology of the San Luis Basin, Colorado – New Mexico with Emphasis on the Geothermal Potential for the Monte Vista Graben. Colorado Geologic Survey Special Publication 17. Denver, CO.

Burt, R., M.A. Wilson, M.D. Mays, and C.W. Lee. 2003. Major and trace elements of selected pedons in the USA. *Journal of Environmental Quality*, 32(6): 2109-2121.

Byun, D.W. and J.K.S. Ching, eds. 1999. Science Algorithms of the EPA Models-3 Community Multiscale Air Quality (CMAQ) Modeling System. EPA/600/R-99/030. U.S. Environmental Protection Agency, Office of Research and Development, Washington, DC.

Caldwell, C.A., C.M. Canavan, and N.S. Bloom. 2000. Potential effects of forest fire and storm flow on total mercury and methylmercury in sediments of an arid-lands reservoir. *Science of the Total Environment*, 260: 125-133.

Caldwell, C.A., R. Arimoto, P. Swartzendruber, and E.M. Prestbo. 2003. Air Deposition of Mercury and Other Airborne Pollutants in the Arid Southwest. Project Number A-00-1. Southwest Consortium for Environmental Research and Policy, San Diego, CA. http://www.scerp.org/projs/00rpts/A-00-l.pdf.

CDOW. 2008. Fishing Regulations March 13, 2008. Colorado Division of Wildlife, Denver, CO. http://wildlife.state.co.us/NR/rdonlyres/279EA0CB-C63F-4B49-8150-8B1DD38FB390/0/Ch01.pdf.

Choe, K.Y., G.A. Gill, R.D. Lehman, and S. Han, W.A. Heim, and K.H. Coale. 2004. Sediment-water exchange of total mercury and monomethylmercury in the San Francisco Bay-Delta. Limnology and Oceanography 49, No 5, 1512-27 S 2004.

Cohen, M., R. Artz, R. Draxler, P. Miller, L. Poissant, D. Niemi, D. Ratte, M. Deslauriers, R. Duval, R. Laurin, J. Slotnick, T. Nettesheim, and J. McDonald. 2004. Modeling the atmospheric transport and deposition of mercury to the Great Lakes. *Environmental Research*, 95: 247-265.

Colorado State Forest Service (CSFS) and Colorado Timber Industry Association. 1998. Colorado Forest Stewardship Guidelines to Protect Water Quality: Best Management Practices (BMPs) for Colorado. Fort Collins, CO.

Doon, B. 2003a. Quarterly Project Performance Report for USDA Rural Utilities Service Solid Waste Management Grant November 2002 – January 2003. Prepared for Costilla County.

Doon, B. 2003b. Quarterly Project Performance Report for USDA Rural Utilities Service Solid Waste Management Grant February – April 2003. Prepared for Costilla County.

Driscoll, C.T., J. Holsapple, C.L. Schofield, and R. Munson. 1998. The chemistry and transport of mercury in a small wetland in the Adirondack region of New York, USA. *Biogeochemistry* 40: 137-146, 1998.

Ecology & Environmental, Inc. (E&E). 1991. Preliminary Assessment Sanchez Reservoir, Costilla County, Colorado. Prepared for US Environmental Protection Agency.

Ecology Center. 2001. Toxics in Vehicles: Mercury. Ecology Center, Great Lakes United. University of Tennessee Center for Clean Products and Clean Technologies.

Elliot, W.J., D.B. Hall, and D.L. Scheele. 1999. WEPP: Road, WEPP Interface for Predicting Road Runoff, Erosion and Sediment Delivery, Technical Documentation. USDA Forest Service Rocky Mountain Research Station and San Dimas Technology and Development Center.

EMNRD. 2001. New Mexico Energy, Minerals and Natural Resources Department, Forestry Division. Commercial Timber Harvesting Requirements. New Mexico Register, November 15, 2001, 19.20.4.

EPRI. 1999. Air Emissions Handbook for Electric Generating Stations. Electric Power Research Institute, Palo Alto, CA.

EPRI. 2000. An Assessment of Mercury Emissions from U.S. Coal-Fired Power Plants. Report TR-1000608. Electric Power Research Institute, Palo Alto, CA.

Eriksen, J., M.S. Gustin, D. Schorran, D. Johnson, S. Lindberg, and J. Coleman. 2003. Accumulation of atmospheric mercury in forest foliage. *Atmospheric Environment*, 37: 1613-1622.

Friedli, H. R., L. F. Radke, R. Prescott, P. V. Hobbs, P. Sinha. 2003. Mercury emissions from the August 2001 wildfires in Washington State and an agricultural waste fire in Oregon and atmospheric mercury budget estimates. *Global Biogeochemical Cycles*, Vol. 17, No. 2, page 1039.

Galloway, M.E. and B.A. Branfireun. 2004. Mercury dynamics of a temperate forested wetland. *Science of the Total Environment*, 325: 239-254.

Glass G., J. Sorensen, K. Schmidt, G. Rapp, D. Yap, and D. Fraser. 1991. Mercury deposition and sources for the Upper Great Lakes region. *Water, Air, and Soil Pollution*, 56: 235-249.

Gray, J.E., D.L. Fey, C.W. Holmes, and B.K. Lasorsa. 2005. Historical deposition and fluxes of mercury in Narraguinnep Reservoir, southwestern Colorado, USA. *Applied Geochemistry*, 20: 207-220.

Gustavsson, N., B. Bolviken, D.B. Smith, and R.C. Severson. 2003. Geochemical Landscapes of the Conterminous United States – New Map Presentations for 22 Elements. Professional Paper 1649. U.S. Geological Survey, Denver, CO.

Haith, D.A., and D.E. Merrill. 1987. Evaluation of a daily rainfall erosivity model. *Transactions of the American Society of Agricultural Engineers* 30(1): 90-93.

Haith, D.A., R. Mandel, and R.S. Wu. 1992. GWLF, Generalized Watershed Loading Functions, Version 2.0, User's Manual. Dept. of Agricultural and Biological Engineering, Cornell University, Ithaca, NY.

Heim, W.A., K. Coale, and M. Stephenson. 2003. Methyl and Total Mercury Spatial and Temporal Trends in Surficial Sediments of the San Francisco Bay-Delta. CALFED Bay-Delta Mercury Project.

Hudson, R.J.M., S.A. Gherini, C.J. Watras, and D.B. Porcella. 1994. Modeling the biogeochemical cycle of mercury in lakes: The Mercury Cycling Model (MCM) and its application to the MCL study lakes. In *Mercury as a Global Pollutant* ed. C.J. Watras and J.W. Huckabee, pp. 475-523. Lewis Publishers, Chelsea, MI.

Hurley, J.P., J.M. Benoit, C.L. Babiarz, M.M. Shafer, A.W. Andren, J.R. Sullivan, R. Hammond, D.A. Webb. 1995. Influences of watershed characteristics on mercury levels in Wisconsin rivers. *Environ. Sci. Technol*. 1995, 29, 1867-1875.

ICF. 2006. Model-Based Analysis and Tracking of Airborne Mercury Emissions to Assist in Watershed Planning, November 2006. ICF International for US EPA Office of Water, Washington, DC.

Ingersoll, G.P. 2000. *Snowpack Chemistry at Selected Sites in Colorado and New Mexico During Winter 1999*B*2000*. Open-File Report 00-394. U.S. Geological Survey, Denver, CO.

Ingersoll, G.P., M.A. Mast, L. Nanus, D.J. Manthorne, D.W. Clow, H.M. Handran, J.A. Winterringer, D.H. Campbell. 2004. *Rocky Mountain Snowpack Chemistry at Selected Sites, 2002*. Open-File Report 2004-1027. U.S. Geological Survey, Denver, CO.

Keeler, G.J, M.E. Hoyer, and C.H. Lamborg. 1994. Measurements of atmospheric mercury in the Great Lakes Basin. In *Mercury Pollution: Integration and Synthesis*, ed. C.J. Watras and J.W. Huckabee, pp. 231-241, Lewis Publishers, Chelsea, MI.

Kirkham, R.M., K.C. Shaver,, N.R. Lindsay, and A.R. Wallace. 2003. Geologic Map of the Taylor Ranch Quadrangle, Costilla County, Colorado. Colorado Geologic Survey Open-File Report 03-15. Denver, CO.

Kirkham, R.M., J.L. Lufkin, N.R. Lindsay, and K.E. Dickens. 2004. Geologic Map of the La Valley Quadrangle, Costilla County, Colorado. Colorado Geologic Survey Open-File Report 04-8. Denver, CO.

Lindberg, S.E., R.R. Turner, T.P. Meyers, G.E. Taylor Jr., and W.H. Schroeder. 1991. Atmospheric concentrations and deposition of Hg to a deciduous forest at Walker Branch watershed, Tennessee, USA. Water, Air, and Soil Pollution 56: 577-594.

Lindberg, S.E., T.P. Meyers, G.E. Taylor Jr., R.R. Turner, and W.H. Schroeder. 1992. Atmosphere-surface exchange of mercury in a forest: results of modeling and gradient approaches. *Journal of Geophysical Research*, 97(D2): 2519-2528.

Lindberg, S.E. and W.J. Stratton. 1998. Atmospheric mercury speciation: concentrations and behavior of reactive gaseous mercury in ambient air. *Environmental Science and Technology*, 36: 1245-1256.

Lindqvist, O., K. Johansson, M. Aastrup, A. Andersson, L. Bringmark, G. Hovsenius, L. Hakanson, A. Iverfeldt, M. Meili, and B. Timm. 1991. *Mercury in the Swedish Environment: Recent Research on Causes, Consequences, and Corrective Methods*. Kluwer Academic Publishers, Dordrecht, Netherlands.

Miller, E.R., A. Vanarsdale, G.J. Keeler, A. Chalmers, L. Poissant, N.C. Kamman, and R. Brulotte. 2005. Estimation and mapping of wet and dry mercury deposition across northeastern North America. *Ecotoxicology*, 14: 53-70.

Nater E. and D. Grigal. 1992. Regional trends in mercury distribution across the Great Lakes states, north central USA. *Nature* 358: 139-141.

Neitsch, S.L., and M. DiLuzio. 1999. ArcView Interface for SWAT99.2, User=s Guide. Blackland Research Center, Texas Agricultural Experiment Station, Temple, TX.

Nydick, K. 2008. Airborne Mercury in the San Juans: An Air and Water Quality Issue. Upper San Juan Water Quality Forum, April 3, 2008. Mountain Studies Institute. http://faculty.fortlewis.edu/ ORTEGA_C/USJWQF/Plenary%20talks/Nydick_Mercury_USJWQF _3Apr08.pdf

Pechan. 2003. Emission & Generation Resource Integrated Database, E-GRID2002. Version 2.01. Prepared for U.S. EPA Office of Atmospheric Programs by E.H. Pechan & Associates.

Popp, C.J., D.K. Brandvold, K. Kirk, L.A. Brandvold, V. McLemore, S. Hansen, R. Radtke, and P. Kyle. 1996. Reconnaissance and Investigation of Trace Metal Sources, Sinks, and Transport in the Upper Pecos River Basin, New Mexico. Cooperative Agreement No. 3-FC-40-13830. New Mexico Institute of Mining and Technology, U.S. Department of the Interior and U.S. Bureau of Reclamation.

Porvari, P., M. Verta, J. Munthe, M. Haapanen. 2003. Forestry Practices Increase Mercury and Methyl Mercury Output from Boreal Forest Catchments. *Environ. Sci. Technol*., 37 (11), 2389-2393, 2003.

PRWG. 2007. Fires, Floods, and Water Quality, Results of Hydrologic and Water-Quality Investigations 2004-07. Pine River Watershed Group. http://www.swhydrologic.com/PRWG.htm.

Rasmussen, P.E. 1995. Temporal variation of mercury in vegetation. *Water, Air, and Soil Pollution*, 80: 1039-1042.

Rea, A.W., S.E. Lindberg, and G.J. Keeler. 2001. Dry deposition and foliar leaching of mercury and selected trace elements in deciduous forest throughfall. *Atmospheric Environment*, 35: 3453-3462.

Reisman, J.I. 1997. Air Emissions from Scrap Tire Combustion. EPA-600/R-97-115. Prepared for U.S.-Mexico Border Information Center on Air Pollution and Office of Air Quality Planning and Standards, U.S. Environmental Protection Agency, Washington, DC.

Risser, P.G. and J.B. Mankin. 1986. Simplified simulation model of the plant producer function in shortgrass steppe. *American Midland Naturalist*, 115(2): 348-360.

RTI. 2001. Electric Power, A Computer Program for Estimating Mercury Air Emissions from Coal Combustion at the Electric Utilities in the United States. Version 3.0.0. Prepared for U.S. EPA by Research Triangle Institute. Available on-line at http://www.epa.gov/ttn/atw/combust/utiltox/natemis1.zip.

SCS. 1986. *Urban Hydrology for Small Watersheds*. Technical Release No. 55, 2nd ed. Soil Conservation Service, U.S. Department of Agriculture, Washington, DC.

Seigneur, C., P. Karamchandani, K. Lohman, K. Vijayraghavan, and R.L. Shia. 2001. Multiscale modeling of the atmospheric fate and transport of mercury. *Journal of Geophysical Research*, 106(D21): 27795-27809.

Seigneur, C., K. Vijayraghavan, K. Lohman, P. Karamchandani, and C. Scott. 2004. Global source attribution for mercury deposition in the United States. *Environmental Science and Technology*, 38: 555-569.

Selker, J.S., D.A. Haith, and J.B. Reynolds. 1990. Calibration and testing of a daily rainfall erosivity model. *Transactions of the American Society of Agricultural Engineers*, 26(1): 1612-1618.

Shacklette, H.T. and J.G. Boerngren. 1984. Element concentrations in soils and other surficial materials of the conterminous United States. Professional Paper 1270. U.S. Geological Survey, Washington, DC.

St. Louis, V.L., J.W.M. Rudd, C.A. Kelly, R.A. Bodaly, M.J. Paterson, K.G. Beaty, R.H. Hesslein, A. Heyes, and A.R. Majewski. 2004. The rise and fall of mercury methylation in an experimental reservoir. *Environ. Sci. Technol*., 38, 1348-1358.

Streufert, R.K. and J.A. Cappa. 1994. Location Map and Descriptions of Metal Occurrences in Colorado with Notes on Economic Potential. Colorado Geologic Survey Map Series 28. Denver, CO.

Tesche, T.W., D.E. McNally, C. Loomis, G.M. Stella, and J.G. Wilkinson. 2004. Scientific Peer Review of the HgCAMx Atmospheric Mercury Model and its Application to the 2002 Annual Cycle. Prepared for WDN Mercury Modeling Team, Wisconsin Dept. of Natural Resources, Madison, WI by Alpine Geophysics, Ft. Wright, KY.

Tetra Tech. 1999a. Total Maximum Daily Load and Implementation Plan for Mercury, Arivaca Lake, Arizona. Report to Arizona Department of Environmental Quality and U.S. Environmental Protection Agency, Region 9. Tetra Tech, Inc., Research Triangle, NC.

Tetra Tech. 1999b. Total Maximum Daily Load and Implementation Plan for Mercury, Peña Blanca Lake, Arizona. Report to Arizona Department of Environmental Quality and U.S. Environmental Protection Agency, Region 9. Tetra Tech, Inc., Research Triangle, NC.

Tetra Tech. 1999c. Dynamic Mercury Cycling Model for Windows 95/NTJ - A Model for Mercury Cycling in Lakes, D-MCM Version 1.0, Users Guide and Technical Reference. Electric Power Research Institute, Palo Alto, CA.

Tetra Tech. 2000. Review of Past and 1999 Mercury Data and Related Information for Six Colorado Reservoirs. Report to U.S. Environmental Protection Agency, Region 8. Tetra Tech, Inc., Lafayette, CA.

Tetra Tech. 2001. Technical Support Document for Developing a Total Maximum Daily Load for Mercury in McPhee and Narraguinnep Reservoirs, Colorado. Report to U.S. Environmental Protection Agency, Region 8. Tetra Tech, Inc., Research Triangle Park, NC.

Tetra Tech. 2006. Technical Support Document for Developing a Total Maximum Daily Load for Mercury in Sanchez Reservoir, Colorado. Report to U.S. Environmental Protection Agency, Region 8. Tetra Tech, Inc., Research Triangle Park, NC.

Tweto, O. 1979. Geologic Map of Colorado. US Geologic Survey Special Geologic Map. Department of the Interior, US Geological Survey. Denver, CO.

Turetsky, M. R., J.W. Harden, H.R. Friedli, M. Flannigan, N. Payne, J. Crock, and L. Radke (2006), Wildfires threaten mercury stocks in northern soils, *Geophys. Res. Lett.*, 33, L16403, doi:10.1029/2005GL025595.

USDA Forest Service, Rocky Mountain Research Station and San Dimas Technology and Development Center. 1999. X-DRAIN Cross Drain Spacing and Sediment Yield Program, Version 2.000. October 1999. http://forest.moscowfsl.wsu.edu/fswepp/docs/xdrain2doc.html

USEPA. 1997. Mercury Study Report to Congress, Vol. 3, Fate and Transport of Mercury in the Environment. EPA-452-R/97-005. U.S. Environmental Protection Agency, Office of Air Quality Planning and Standards and Office of Research and Development, Washington, DC.

USEPA. 2001. *Water Quality Criterion for the Protection of Human Health: Methylmercury*. EPA-823-R-01-001. Office of Science and Technology, Office of Water, USEPA, Washington, DC.

USEPA. 2004a. Facilities Emissions Report – Hazardous Air Pollutants. U.S. Environmental Protection Agency, National Emissions Inventory. http://www.epa.gov/air/data/reports.html

USEPA. 2004b. Facility Report. U.S. Environmental Protection Agency, Toxics Release Inventory. http://www.epa.gov/triexplorer/facility.htm

USEPA. 2005. Technical Support Document for the Final Clean Air Mercury Rule – Air Quality Modeling. US Environmental Protection Agency, Office of Air Quality Planning and Standards, Research Triangle Park, NC. March 2005. http://www.epa.gov/ttn/atw/utility/agm_oar-2002-0056-6130.pdf

USEPA. 2007. Options for Expressing Daily Loads in TMDLs. U.S. Environmental Protection Agency, Office of Wetlands, Oceans & Watersheds. June 22, 2007 Draft.

USEPA. 2008. Facility Report. U.S. Environmental Protection Agency, 2006 TRI Public Data Release. http://www.epa.gov/tri/tridata/tri06/index.htm

Walker, M.D., P.J. Webber, E.H. Arnold, and D. Ebert-May. 1994. Effects of interannual climate variation on aboveground phytomass in alpine vegetation. *Ecology*, 75(2): 393-408.

Watras, C.J., N.S. Bloom, R.J.M. Hudson, S. Gherini, R. Munson, S.A. Claas, K.A. Morrison, J. Hurley, J.G. Wiener, W.F. Fitzgerald, R. Mason, G. Vandal, D. Powell, R. Rada, L. Rislov, M. Winfrey, J. Elder, D. Krabbenhoft, A.W. Andren, C. Babiarz, D.B. Porcella, and J.W. Huckabee. 1994. Sources and fates of mercury and methylmercury in Wisconsin lakes. In *Mercury Pollution: Integration and Synthesis*, ed. C.J. Watras and J.W. Huckabee. Lewis Publishers, Chelsea, MI.

Wesley, M.L. 1989. Parameterization of surface resistances to gaseous dry deposition in regional-scale numerical models. *Atmospheric Environment*, 23:1293-1304.

Wischmeier, W.H., and D.D. Smith. 1978. Predicting Rainfall Erosion Losses: A Guide to Conservation Planning. Agricultural Handbook 537. U.S. Department of Agriculture, Washington, DC.

Xu, X., X. Yang, D.R. Miller, J.J. Helble, and R.J. Carley. 1999. Formulation of bi-directional atmosphere-surface exchanges of elemental mercury. *Atmospheric Environment*, 33: 4345-4355.